Elucidation of plasmacytoid dendritic cell development

Elucidation of plasmacytoid dendritic cell development

A dissertation presented

by

Ilka Arun Netravali

to

The Division of Medical Sciences

in partial fulfillment of the requirements

for the degree of

Doctor of Philosophy

in the subject of

Immunology

Harvard University

Cambridge, Massachusetts

January 2014

Dissertation Advisor: Dr. Shiv S. Pillai Ilka Arun Netravali

Elucidation of plasmacytoid dendritic cell development

Abstract

Most currently defined hematopoietic progenitor pools are heterogeneous, contributing to uncertainty regarding the development of certain blood cells. The origins of plasmacytoid dendritic cells, for instance, have long been controversial and progenitors exclusively committed to this lineage have never been described. We show here that the fate of hematopoietic progenitors is determined in part by their surface levels of 9-*O*-acetyl sialic acid. Pro-plasmacytoid dendritic cells were identified as lineage negative 9-*O*-acetyl sialic acid low progenitors that lack myeloid and lymphoid potential but differentiate into pre-plasmacytoid dendritic cells. The latter cells are also lineage negative, 9-*O*-acetyl sialic acid low cells but are exclusively committed to the plasmacytoid dendritic cell lineage. Levels of 9-*O*-acetyl sialic acid provide a distinct way to define progenitors and thus facilitate the study of hematopoietic differentiation.

For Arun, Chitra, and Ravi Netravali,

I cherish your unconditional love and affection.

Live as if you were to die tomorrow.
Learn as if you were to live forever.

– Mahatma Gandhi

Science does not know its debt to imagination.

– Ralph Waldo Emerson
from *Letters and Social Aims*

Relatedness of the unrelated

Common threads
run through
seemingly
unrelated
human actions
and
behavior.
Look for the
common thread
to understand
that the fabric of Life
is not a patchwork
of black and white
but a continuum
of swirling designs
and many colors.

– Cariappa Annaiah
from *Truisms – mostly. Reflections on life, living, and relationships, volume I*, 2010.

Acknowledgements

There are several individuals who have enriched my life throughout my studies. They are as much a part of this thesis as I am.

To Shiv Pillai: I am indebted to your unfailing guidance and mentorship. Your confidence gave me the courage to pursue my research with an unbiased and open mind, never allowing the fear of failure to prevent me from taking bold directions. Thank you for always urging me to aim high in the lab, in the clinic, and in my life. I am a better person and will become a better physician-scientist because of you.

To Cariappa Annaiah and Amitinder Kaur: I am grateful for your kindness, generosity, and love. Miti, you have an unparalleled inner strength and a zest for life and I strive to be more like you each day. Cariappa, you are an amazing mentor, physician-scientist, and human being. You have taught me lifelong lessons on how to learn and how to love that I will call upon for the rest of my life. I treasure your friendship.

To Shannon Turley, Rachael Clark, Andrew Lichtman, and Arlene Sharpe: Thank you for your thoughtful suggestions, engaging discussions, and constant support.

To David Cardozo: Thank you for believing in me as a student and as a person.

To Ian Rosenberg: Thank you for helping me learn how to do a Western blot, Southern blot, and everything in between. You are a truly gifted teacher.

To Brian Brannigan: Thank you for always making the time to help me troubleshoot my experiments and reminding that there is a solution to every problem.

To Emanuel Della Torre, Ezana Demissie, Carlos Donado, Kendra Taylor, and Kai Xin: Thank you for your insightful discussions and creating a fun lab atmosphere.

To Bobby Cherayil, Mo Motamedi, Miguel Rivera, and David Ting: Thank you for sharing your broad perspectives, constructive suggestions, and valuable advice.

To Dorothy Binford: Thank you for being my second mother.

To Khaleda Haider: Thank you for looking after the little things so that I could focus on the big ones.

To Raphael Sinclair: Thank you for your resourcefulness and reliability.

To Kathryn Pedrick and Patrick Hopkins: Thank you for your being there when I needed you the most.

To Diana Collins: Thank you for encouraging my nine-year-old self to think outside the box and following my journey to become a physician-scientist with enthusiasm and support.

To Venky Soundararajan: Your pep talks helped me overcome the most difficult times. I am grateful for your friendship.

To Ravi, my brother: I am proud of the person you have become. Thank you for always reminding me to enjoy life. Please don't stop!

To Chitra, my mother: Thank you for always encouraging me to reach for the stars and doing everything to help me get there… but keeping me grounded.

To Arun, my father: Thank you for never letting me give up. You are my best friend.

Table of Contents

Commonly used abbreviations

9-*O*-AcSia	9-*O*-acetylated sialic acid
CDP	Common dendritic cell progenitor
CDC	Conventional dendritic cell
CLP	Common lymphoid progenitor
CMP	Common myeloid progenitor
CMAH	CMP-Neu5Ac hydroxylase
HSC	Hematopoietic stem cell
IFN	Interferon
MDP	Macrophage-dendritic cell progenitor
Neu5Ac	*N*-acetyl neuraminic acid
Neu5Gc	*N*-glycolyl neuraminic acid
PBA	PBS and 0.2% bovine serum albumin
PDC	Plasmacytoid dendritic cell
PSA	Polysialic acid
Pre-cDC	Pre-conventional dendritic cell
Pre-pDC	Pre-plasmacytoid dendritic cell
Pro-pDC	Pro-plasmacytoid dendritic cell
Sia	Sialic acid
SIAE	Sialic acid acetyl esterase

Chapter One:

Introduction

In this introductory chapter I have provided background information on a number of topics that are relevant to the main thrust of this thesis. I discuss the biology of sialic acids with specific reference to the immune system, some specific modifications of sialic acids, and the enzymes that are responsible for these modifications. In addition, I provide background information regarding dendritic cells, with a focus on plasmacytoid dendritic cells.

Sialic acids and the immune system

Standard teaching of molecular and cellular biology still focuses on Crick's 1970 "central dogma" that "DNA makes RNA makes protein," rooted in descriptions of cells, membranes, and tissues (Crick, 1970). This gives budding scientists the impression that nucleic acids and proteins are the major constituents of living organisms. In fact, another major class of macromolecules was largely ignored during the recent molecular biology revolution, namely sugar chains or glycans (Sharon and Lis, 1982). Reasons for this omission were largely technical, as glycans are complex and relatively difficult to study. Modern advances in chemical biology, however, have enabled this class of molecules to emerge from historical obscurity, and we now appreciate their significance in all biological systems. Glycan biosynthesis is not template driven, is encoded only indirectly in the genome, and a range of variation in glycan structures can be found on any given glycosylation site on a given glycoprotein (Kornfeld R and Kornfeld S,

1985). Thus, a given protein encoded by a single gene can have multiple "glycoforms," which must be considered when interpreting the original "central dogma."

This thesis focuses on a specific modification of one class of sugars called sialic acids (Sias), which are typically found on all vertebrate cell surfaces at the outermost end of *N*- and *O*-linked glycans on membrane proteins and on glycosphingolipids, as well as on secreted glycoproteins (Varki A and Angata T, 2006). These acidic sugars are thus strategically poised to facilitate initial cellular interactions in the context of key physiological and pathological processes. While all Sias have a nine-carbon backbone with a carboxyl group at the 1-position, and form a linkage to the underlying sugar chain from the 2-position, great variation is superimposed on this core structure (Kelm and Schauer, 1997; Varki and Schauer, 2009). There are two major types of Sia, neuraminic acid or Neu (5 amino 3,5 dideoxy-*D-glycero-D-galacto*-2nonulosnic acid) and KDN (2-keto-3-deoxy-D-glycero-D-galacto-nononic acid) in which there is a hydroxyl group at the C5 position instead of the amino group in neuraminic acid (Varki and Gagneux, 2012). All currently recognized Sias are biosynthetically derived either from *N*-acetyl neuraminic acid (Neu5Ac) or from KDN. A major species of Sia in most vertebrates is *N*-glycolyl neuraminic acid or Neu5Gc. CMP-Neu5Ac is modified by the addition of an oxygen atom to the *N*-acetyl group, in a reaction catalyzed by an enzyme called CMP-Neu5Ac hydroxylase (CMAH) (Varki and Gagneux,

2012). This enzyme is found in most vertebrates, but exists in mutant form in humans (Varki, 2001). As a result, human glycans contain only Neu5Ac.

Beyond the above noted differences at the C5 position, multiple types of substitutions at the C4, 7, 8, and 9 positions (e.g., esterification with acetyl, lactyl, sulfate, or phosphate groups, or modification by methyl ethers), different α-linkages between C2 and the underlying structures (most commonly α2-3 or α2-6 to various sugars, or α2-8 to another Sia), and the nature of the underlying glycoconjugate (e.g., *N*-glycans or *O*-glycans on proteins, or glycan chains attached to lipids in gangliosides) all contribute to a hierarchical complexity that enables the diverse functions of Sias (Kelm and Schauer, 1997; Varki and Schauer, 2009; Angata and Varki, 2002; Troy, 1992). *O*-acetylation at the C-9 position of Sia is one of the most common modifications found on these sugars, but very little is known about its function (**Figure 1.1**). In the immune system, Sias are key components of intrinsic ligands for the selectin class of adhesion receptors and for members of the Siglec (sialic-acid-binding immunoglobulin-like lectins) family, which function as regulators of adhesion, cell signaling, and endocytosis (Crocker et al., 2007; Varki and Crocker, 2009; Pillai et al., 2012). A large number of Siglecs including Siglec-2/CD22, Siglec -6 and Siglec-10 among others in humans, and Siglec-2, Siglec-E, and Siglec-G among others in mice contain cytosolic ITIMs (immunoreceptor tyrosine based inhibitory motifs). The tyrosines in these motifs can be phosphorylated by Src family kinases allowing

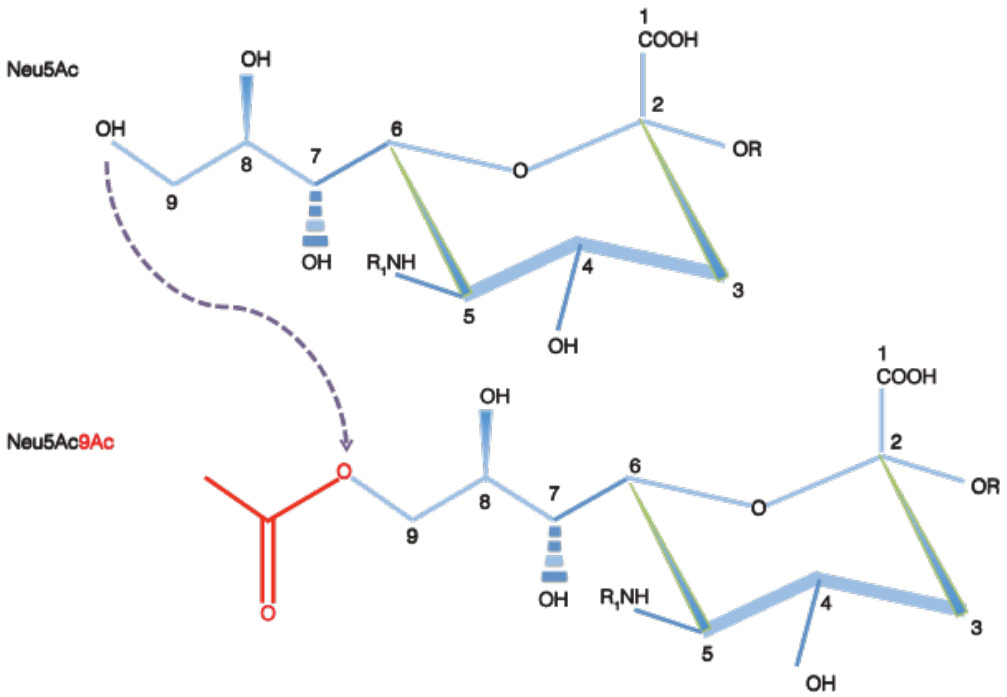

Figure 1.1. A schematic view of sialic acid structure. Sialic acids (Sias) are a family of sugars that decorate the termini of several cell surface glycoconjugates, including N-linked glycans chains on proteins, *O*-linked mucins, and glycosphingolipids. All class members are negatively charged and possess a nine-carbon backbone. The first numbered carbon atom is the carboxylic carbon. The remaining carbons form a ring (C-2 through C6) and an exocyclic side chain that includes C-7, C-8, and C-9. Even with several conserved features, a variety of linkages to the underlying sugar chain from the 2-position, and multiple types of substitutions at C-4, C-5, C-7, C-8, and C-9, combine to generate close to fifty family members. The most common modification of Sia is *O*-acetylation at the C-7 position; however at physiological extracellular pH, the ester group spontaneously migrates to the C-9 position. Thus, 9-*O*-acetylated Sias predominate on cell surface glycoconjugates.
(Upper panel) Neuraminic acid (Neu), the most commonly occurring Sia, has an amino group at the C-5 position that is N-acetylated to form N-acetyl neuraminic acid (Neu5Ac).
(Lower panel) *O*-acetylation of Neu5Ac at the 9-OH position.

them to recruit SH2 domain containing tyrosine phosphatases in order to dampen signaling in a range of hematopoietic cell types. Siglecs are therefore critical players in immune cell development and signaling.

The first immune cells in which 9-*O*-acetylation of Sia was described were $CD4^+$ T cells, although the functional role of this modification in these cells remains to be elucidated (Krishna and Varki, 1997). Recent work in our laboratory has shown that this modification also occurs in and regulates the development and function of B cells (Cariappa et al., 2009; Pillai et al, 2009). I chose to investigate whether 9-*O*-acetylation of Sia is also relevant in innate immune cells, with a specific focus on dendritic cells.

9-*O*-acetylation of Sia in T cells

As mentioned above, in addition to our investigation of 9-*O*-acetylation of Sia (9-*O*-AcSia) in B cells, the only other demonstration of this modification on immune cells has been in T cells. Work from Krishna et al., has established that 9-*O*AcSia is intricately regulated during murine T cell ontogeny and that the high density of Sia *O*-acetylation observed on $CD4^+$ T cells serves as a marker of maturation that is modulated downwards upon activation (Krishna and Varki, 1997). Analysis of Sia 9-*O*-acetylation patterns on thymocytes reveals some enrichment in the $CD4^-$ $CD8^-$ DN fraction, but the lowest levels are in the $CD4^+CD8^+$ DP cells. Thereafter, there is a progressive increase to the highest levels of Sia 9-*O*-

acetylation as cells mature from the DP stage through the $CD4^+$ SP stage. In contrast, the cells progressing towards the $CD8^+$ SP lineage show only a minimal increase, not reaching levels observed in the DN cells. Peripheral $CD4^+$ and $CD8^+$ T cells maintain these patterns of expression. Further biochemical analyses of the Sia-containing glyconjugates on these cells indicate that the 9-*O*-acetylation on $CD4^+$ T cells is predominantly on *O*-linked glycoproteins (mucins), and to a lesser degree, on sialylated glycolipids (gangliosides), while in $CD8^+$ T cells, only gangliosides are *O*-acetylated. Interestingly, activation by either anti-CD3 crosslinking or PMA/ionomycin reduces 9-*O*-acetylation in the mucin, but not the ganglioside fraction in $CD4^+$ T cells. The glycosylation patterns observed have not been linked mechanistically to specific T cell function. Taken in concert with our studies in B cells (described below), however, the association between the 9-*O*-acetyl modification of Sia and both development and activation of lymphocytes is evident.

Sialic acid acetyl esterase modulates BCR signaling and tolerance

Our laboratory has focused on how CD22 (Siglec-2), a prominent B cell Siglec, inhibits B cell receptor (BCR) signaling to set a threshold for B cell activation when it is bound to its ligands, that are N-glycans containing α2-6 linked Sia. A critical question was how such inhibitory signaling by CD22 is regulated. Because CD22 does not bind to 9-*O*-AcSia in vitro, we proposed that the function

of this Siglec might be modulated in vivo by the enzymatic acetylation and deacetylation of Sia (**Figure 1.2**; Sjoberg et al., 1994). Sialic acid acetyl esterase (SIAE) was molecularly characterized as an enzyme that removes acetyl groups from the 9-OH position of α2-6 linked Sia and was also identified as a gene that is upregulated during B cell maturation (Guimaraes et al., 1996; Stoddart et al., 1996). We therefore used mice with an engineered deletion of exon 2 of the *Siae* gene to investigate a permissive role for this enzyme to maintain CD22 ligands in an accessible deacetylated state, and thus serve as a novel catalytic regulator of B cell signaling (Cariappa et al., 2009). Our studies have established that in the absence of functional SIAE, BCR signaling in murine B cells is both enhanced and accelerated, as shown in calcium flux studies. *Siae*$^{-/-}$ mice have a major defect in the development of marginal zone B cells and a reduction in bone marrow perisinusoidal B cells, consistent with enhanced BCR signaling. The mice develop a lupus like syndrome suggesting a role for the Siglec/SIAE pathway in the maintenance of peripheral B cell tolerance (Cariappa et al., 2009; Pillai et al., 2009).

By re-sequencing the *SIAE* gene in a large number of subjects with autoimmunity and in controls, our laboratory established the importance of SIAE in human autoimmunity and the broader importance of rare genetic variants (as opposed to common variants studied by genome wide association studies) in the

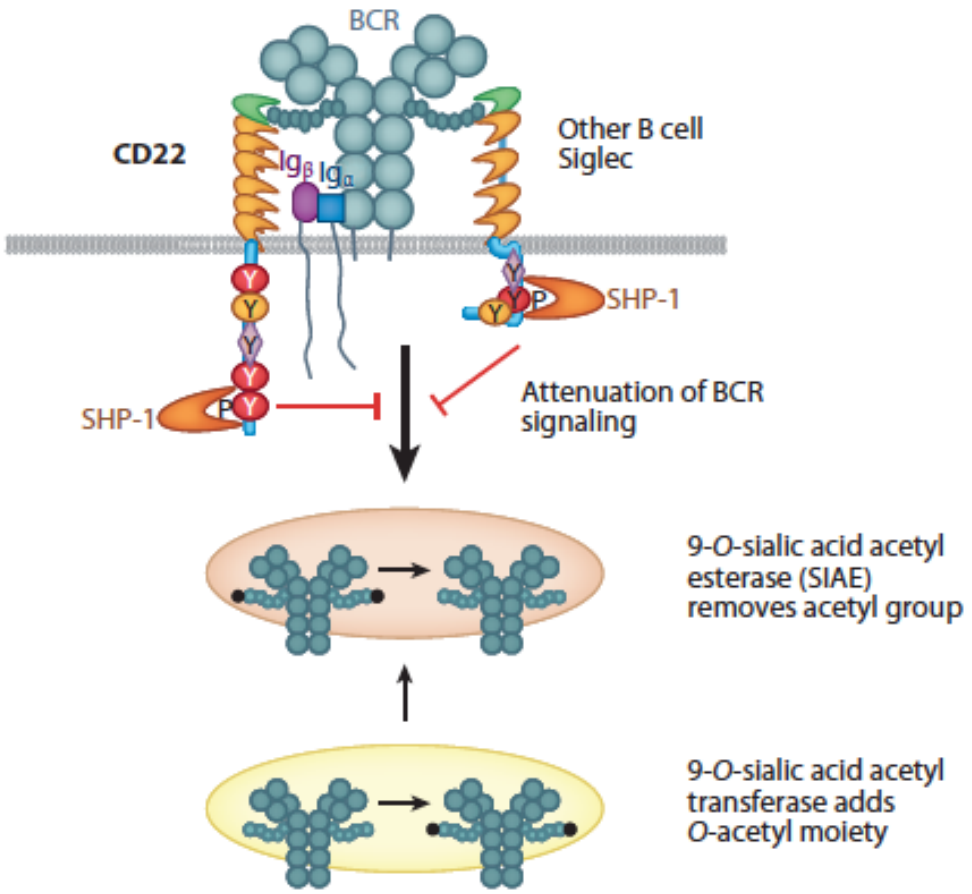

Figure 1.2. 9-*O*-acetylation of sialic acid regulates BCR signal strength. In this pathway CD22 and other Siglecs function to inhibit (B-cell receptor) BCR signaling. Although our bias is to consider the BCR a key source of Siglec binding *N*-glycans, other sialoglycoproteins may also function as CD22 ligands. Sialoglycoproteins are acetylated (black filled circles) on the 9-OH position of terminal α2-6 linked sialic acid moieties in the Golgi by sialic acid acetyltransferase (SIAT). In a post-Golgi compartment, a specific acetylesterase, SIAE, removes the acetyl moiety allowing ligation of CD22 and other Siglecs, thus facilitating ITIM tyrosine phosphorylation, SHP-1 recruitment, and BCR signal attenuation. The attenuation of BCR signaling by inhibitory receptors is crucial for the maintenance of peripheral B cell tolerance (Pillai et al., 2012).

pathogenesis of human autoimmune disorders (Surolia et al., 2010; Chellappa et al., 2013).

Apart from its role in B cells, SIAE and its regulation of 9-*O*-acetylation of Sia may be functionally relevant in effector cells of innate immunity as well as in dendritic cells.

Functional Roles for Sia in Dendritic Cells

Studies of sialylation patterns in dendritic cells are scarce. Preliminary investigation to uncover a role for glycosylation in conventional dendritic cells considered the unique ability of these cells to restore antigen-specific responses in T cells from mice with a point mutation in the MHC class-I H-2D^b gene. A pioneering study from Boog et al., utilized the class I H-2D^b mutant mouse strain bm14, in which female mice are unable to mount a CTL response against the male specific antigen HY, although females with a wild type H-2D^b molecule are competent (Boog et al., 1989). This group demonstrated that the use of conventional dendritic cells as APCs could overcome the defective response seen with total splenocytes, and intriguingly that removal of Sia by neuraminidase (NANAse) treatment could restore the ability of nonresponder bm14 APCs (e.g., total splenocytes) as well. Flow cytometric and biochemical analysis revealed that the superior efficiency of dendritic cells driven responses was due to not only quantitatively greater MHC expression on conventional dendritic cells, but a

qualitative difference: the presence of fewer Sias on MHC molecules on conventional dendritic cells versus other APC types. These studies signified that a generally low degree of sialylation on conventional dendritic cells enhances their APC function as compared to other innate immune cells, but the underlying basis for this phenomenon remains unclear and there is no evidence to suggest that altered sialylation on MHC molecules themselves alters APC function.

In the two decades since the initial suggestion that reduced Sia content contributed to conventional dendritic cells activation additional studies have spawned limited insight regarding the functional role of Sia in dendritic cells. The majority of these studies have used a combined approach of lectin binding assays and the analysis of sialyltransferases (ST) at the mRNA level to characterize changes in the sialome during human (monocyte-derived dendritic cell generation and maturation (Bax et al., 2007; Cabral et al., 2010; Crespo et al., 2009; Jenner et al., 2006; Stamatos et al., 2010; Stamatos et al., 2005; Videira et al., 2008). A key observation is that differentiation of monocyte-dendritic cells is accompanied by an increased expression of sialylated cell surface structures, specifically, α2-3-sialylated *O*-glycans and α2-6- and α2-3-sialylated *N*-glycans. Enhanced activity of three core STs are putatively responsible for this change: ST6Gal1 for α2-6-sialylated *N*-glycans; ST3Gal1 for α2-3-sialylation of *O*-glycans, particularly T antigens; and ST3Gal4 for the increased α2-3-sialylated *N*-glycans (Bax et al., 2007; Jenner et al., 2006; Videira et al., 2008). Recent HPLC

studies have verified that monocyte-dendritic cells contain a greater amount of Sia than monocytes, but have also uncovered that the amount of Sia/mg total protein declines during differentiation to dendritic cells (Stamatos et al., 2010). This finding may be linked to substrate specificity of the sialidases (Neu1 and Neu3) that show a corresponding increase in protein expression during the differentiation process. The Sia patterns that decorate dendritic cell surfaces are clearly complex.

Moreover, these patterns are far from static, as upon cytokine (e.g., IL-1 & TNF-α) and TLR (e.g., LPS) induced monocyte-dendritic cell activation, relative hyposialylation characterized by a selective reduction in α2-6-linked, but unchanged levels of α2-3-linked, Sia is observed (Jenner et al., 2006). The associated decrease in ST6Gal1 and ST3Gal4 transcripts, but intensified ST3Gal1 expression is a potential explanation for these trends, but fall short of providing a complete picture (Videira et al., 2008). Conversely, sialidase (neuraminidase)-treatment of monocyte-dendritic cells that nonspecifically strips off all Sia species provokes conventional dendritic cell maturation, as exhibited by reduced endocytic capacity, enhanced expression of MHC and costimulatory molecules, and increased transcription of proinflammatory and Th1-promoting cytokines (Crespo et al., 2009; Videira et al., 2008). The "naked" conventional dendritic cells also induce greater T cell proliferation in mixed leukocyte reactions. Of note, however, is a recent independent report that demonstrates an increase in α2-

8-linked polysialic acid (polySia) and in corresponding ST8Gal4 activity in LPS-stimulated monocyte-dendritic cells. This polySia in mature monocyte-dendritic cells enhances CCR7-mediated chemotaxis (Bax et al., 2009). Specifically, the polysialylation serves as a posttranslational modification of neuropilin (NRP2) that enables the interaction of the *O*-glycan on this plasma membrane glycoprotein with the C-terminal domain of CCL21 (Rey-Gallardo et al., 2011; Rey-Gallardo et al., 2010). In this model, polySia-NRP2 may trap CCL21 to increase local chemokine concentration or facilitate optimal CCL21-CCR7 docking. The conclusion that monocyte-dendritic cells activation is accompanied by a straightforward reduction in sialylation is perhaps an oversimplification. Still, the majority of outcomes from these in vitro experiments begged a further investigation to establish if the reduction of a particular type of sialylation is involved in the conventional dendritic cell activation process in vivo.

To correlate a linkage-specific sialylation deficiency with triggering of dendritic cell maturation, Crespo et al., considered the findings regarding STs described above, and chose to examine ex vivo splenic dendritic cells from *ST3GalI*$^{-/-}$ and *ST6Gal1*$^{-/-}$ mice (Crespo et al., 2009). Analysis of maturation markers revealed an expected increase of MHC II in total dendritic cells from only *ST6Gal1*$^{-/-}$ animals, but closer inspection revealed this change to originate exclusively in plasmacytoid dendritic cells. In addition, a percentage increase in total DCs in *ST3GalI*$^{-/-}$ mice was due solely to an expanded plasmacytoid

dendritic cell compartment. Since the in vitro work described above used IL-4 and GM-CSF cytokine cocktails suited exclusively to conventional dendritic cell and not to plasmacytoid dendritic cell generation, the lack of significant changes in cDCs from the mouse models was unexpected. The findings nonetheless suggest that Sia linkages mediated by certain STs are functionally distinct in dendritic cells and influence dendritic cell immunogenicity, perhaps most meaningfully in plasmacytoid dendritic cell subsets in vivo.

Deliberate interrogation of linkage-specific sialylation patterns on plasmacytoid dendritic cells has not previously been undertaken, and it follows that any potential modification of Sia, including 9-*O*-acetylation have not been considered.

Reagents for detection of *O*-acetylated Sia

Cell surface detection of 9-*O*-AcSia is achieved with a fusion protein containing the Fc portion of human IgG and the influenza C hemagglutinin esterase treated with diisopropylfluorophosphate (DFP). Modification of the catalytic serine nucleophile in this fusion protein by DFP permits the viral protein to bind to 9-*O*-AcSia, but not to cleave it (Klein et al., 1994; Krishna and Varki, 1997). This well-established reagent, designated CHE-FcD **(Figure 1.3)**, is used in concert with flow cytometric analysis as part of the ex vivo staining data presented in this thesis.

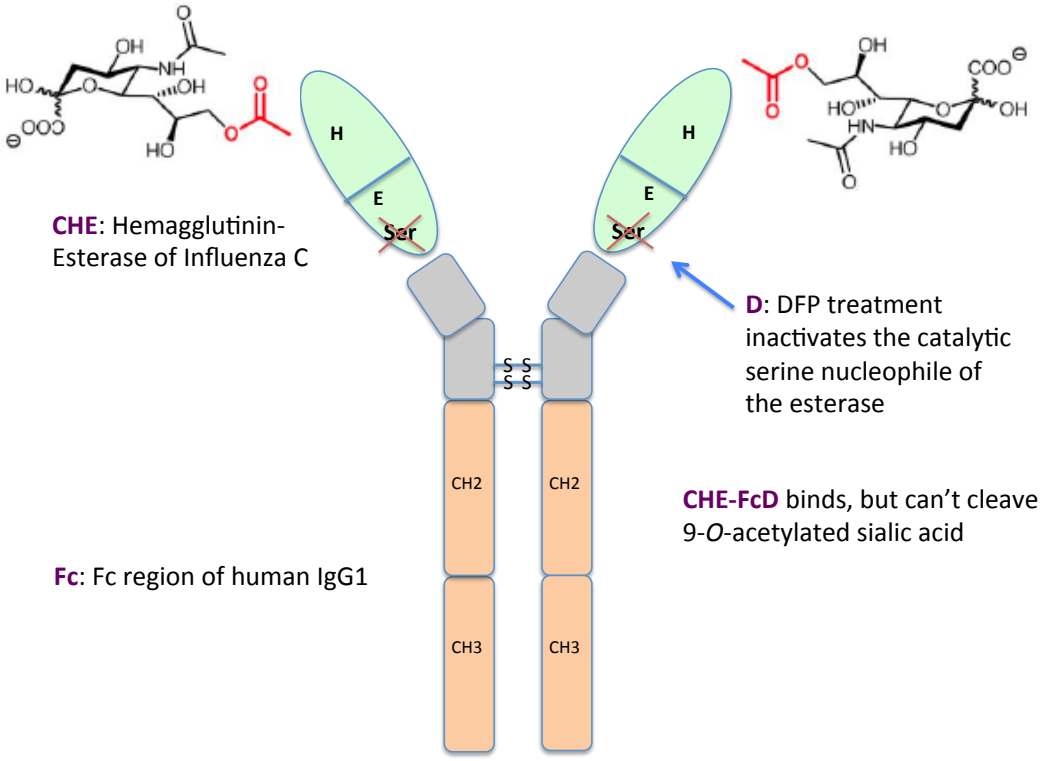

Figure 1.3. CHE-FcD is a highly specific tool to detect 9-*O*-acetylated sialic acid. CHE-FcD is a chimeric Fc-fusion protein that uses the hemagluttinin activity of the influenza C virus to bind to 9-*O*-acetylated sialic acid. To enhance binding, the viral esterase, which cleaves the 9-*O*-acetyl moiety from sialic acid, is inactivated by treatment with diisopropyl fluorophosphate (DFP). DFP inactivates the catalytic serine nucleophile of the esterase. CHE-FcD can be used in combination with an appropriate flurochrome-conjugated secondary antibody on flow cytometry assays and serves as a robust method to detect cell surface levels of 9-*O*-acetylated sialic acid.

Several studies have contributed to establishing the specificity of CHE-FcD for 9-*O*-AcSia (Herrler et al., 1985; Rogers et al., 1986; Muchmore and Varki, 1987; Vlasak et al., 1989; Zimmer et al., 1992; Klein et al., 1994). Human RBCs whose surfaces are decorated only by Sias lacking *O*-acetylation were not agglutinated by influenza C hemagglutinin in their native state, but became agglutinable when desialyated and then enzymatically modified to terminate in 9-*O*-AcSia (Rogers et al., 1986). Importantly, this agglutination occurred regardless of the linkage (α2-3, α2-6, or α2-8) between 9-*O*-AcSia and the underlying glycan. In contrast to influenza C, the host cell determinants engaged by influenza A and B hemagglutinins are Sias (in specific linkages) that lack *O*-acetylation. In line with this data, influenza C pretreatment of human RBCs that were modified to contain only 9-*O*-AcSia enabled subsequent agglutination with influenza A and B (in accordance with their linkage specificities) and simultaneously prevented agglutination with influenza C. These results were due to the esterase activity of influenza C that removed the 9-*O*-acetyl moieties from Sia. In a similar study, prior incubation of influenza C with bovine submaxillary mucin and rat serum glycoproteins that are abundant in 9-*O*-AcSia drastically reduced its hemagglutination abilities (Herrler et al., 1985).

Experiments utilizing CHE-Fc, in which DFP treatment has not been administered and acetylesterase activity is intact have also helped demonstrate the specificity of CHE-FcD. Prior *O*-deacetylation by CHE-Fc abolished staining of

CHE-FcD on Western blots of rat serum glycoproteins and prevented CHE-FcD detection of 9-*O*-acetylated gangliosides from human melanoma cell lines on lipid thin layer chromatography overlay assays (Klein et al., 1994). Our own flow cytometric analysis of murine cells presented in Chapter 2 demonstrates that CHE-FcD detection of 9-*O*-AcSia is abolished by prior incubation of the cells with CHE-Fc. It should be noted that other viral hemagglutinin esterases, including the protein from bovine coronaviruses, have been used by others to detect *O*-acetylated Sia (Zeng et al., 2008).

Salient features of plasmacytoid dendritic cells

DCs play critical roles in immunity because of their ability to recognize invading pathogens and mobilize multiple immune cell types to combat them. Conventional DCs (cDCs) efficiently detect and present foreign antigens to antigen-specific T lymphocytes in the context of major histocompatibility (MHC) molecules. On the other hand, plasmacytoid DCs (pDCs) represent a distinct DC type specialized for rapid secretion of type I interferons (type I interferons in humans include include 13 variants of interferon-α, two of interferon-β. as well as one each of interferon-κ and -ω) in response to viruses (Asselin-Paturel and Trinchieri, 2005; Barchet et al., 2005; Cao and Liu, 2007). The resulting type I interferons (IFNs) act both directly to block viral replication and as an adjuvant to activate multiple immune cell types. In particular, pDCs efficiently suppress HIV

replication, and their infection and eventual depletion contributes to immunodeficiency caused by HIV (Meyers et al., 2007). Conversely, persistent activation of pDCs causes elevated IFN levels in autoimmune diseases such as lupus and psoriasis (Banchereau and Pascual, 2006). In both conditions, aberrant activation of PDCs by complexes of self-DNA has been demonstrated (Lande et al., 2007). Thus, pDCs are primary type I IFN-producing cells that play central roles both in protective antiviral responses and in immunopathology.

pDCs express a combination of Toll-like receptors (TLRs) including TLR7/8 and TLR9, allowing the recognition of virus associated nucleic acids such as single-stranded RNA and unmethylated CpG-containing DNA (CpG), respectively. After TLR-mediated virus recognition, pDCs produce IFN and other cytokines and appear to differentiate into activated cDCs through poorly understood mechanisms. The secretion of IFN by pDCs is characterized by rapid kinetics, high level (up to 1000-fold higher than most cell types), and broad spectrum of IFN types (α and β). This is facilitated by multiple mechanisms, including high secretory capacity reflected in "plasmacytoid" secretory morphology resembling antibody-secreting plasma cells; high basal expression of IRF7, a key transcriptional regulator of the IFN response; and prolonged retention of TLR ligands in early endosomes (Honda et al., 2005; Barchet et al., 2002). In addition, pDCs specifically express several unique receptors that modulate type I IFN production, including human BDCA-2/CD303 and ILT7 and murine Siglec-

H (Gilliet et al., 2008). Thus, the unique functional properties of pDCs are reflected in their distinct cellular features and specific gene expression program.

Lineage-defining inhibitory receptors in murine pDCs

A notable feature of pDCs is that multiple cell-type specific membrane proteins used in their identification also inhibit their function. In light of the potential danger of unchecked type I IFN secretion, the teleological rationale for such tight control is clear. Receptors in this category include murine Siglec-H and human BDCA-2 and ILT7. These human inhibitory receptors signal through ITAM motifs of DAP12 or FCεRIγ, respectively, and converge on a BCR-like pathway that involves SRC family protein tyrosine kinases, Syk, and the B-cell-specific adaptors BLNK (B-cell linker) and BCAP (B-cell adaptor) (Blasius and Colonna, 2006; Gilliet et al., 2008). This ITAM-mediated pathway potently inhibits type I IFN and proinflammatory cytokine (e.g., IL-6, TNF-α) production by pDCs in response to TLR7/9 activation (Cao et al., 2006; Cao et al., 2007). While the mechanism of attenuation remains unknown, evidence to support the proposal that ITAM-associated "activating" receptors dampen pDC responses is emerging (Pillai et al., 2012).

Siglec-H is a specific marker for murine pDCs, although a human homolog has not been identified. Unlike for other members of this lectin family, binding to Sia has not been demonstrated for Siglec-H and its in vivo ligand

remains unknown (Blasius et al., 2004; Blasius et al., 2006a; Blasius and Colonna, 2006; Zhang et al., 2006). In addition, this Siglec lacks its own cytoplasmic signaling domain, and instead requires association with a DAP12 homodimer (that contains ITAM motifs) for transport to the cell surface (Blasius et al., 2006a). Antibody cross-linking of Siglec-H on murine pDCs attenuates TLR9 induced type I IFN synthesis and secretion and a role for Siglec-H as a negative regulator of pDC function has been proposed (Blasius et al., 2004). A mechanism for this inhibition may involve signaling through DAP12 ITAMs, and it was demonstrated that pDCs from DAP12-deficient mice produce increased levels of IFN-α in response to TLR9 activation, presumably because of defective Siglec-H function (Blasius et al., 2006a). Most recently, the functions of Siglec-H have been examined using a gene targeting approach demonstrating an in vivo negative regulatory role for Siglec-H in TLR-mediated type I IFN and IL-12 production (Takagi et al, 2011).

Recently, murine pDCs have been divided into two functionally distinct subsets. One subset expresses the CD9 tetraspannin and low (but clearly discernible levels) of Siglec-H (Bjorck et al., 2011). This subset secretes large amounts of type I IFN following stimulation with TLR-7/8 or -9 agonists, induces CTL activation, and generates protective anti-tumor immunity. A second pDC subset does not express CD9, expresses high levels of Siglec-H, and secretes

negligible levels of type I IFN. This subset can contribute to the generation of antigen-specific Foxp3 Tregs, and is inefficient at inducing anti-tumor immunity.

In addition to the role of Siglec-H, insight into negative regulation of murine pDC function has been revealed through the identification of BST2 (PDCA-1) as a ligand of human ILT7 (Cao et al., 2009). PDCA-1 is an IFN-inducible membrane protein that directly restricts viral replication; thus, its expression provides negative feedback to pDCs by confirming a successful type I IFN signal. Interestingly, murine pDCs lack an ILT7 ortholog, but instead specifically express PDCA-1 (Blasius et al., 2006b). Moreover, as demonstrated for Siglec-H, antibody cross-linking of PDCA-1 on mouse pDCs reduces secretion of IFN-α in response to CpG, fueling the suggestion that it functions as a modulator of IFN release (Blasius et al., 2006b). An additional role for PDCA-1 in blocking viral spread has also been proposed. This view stems from the recent demonstration that PDCA-1 inhibits the release of HIV-1 and other viruses from infected cells and that several viruses have evolved mechanisms to counteract its antiviral activity (Jouvenet et al., 2009; Neil et al., 2008; Van Damme et al., 2008). For example, the HIV genome encodes a viral accessory protein, Vpu, which antagonizes PDCA-1 and downregulates its surface expression (Neil et al., 2008; Van Damme et al., 2008; Miyagi et al., 2009). Thus, pDC-specific constitutive expression of PDCA-1 may help retain viruses at sites where they are

easily degraded or in endosomes where they can be sensed by TLRs, and drive pDC synthesis of type I IFN.

Cellular origins of pDCs

Although pDCs clearly represent a distinct hematopoietic cell lineage, the molecular and cellular bases for their development are poorly understood (**Figure 1.4**). A major stride was taken, however, when independent work from the Manz and Shortman labs identified a common dendritic cell progenitor (CDP) in the bone marrow (BM) with both pDC and cDC differentiation capacity, that lacked alternative developmental options (Naik et al., 2007; Onai et al., 2007). In isolating a common DC precursor, the two groups predicted, quite judiciously, that such a cell would be present in the BM in the steady state, and would possess two key properties:

The first predicted property was that a DC precursor should respond to the cytokine, Flt3 ligand (Flt3L), and also have high expression of its receptor, fms-like tyrosine kinase 3 (Flt3). This prediction was based on in vitro and in vivo evidence that implicates the Flt3-Flt3L pathway in the development and maintenance of lymphoid organ DCs in a nonredundant way. Supplementation of BM cultures with Flt3L singularly drives differentiation of pDCs and cDCs (Brawand et al., 2002; Gilliet et al., 2002; McKenna et al., 2000).

In addition, $Flt3L^{-/-}$ mice, as well as mice in which STAT3 (a transcription

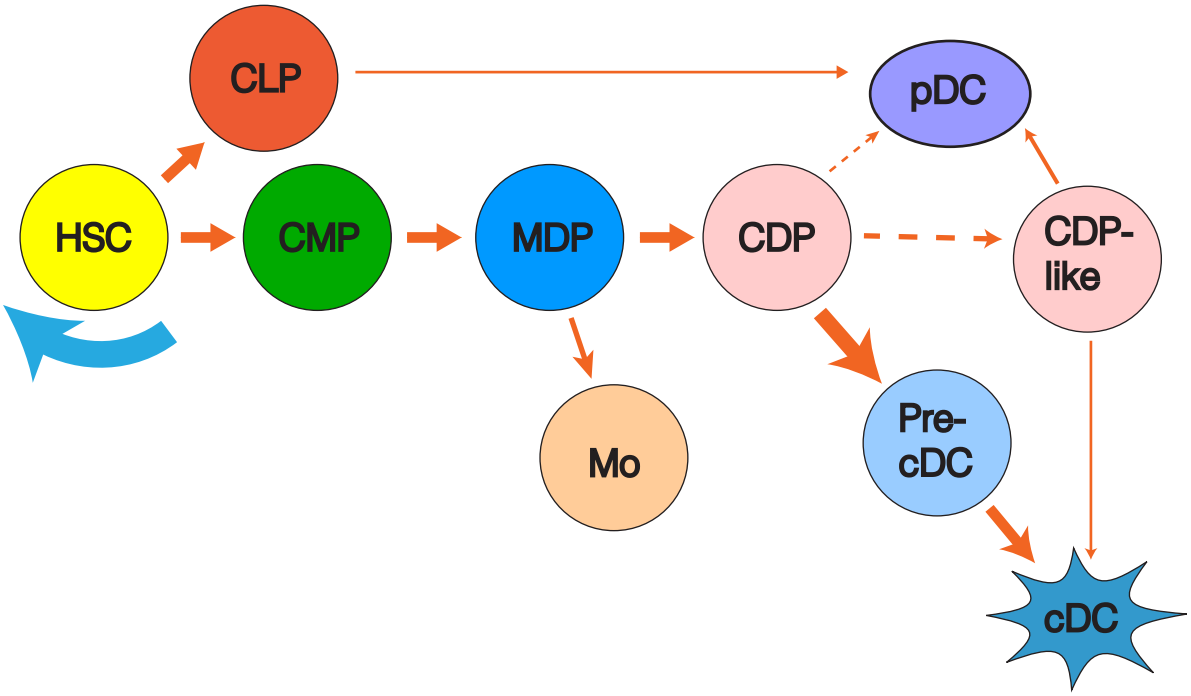

Figure 1.4. A current model for pDC development in the bone marrow. The pathway for conventional dendritic cell (cDC), but not plasmacytoid dendritic cell (pDC), development is well understood. Common myeloid progenitors (CMPs) give rise to macrophage-dendritic cell progenitors (MDPs) that further differentiate into monocytes (Mos) or common dendritic cell progenitors (CDPs). CDPs are restricted to develop only into DCs, but are far more effective at generating cDCs versus pDCs. A precursor committed to cDC development (Pre-cDC) has been identified downstream of the CDP. CDP-like cells have a phenotype very similar to that of CDPs and may originate from CDPs. Like CDPs, CDP-like cells have greater cDC versus pDC potential. Common lymphoid progenitors (CLPs) also give rise to pDCs. Hematopoietic stem cells (HSCs) have significantly greater pDC developmental capacity than any other defined progenitor pool and the identity of a committed pDC progenitor remains unknown.

factor relevant in signaling downstream of Flt3) was deleted in hematopoietic cells, and also mice treated with Flt3 kinase inhibitors all show marked reductions in the pDC and cDC compartments, approaching 10% of the absolute numbers of these cells in their untreated counterparts (Brawand et al., 2002; Gilliet et al., 2002; McKenna et al., 2000; Laouar et al., 2003; Tussiwand et al., 2005). Conversely, Flt3L injection increases pDCs and cDCs, and enforced expression of Flt3 in both $Flt3^-$ and $Flt3^+$ BM progenitors restores and enhances their in vitro and in vivo development into pDCs and cDCs (Karsunky et al., 2003; Maraskovsky et al., 1996; Miller et al., 2003). Furthermore, all steady-state spleen DC subtypes, but no other mature hematopoietic cell population, express Flt3 (Karsunky et al., 2003).

The second property was that a DC precursor should arise downstream of the common lymphoid and myeloid progenitors (CLPs and CMPs, respectively) and progressively become restricted to the DC lineage. This prediction stemmed from studies in which the $Flt3^+$ fraction of the CMPs and CLPs were both able to efficiently give rise to cDCs and pDCs in vitro and in vivo (D'Amico and Wu, 2003; Karsunky et al., 2003).

The above considerations translated into searching the Lin^-c-$kit^{int/+}Flt3^+$ cells of the murine bone marrow that would lack markers of mature cell types (Lin^-), including those with broad developmental potential (c-$kit^{int/+}$), and enriching for proficient DC generation capacity ($Flt3^+$), in order to identify the

restricted DC progenitor. Since Flt3 also supports the development of other hematopoietic lineages, Onai et al., also looked for other relevant DC commitment-defining cytokine receptors (Onai et al., 2007). The best candidate to emerge was M-CSFR (also a receptor tyrosine kinase), given its expression on both pDCs and cDCs, and also because M-CSFR$^+$ human bone marrow progenitor cells have the ability to differentiate into pDCs (MacDonald et al., 2005; Olweus et al., 1997). Their strategy of phenotypic expression analysis enabled identification of a CDP that was Lin$^-$Sca-1$^-$c-Kit^{lo}Flt3$^+$M-CSFR$^+$ that accounted for 0.1% of BM nucleated cells. Limiting-dilution analysis demonstrated that single-sorted CDP clones could give rise to CD11c$^+$ pDCs and cDCs in Flt3L$^+$ supplemented cultures; additionally, these cells lacked significant myeloid, erythroid, or lymphoid (pre-B) differentiation potential in permissive *in vitro* colony-forming assays. Most convincingly, CDPs that were transferred into unirradiated recipient mice expanded and differentiated into both CD11c$^+$PDCA-1$^+$ pDCs and CD11c$^+$PDCA-1$^-$ cDCs, and even in animals treated with Flt3L, in which absolute numbers of DCs increased, other cell lineages were not detected, confirming exclusive in vivo DC reconstitution potential.

Naik and colleagues identified the CDP independently with a different approach using Flt3-supplemented BM cultures to seek out putative DC precursors (Naik et al., 2007). An initial observation was that total numbers of viable cells dropped over the first 3 days of culture and then increased over the

ensuing 5 days to yield only DCs (as expected). The group therefore labeled bone marrow cells prior to culture with CFSE, and reasoned that selection of CFSE-low dividing cells shortly after day 3 would enrich for DC progenitors. Purification steps to exclude dead cells and those bearing lineage markers, followed by an in vitro evaluation of the DC generation capacity of the remaining fractions led to identification of the CDP with a phenotype akin to the cell isolated by the Manz group (Onai et al., 2007). Elegant clonal assays were used to track progeny of single-sorted fluorescent CDPs from BM of UBC-GFP mice, which express GFP under control of the ubiquitin c promoter. These corroborated the finding of Onai et al., that CDPs were exclusive pDC and cDC precursors. Additional adoptive transfer experiments confirmed their developmental proficiency in vivo (Naik et al., 2007; Onai et al., 2007).

These experiments provided clear support of the CDP as a restricted DC precursor, and other evidence in support of this claim has since emerged. M-CSF addition has been shown to drive pDC and cDC development in $Flt3L^{-/-}$ mice and op/op mice that lack M-CSF exhibit reduced numbers of DCs (Dai et al., 2002; Fancke et al., 2008). In addition, the even more upstream macrophage/DC progenitor (MDP) that was originally thought to give rise to monocytes, macrophages, and cDCs, has recently been confirmed to have CDP and even pDC potential (Auffray et al., 2009; Liu et al., 2009). These adoptive transfer studies made use of *LysM-CrexRosa26-StopfloxEGFP* mice, in which monocytes and

their progeny are irreversibly marked with EGFP expression (because lysozyme promoter-driven Cre expression leads to deletion of the Stop sequence from *Rosa26-StopfloxEGFP*) to confirm a point of divergence between monocyte and DC lineage (Liu et al., 2009; Jakubzick et al., 2008). In contrast to bone marrow and blood monocytes and their progeny, MDPs, CDPs, cDCs, and pDCs did not express EGFP and therefore never traversed a monocyte intermediate (Liu et al., 2009). Thus, monocytes separate from the DC lineage during the transition from MDPs to CDPs. Nonetheless, the progressive differentiation of early myeloid progenitors to MDPs and then to CDPs appeared to represent a major cellular source of DC development, especially for cDCs, although the identity of the committed steady-state pDC progenitor in the bone marrow was still unclear.

Characterization of the CDP, however, indicated that pre-commitment to either the cDC or pDC lineage may already exist among some members of this pool. The in vitro assays carried out by both the Manz and Shortman groups to analyze clones derived from a single CDP yielded interesting results: some clones contained both $CD8\alpha^-$ and $CD8\alpha^+$ cDCs and pDCs, others comprised both types or one type of cDC only, and another group pDCs only (Naik et al., 2007; Onai et al., 2009).

In complementary assays, Naik et al., used their GFP-labeling strategy to check if single-sorted developmentally "upstream" LSK ($Lin^-Sca\text{-}1^+c\text{-}Kit^+$) hematopoietic stem cells (HSCs) were able to give rise to all DC subtypes. While

the proportion of DC clones containing all DC subtypes was much higher from these earlier precursors cells than from CDPs, some clones were still restricted to particular DC types. Importantly, the LSK HSCs gave rise to 10-fold more pDC-restricted clones, but significantly fewer clones limited to either of the cDC subtypes, compared to those derived from CDPs in which cDC-only clones far outnumbered both cDC/pDC-clones and pDC-only clones, the latter being the least represented (Naik et al., 2007). It appears then, that some commitment to DC subtypes, particularly to pDCs, occurs at a significantly earlier developmental stage than the CDP. This possibility is supported by certain in vivo adoptive transfer studies that have demonstrated that the highest yield of pDCs is obtained from the LSK fraction of HSCs, compared to generation from even $Flt3^+$ CLPs or CMPs (Pelayo et al., 2005).

Several investigations have raised doubts regarding the contribution of CDPs to the pDC pool. CDPs have been demonstrated to derive from CMPs and to give rise to committed precursors of cDCs (pre-cDCs) that lack pDC potential; similar attempts to isolate a committed steady-state pDC progenitor downstream of the pDC have been unsuccessful (Naik et al., 2006; Liu et al., 2009). Instead, CDPs give rise to BM $CD11c^+PDCA\text{-}1^+$ precursor cells that lack CCR9, a marker found on mature pDCs (Schlitzer et al., 2011; Schlitzer et al., 2012). These $CCR9^-$ pDC-like cells differentiate into mature $CCR9^+$ pDCs, but also into cDCs, and at a pDC:cDC ratio similar to that of CDPs. In addition, a lineage tracing

study that examined the expression history of DNGR1 suggests that CDPs are largely cDC-restricted precursors, lacking pDC potential (Schraml et al., 2013). It is also possible that the reported pDC potential of CDPs may reflect the presence of a small subset of pDC committed cells in this heterogeneous but cDC biased progenitor pool. The expression of Siglec-H, considered to be a unique pDC lineage marker, has been described recently on a fraction of CDPs and pre-cDCs that are committed to cDC development (Satpathy et al., 2012). These Siglec-H^{+} CDPs may represent contaminant pDCs or their progenitors that contribute to the small pDC potential observed in the original studies describing CDPs (Naik et al., 2007; Onai et al., 2007).

The low yield of pDCs from CDPs prompted a search for additional pDC precursors down the myeloid route. In a recent study, Onai et al. focused on cells that differ from conventional CDPs by their lack of M-CSFR expression (Onai et al., 2013). These M-$CSFR^{-}$ cells had greater pDC potential than CDPs, but still maintained significant cDC potential (about 50% of the M-$CSFR^{-}$-derived cells were cDCs). In line with the latter result, in vivo transfers suggested that these progenitors derive from a fraction of CDPs that downregulates M-CSFR expression and demonstrate that they are as effective as CDPs at generating the $CCR9^{-}$ precursors that maintain pDC and cDC differentiation capacity.

It may be that the widely accepted reductionist model of hematopoiesis originally set forth by Weissman and colleagues, in which all cells of the myeloid

lineage arise from committed CMPs and those of the lymphoid lineage from committed CLPs, may not be applicable to dendropoeisis (Reya et al., 2001). Successful characterization of committed pDC progenitors, specifically, may necessitate debunking this paradigm and acknowledging the existence of broader developmental plasticity among progenitor cells. In fact, multiple reports support this approach. Recent work from Allman's group demonstrated that estrogen treatment that depletes lymphoid progenitors does not affect pDCs (Harman et al., 2006). While a primary interpretation is that the latter develop largely from non-lymphoid cell sources, crucial insight was obtained by dissecting the identity of the specific pDC progenitors in this context. The investigators used Rag2/GFP knockin mice to demonstrate that a fraction of estrogen-resistant CMPs was also Rag2/GFP^{+}, and that these cells were more effective in generating pDCs (and less efficient in producing myeloid cells) than their Rag2/GFP^{-} counterparts (or CLPs) in competitive BM chimeras. In addition, the Rag2/GFP^{+}, but not Rag2/GFP^{-} CMPs were characterized by low-level expression of TdT (terminal deoxynucleotidyl transferase) and sterile IgH (μ_0), and transcripts for each of these were also detected in BM pDCs (Harman et al., 2006). Thus, it appears that certain lymphoid-associated genes are ectopically activated within pDC-biased members of the conventionally defined CMP pool.

The view that pDCs express lymphoid genes as a conserved part of their cellular development is not without precedence. Corcoran et al., have

independently demonstrated that pDCs from murine spleen, but not cDCs, express mRNA for CD3ε and pre-Tα, indicative of a past T lineage relationship, and contain D-J rearrangements of IgH genes as in indelible clonal marker of past lymphoid origin (Corcoran et al., 2003). Work from Akashi's laboratory extended these findings to show that pDCs were the only cells that activated murine RAG1 knockin reporters outside the lymphoid lineage and that RAG transcripts were found in 30% of both myeloid- and lymphoid-derived pDCs (Shigematsu et al., 2004). Pelayo et al. demonstrated that the pDCs in RAG1/GFP knock-in mice could be subdivided, and D_H-J_H rearrangements, as well as transcripts for the B-lineage-related genes *Pax5*, *mb1/CD79a*, *ebf*, and *Bcl11a*, were identified only in the GFP^+ pDC subset (Pelayo et al., 2005). All pDCs expressed TdT as well as TLR9, although IFNα production in response to CpG stimulation was greater in the GFP^- pDCs. Recent work from Kincade's group, however, used a *RAG1-CrexRosa26-StopfloxtdRFP* mice to mark all cells with a history of RAG1 expression and confirmed that while a substantial subset of pDCs express RAG1, CDPs are uniformly *Rag1*-negative (Welner et al., 2009). Interestingly, while CLPs in this system were heterogeneous for RAG1 expression, both subsets could give rise to pDCs in culture, although CDPs were never detected in these differentiation experiments. It thus appears that classical CLPs do not pass through a CDP stage en route to pDCs and commitment to the

pDC lineage may include the establishment of promiscuous lymphoid gene expression.

Taken together, the data suggests that a bonafide pDC restricted precursor may emerge from the asynchronous, stochastic activation and implementation of discrete transcriptional regulatory circuits within a broad spectrum of HSC-proximal progenitors.

PDC to cDC conversion

Multiple studies support the notion that pDCs can undergo a full transformation into cDCs. pDCs were originally described as efficient type 2 precursors of cDCs from human peripheral blood (Grouard et al., 1997). Indeed, mature human pDCs cultured with cytokines and/or activation stimuli (e.g., IL-3, CD40L, viruses, TLR ligands) exhibit full phenotypic and functional differentiation to cDCs (Soumelis and Liu, 2006). Although this provides a proof of principle for pDC-to-cDC conversion, evidence for this event in vivo has been scarce. Lindstedt et al. characterized human DC populations in resected tonsils and in the peripheral blood (Lindstedt et al., 2005). Notably, the tonsils appear to contain a minor intermediate population between $CD123^+$ pDCs and BDCA-3^+ cDCs; moreover, increased expression of pDC-specific genes was observed in BDCA-3^+ cDCs from the tonsils. These results may reflect ongoing pDC differentiation into BDCA-3^+ cDCs, the human counterpart of mouse $CD8\alpha^+$ cDCs, at the site of

active chronic infection. In mice, phenotypic changes consistent with $CD8\alpha^+$ cDC differentiation (including loss of B220, and increase in CD11c and CD8α) have been described in adoptively transferred splenic pDCs 10 hrs after injection of recipients with inactivated influenza virus (O'Keeffe et al., 2002). Of note, the pDC purification scheme used at the time ($CD11c^+B220^+$) lacked specific pDC markers (Siglec-H or PDCA-1), and likely included other cell types, such as the recently described $CD11c^+B220^+CCR9^-$ cDC precursors unrelated to pDCs (Segura et al., 2009).

Subsequently, Zuniga and colleagues have provided a compelling case for IFN-dependent pDC conversion to $CD8\alpha^-$ ($CD11b^+$) cDCs following lymphocytic choriomeningitis virus (LCMV) infection in vitro and in vivo (Liou et al., 2008; Zuniga et al., 2004). In a series of adoptive transfer experiments, BM pDCs from LCMV infected animals ($CD45.2^+$) were transferred into congenic naïve recipients ($CD45.1^+$) where they generated $CD11b^+$ cDCs ($CD45.2^+$). These pDC-derived DCs exhibited similar morphology (characteristic dendrites), and increased expression of CD11c, costimulatory molecules (B7.1 and B7.2), and MHC class II, as the $CD11b^+$ cDCs of recipient origin. Importantly, only BM pDCs, but not those from the spleen, were capable of such conversion, suggesting that fully mature peripheral pDCs have lost this capacity (Liou et al., 2008). The same group also addressed whether type I IFNs are involved during the in vivo conversion. Interestingly, when pDCs from LCMV-infected IFN-αβ receptor

knockout mice were used in similar transfer experiments, conversion to $CD11b^+$ cDCs could not be detected. This result implies an important role for a type I IFN signal in "reprogramming" of pDCs in vivo.

In addition, elegant experiments demonstrated that the pDC-derived $CD11b^+$ cDCs were able to prime LCMV-specific T cells in vivo to a similar extent as endogenous $CD11b^+$ cDCs from LCMV-infected mice. $Thy1.1^+$, TCR transgenic CD8 T cells (P14-Thy1.1) specific for the LCMV GP_{33-41} epitope presented in the context of $H\text{-}2D^b$ were labeled with CFSE and transferred into C57BL/6 $D^{b-/-}$ ($Thy1.2^+$) mice. Twenty-four hours later, DCs from LCMV infected wild type mice were transferred into the same $D^{b-/-}$ mice. Proliferation of the P14-Thy.1 cells was assessed by CFSE dilution nine days later. In this system, the donor DCs expressing $H\text{-}2D^b$ molecules are the only cells that could prime LCMV-specific-P14 T cells, as indicated by the lack of P14 division when $D^{b-/-}$ mice were infected with LCMV without receiving wild type DCs. Transfer of BM pDCs from LCMV infected mice that had been shown to differentiate into $CD11b^+$ cDCs in vivo induced significant proliferation of $P14\text{-}Thy1.1^+$ cells to a similar extent as spleen $CD11b^+$ cDCs from LCMV-infected mice. In contrast, transfer of spleen pDCs from the same LCMV-infected mice (which do not generate $CD11b^+$ cDCs) induced only background levels of T cell proliferation (Liou et al., 2008). These data support the view that pDC-derived $CD11b^+$ cDCs are *bona fide* cDCs. Teleologically, the differentiation of activated pDCs to cDCs

would appear to be both desirable and plausible. It would automatically terminate high-level IFN secretion that could cause immunopathology and shorten the lifespan of an infected pDC; at the same time, it would facilitate T cell priming to viral antigens, and the switch from innate to adaptive immunity.

Most recently, Reizis et al., have shown that upregulation of the basic helix-loop-helix transcription factor (E protein) E2-2 serves as a key lineage commitment event in pDC development, as E2-2-deficient hematopoietic progenitors fail to produce pDCs (Cisse et al., 2008). It is noteworthy that E2-2 is expressed at significant levels in hematopoietic stem/progenitor cells and B cells; thus, a merely quantitative several-fold upregulation of E2-2 underlies pDC commitment. Importantly, pDCs show particularly low expression of the E protein inhibitor Id2 (in contrast to its abundant expression in T, NK, and myeloid cells), and this absence likely serves as an important counterpart of E2-2 upregulation, increasing the effective E2-2 concentration in pDCs (Cisse et al., 2008; Crozat et al., 2010). Furthermore, genome-wide binding analysis of E2-2 binding to promoters and other regulatory sequences in a human pDC cell line using ChIP Seq suggest that E2-2 is directly involved in establishment of a pDC-specific gene expression program (e.g., through binding to *ILT7* and *PACSIN1*), and the suppression of an alternative cDC-lineage program (e.g., by binding *CD11c* and *ID2*). This same group went on to test if the pDC lineage shows plasticity by deleting E2-2 from mature pDCs in vivo (Ghosh et al., 2010). They

found that such E2-2 deficient mature pDCs spontaneously differentiate into cDC-like cells, acquiring a cDC phenotype, morphology, and antigen-presenting capacity, and gene expression profile. Such differentiation is consistent with the rapid (within one week) disappearance of peripheral pDCs after E2-2 deletion. Thus, continuous E2-2 expression appears necessary to maintain the lineage identity of pDCs and to prevent their spontaneous differentiation into cDC-like cells. Interestingly, E2-2 expression is reduced several-fold after pDC activation through TLR9 stimulation, raising the possibility that E2-2 deletion may also drive the activation-induced conversion of pDCs demonstrated by Zuniga's group.

These results indicate that pDC cell fate is reversible in principle, likely occurring in concert with activation, although the mechanism of such conversion in a natural infection model remains to be elucidated.

The role of pDCs in autoimmune disease

The release of host-derived (self) DNA into the extracellular environment is a common feature of both necrotic and apoptotic cell death (Pisetsky et al., 2007). It is therefore of pivotal importance that the immune system avoids recognition of extracellular self-DNA, while retaining the ability to sense pathogen-derived nucleic acids. For pDCs, the discrimination between pathogen-derived and self-DNA seems to be controlled at three distinct levels. First, the endosomal localization of TLR9 allows immune responses to DNA from pathogens that

invade the cells by endocytosis, whereas self-DNA fails to spontaneously access this subcellular compartment (Barton et al., 2006; Yasuda et al., 2005). Second, the high extracellular concentration of DNases ensures a rapid degradation of self-DNA released by dying cells, but not DNA that is contained in viruses or microorganisms. The importance of this pathway in preventing autoimmune responses is underscored by the fact that mice deficient in DNase I develop a SLE-like syndrome, and that some patients with SLE have mutations in *DNase I* (Napirei et al., 2000; Yasutomo et al., 2001). Finally, viral or bacterial DNA contains multiple unmethylated CpG motifs that can bind and activate TLR9, whereas mammalian self-DNA contains fewer such motifs, and these are mostly masked by methylation (Krieg, 2002; Stacey et al., 2003). Hypomethylated CpG islands that show reactivity to TLR9, however, have been found in mammalian DNA (Sano et al., 1982). Moreover, these islands are preferentially enriched in DNA fragments released by apoptotic or necrotic cells and in immune complexes associated with SLE.

The barriers that prevent pDCs from sensing self-DNA are not infallible, and the strongest evidence of their response to self-DNA and established role in autoimmune pathogenesis has accumulated from the study of two diseases: SLE and psoriasis. In lupus patients, pDCs are continuously activated by circulating immune complexes comprised of self-DNA and antibodies to DNA or nucleoproteins (Means et al., 2005; Barrat et al., 2005; Ronnblom et al., 2003).

The ongoing production of type I IFNs by pDCs in these patients induces an unabated activation and maturation of cDCs that stimulate autoreactive T cells (Blanco et al., 2001). Furthermore, pDC-derived type I IFN together with IL-6, stimulate the differentiation of autoreactive B cells into autoantibody-secreting plasma cells (Jego et al., 2003). In psoriasis, pDCs sense self-DNA that is released locally following skin injury (Lande et al., 2007). The resulting activation of pDCs triggers autoreactive T-cell activation and initiates the development of skin lesions through type I IFNs (Nestle et al., 2005). Interestingly, decreased numbers of circulating pDCs are found in the blood of both SLE and psoriasis patients (Nestle et al., 2005; Farkas et al., 2001). In psoriasis, this corresponds to infiltration of early skin lesions with activated pDCs, while in SLE, IFN-producing pDCs accumulate in cutaneous lesions, kidney glomeruli, and other affected sites.

Several host factors have been implicated in converting self-DNA into triggers of pDC activation— these are LL37, autoantibodies, and high mobility group box 1 protein (HMGB1). LL37 is an endogenous antimicrobial peptide that is produced by keratinocytes and neutrophils in wounded skin and is overexpressed in psoriatic skin (Lande et al., 2007; Zasloff, 2002). Lande et al. have recently revealed a direct link between LL37 and pDC activation in psoriasis: through its unique cationic and α-helical properties, LL37 was found to bind self-DNA fragments released by dying cells, forming large aggregated

structures that are resistant to extracellular nuclease degradation (Lande et al., 2007). In addition, self-DNA-LL37-complexes can enter pDCs through a process that seems to involve lipid-raft and proteoglycan dependent endocytosis (Sandgren et al., 2004). The aggregated self-DNA-LL37 complexes are retained in the early endosomes of pDCs where they trigger the TLR9-MyD88-IRF7 pathway to induce type I IFN production. In this way, LL37 overexpression might encourage a break in tolerance to self-DNA in psoriatic skin, leading to sustained activation of pDCs and type I IFN production.

In SLE, the breakdown of innate tolerance to self-DNA has been attributed classically to complex formation between self-DNA and DNA-specific antibodies (Marshak-Rothstein, 2006). DNA-containing immune complexes isolated from the sera of patients with SLE trigger type I IFN production by pDCs through binding of the DNA-specific autoantibody to the low-affinity Fc receptor for IgG (FcγRIIA). Self-DNA containing immune complexes can then be internalized by FcγRIIA and translocated to TLR9-containing endosomal compartments (Lovgren et al., 2004). Interestingly, antibodies to DNA and nucleoprotein alone seem to be unable to protect extracellular DNA fragments from nuclease activity. Instead, Gilliet and colleagues have found that immune complexes isolated from patients with SLE contain LL37 and that presence of LL37 is a prerequisite for the ability of DNA-specific antibodies to promote an FcγRIIA-mediated uptake of self-DNA into pDCs to trigger an early endosomal TLR9 response (Lande et al., 2011). In

line with these findings, Pascual's group found that the gene encoding LL37 is among the most upregulated in blood cells from SLE patients and correlates with high level expression of type I IFN and IFN-induced genes (i.e., the "IFN signature") and disease activity (Bennett et al., 2003).

Although the exact origin of LL37 in SLE-associated immune complexes was initially obscure, preliminary studies linked its expression to the presence of immature granulocytes in the peripheral blood of patients with SLE (Bennett et al., 2003). In subsequent follow-up work, Lande et al., determined that neutrophils in SLE patients undergo extensive NETosis, a cell death process in which activated neutrophils extrude large amounts of nuclear DNA into the extracellular space in the form of web-like structures called neutrophil extracellular traps (NETs) (Lande et al., 2011). The group showed that immune complexes in NETs from SLE patients could potently activate pDCs through TLR9 because of the high levels of LL37 bound to DNA in these NETs. In parallel experiments, Garcia-Romo and colleagues demonstrated that pDC secreted IFN-α promoted accelerated neutrophil death that contributed to the heightened NETosis in SLE patients (Garcia-Romo et al., 2011). These studies not only underscore the importance of TLR engagement in pDCs as a part of SLE pathogenesis, but also underscore the feed-forward nature of immune system activation that is a hallmark of this disease.

HMGB1 is a nuclear DNA-binding protein that is released by dying cells and has the ability to enhance type I IFN production by pDCs in response to DNA-containing immune complexes (Tian et al., 2007). Interestingly, in contrast to LL37, HMGB1 can only bind multimeric aggregated DNA structures, but not monomeric DNA sequences. The DNA-HMGB1 complex binds to a surface receptor on pDCs known as RAGE (receptor for advanced glycation end-products). The interaction between RAGE and the DNA-HMGB1 complex is not involved in the uptake of the complex, but potently enhances type I IFN production by facilitating association of the DNA with TLR9 in early endosomes (Tian et al., 2007).

Based on these observations, a model for the breakdown of pDC tolerance to self-DNA in SLE can be offered. In the proposed sequence, LL37 binds first to self-DNA fragments released by apoptotic cells and forms aggregated structures that are protected from nuclease degradation. The aggregated self-DNA-LL37 complexes are then bound by HMGB1. After internalization, the self-DNA-LL37-HMGB1 complex associates with TLR9 in early endosomes. DNA-specific IgG antibodies can bind self-DNA and potently enhance internalization of the resulting complex through FcγRIIA.

Similar to self-DNA, host-derived self-RNA released by damaged cells normally fails to activate pDCs, owing to its rapid extracellular degradation by abundant RNases, which thereby limits accessibility to the TLR7-containing

endosomes. Furthermore, vertebrate-specific RNA modifications, including polyA tails and nucleotide methylations, contribute to a low immunogenicity (Kariko et al., 2005; Koski et al., 2004). Vollmer et al., have shown, however, that self-RNA molecules that are rich in uridine or uridine and guanosine (U/UG-snRNP), trigger pDCs to produce type I IFN through TLR7 when delivered to endosomes by autoantibodies or liposomes (Vollmer et al., 2005). In addition, these self-RNA and autoantibody complexes activated autoreactive B cells through both the BCR and endosomal TLR7 (Vollmer et al., 2005; Lau et al., 2005). In line with these findings, SLE patients have autoantibodies to not only self DNA/chromatin, but also to snRNPs that contain U/UG-RNA (Marshak-Rothstein, 2006; Krieg and Vollmer, 2007). More recently, elegant work from Bolland's group has implicated key changes in the pDC compartment in the development of the SLE-like syndrome seen in *Yaa* mice that harbor a *Tlr7* gene duplication (Deane et al., 2007). Specifically, increased Tlr7 gene dosage resulted in expansion of "inflammatory" blood and splenic pDCs that expressed high levels of activation-related molecules such as MHC class II and CD80, and produced elevated amounts of inflammatory cytokines including TNF-α, IL-6, and MCP-1. Moreover, analysis of pDC cDNA from these animals revealed a strong IFN signature, with significantly increased expression of IRF-5 and SOCS-1. Such findings endorse the contributions of self-RNA triggered TLR7 signaling in pDCs as an important instigator in development of SLE.

Most recently, Guiducci et al., have shown that TLR-activated pDCs become resistant to glucocorticoids, which could underlie the limited efficacy of these drugs in lupus (Guiducci et al., 2010). At the cellular level, glucocorticoids inhibit NF-κB activity, thought to be a main mechanism by which they exert their anti-inflammatory effects. In pDCs, TLR7/9 triggering not only induces type I IFN production, but also activates the NF-κB pathway essential for pDC survival. Interestingly, while naïve murine pDCs were extremely sensitive to glucocorticoid-induced cell death, in vivo activation with immune complexes (as a TLR9 agonist) increased NF-kB transcriptional activity as assessed on DNA-binding assays and p65 phosphorylation. Neither of these was inhibited upon subsequent glucocorticoid treatment, corresponding to the preservation of pDC viability. In addition, gene expression analysis of whole blood after the sequence of TLR9 stimulation and glucocorticoid treatment revealed a robust IFN signature. Importantly, co-injection of IRS (immunoregulatory sequences), short DNA sequences that are a known bifunctional TLR7/9 inhibitor, with the immune complexes restored pDC death in response to glucocorticoids. Thus, it appears that chronic stimulation of pDCs through TLR7/9 results in induction of type I IFN, but additionally may contribute to the reduced therapeutic activity of glucocorticoids. Self-recognition of nucleic acids by TLRs is widely accepted as an important amplifier of inflammation in SLE. A mechanistic relationship between pDC-derived type I IFN production and lupus progression and severity

remains to be fully elucidated. Nevertheless, the likely connection between the formation of nucleic acid containing immune complexes, pDC activation, and IFN secretion, as well as the pronounced IFN signature of the disease, make a strong case for the pDC as a major player in lupus pathogenesis.

PDC production of type I IFN has also been implicated in type 1 diabetes (T1D). IFN-α can be detected in the pancreatic β-islet cells of patients with T1D and in experimental models of T1D, and the induction of a type I IFN response accelerates T1D development (Huang et al., 1994; Huang et al., 1995). In addition, pDCs have been demonstrated to infiltrate the pancreatic islands and pancreatic lymph nodes of non-obese diabetic (NOD) mice; importantly, antibody-mediated blockade of type I IFN-mediated signaling reduced T1D development in this model (Li et al., 2008). In a recent study, Diana et al. revealed that pDCs in the β-islets produce type I IFN that is essential for the induction of T1D (Diana et al., 2013). The authors proposed that dying β-islet cells release DNA that complexes with DNA-specific antibodies and cathelin-related antimicrobial peptide (CAMP), which are produced by B cells and neutrophils, respectively. The resulting immune complexes activate type I IFN production by pDCs in a TLR9-dependent manner, possibly promoting cDC activation dependent autoreactive T cell priming (Guiducci et al., 2006). In another investigation, pDCs were shown to present β-islet cell-derived antigens

that were obtained by immune complex capture more efficiently than cDCs, acting directly to activate diabetogenic T cells (Allen et al., 2009).

Thus, aberrant pDC-mediated type I IFN production appears to be a common mechanism that drives pathogenesis in several autoimmune diseases, including SLE, psoriasis, and TID**.**

Chapter Two:

9-*O*-acetyl sialic acid levels identify committed progenitors of plasmacytoid dendritic cells

Introduction

A prevailing model of hematopoiesis proposes that a multipotent and self-renewing HSC gives rise to either CMPs or CLPs, making an irrevocable choice between myelo-erythroid and lymphoid fates (Kondo et al., 1997; Akashi et al., 2000). Several studies have challenged such an obligatory split (Mebius et al., 2001; Chi et al., 2011; Luc et al., 2012; Bell et al., 2008; Wada et al., 2008), however, reflecting the heterogeneity of early progenitor pools that are comprised of cells with distinct, often multipotent lineage capacity which cross the myelo-erythroid/lymphoid boundary.

Single cell cloning studies (Naik et al., 2013; Yamamoto et al., 2013) have helped dissect the heterogeneity of progenitor populations and underscore the difficulty in identifying specific progenitors for many hematopoietic lineages, including pDCs. PDCs specialize in type I IFN production that is crucial to the antiviral response, but also drives autoimmune pathogenesis in diseases like psoriasis and lupus. In addition, pDCs can induce central and peripheral tolerance (Liu, 2005; Swiecki and Colonna, 2010; Reizis et al., 2011). In spite of their critical roles in the immune system, the molecular and cellular bases for pDC development remain poorly understood.

CDPs that only give rise to cDCs and pDCs (Onai et al., 2007; Naik et al., 2007; Liu et al., 2009) have been defined among the descendants of CMPs

(**Figure 1.4**). In cell transfer studies CDPs were seven times more effective at differentiating into cDCs than pDCs (Onai et al., 2007). Single cell cloning of CDPs revealed their skewed heterogeneity as the largest number of clones gave rise to only cDCs, a smaller fraction to cDCs and pDCs, and the fewest to pDCs only (Naik et al., 2007). While CDPs differentiate into committed precursors of cDCs, pre-cDCs that lack pDC potential, attempts to identify committed progenitors of pDCs downstream of these cells have been unsuccessful (Liu et al., 2009; Naik et al., 2006; Schlitzer et al., 2011; Schlitzer et al., 2012). "CDP-like" cells are very similar to CDPs and have greater pDC potential than CDPs. However approximately 50% of the progeny of CDP-like cells are cDCs (Onai et al., 2013), underscoring the absence so far of any defined progenitor that exclusively gives rise to pDCs (**Figure 1.4**). That CDPs, which are myeloid in origin, may not be the major source of pDCs is also supported by a recent lineage tracing study demonstrating CDPs to be largely cDC-restricted precursors, lacking pDC potential (Schraml et al., 2013).

A lymphoid origin for pDCs has also been proposed. In side-by-side adoptive transfer experiments, CLPs gave rise to more pDCs than CDPs (Onai et al., 2007). However, estrogen treatment that effectively depleted lymphoid progenitors did not affect pDC development (Harman et al., 2006).

Uncertainty regarding the origin of pDCs suggests that the development of these cells may be revealed by an unbiased investigation of hematopoiesis,

liberated from a presumed dichotomy between the myelo-erythroid and lymphoid lineages. One such unbiased approach involves the analysis of a post-synthetic modification of Sia on hematopoietic cells, namely acetylation at the 9-OH position (**Figure 1.1**; reviewed in Pillai et al., 2012).

The in vivo biological function of 9-*O*-AcSia has been explored only in the B lymphoid lineage. One tool utilized to detect 9-*O*-AcSia is a fusion protein of the Fc portion of human IgG with the Influenza C hemagglutinin that binds specifically to 9-*O*-AcSia (Klein et al., 1994). We have used this reagent, termed "CHE-FcD", to demonstrate that the 9-*O*-acetylation state of Sia plays a role in modulating the strength of B cell receptor signaling (Cariappa et al., 2009).

Given the heterogeneity of CDPs and canonical CLPs and CMPs that have been defined primarily by expression patterns of growth factor receptors, we sought to use 9-*O*-AcSia as a marker to provide an independent and novel approach to delineate categories of hematopoietic progenitors. We show that high levels of 9-*O*-AcSia characterize myeloid cells including cDCs, while low levels are found on most lymphoid cells and pDCs. High versus low levels of 9-*O*-AcSia also segregate early Lin^- bone marrow progenitors into two large pools that, as we demonstrate, represents a new approach to dissecting the heterogeneity of hematopoietic progenitors and has the potential to provide new insights regarding hematopoiesis. In vivo studies of the 9-*O*-$AcSia^{Lo}$ pool of bone marrow progenitors delineated unique sequential progenitors of pDCs that are not linked

to either CLPs or CMPs, and include a precursor exclusively committed to pDC development. Demarcating cells with low levels of 9-*O*-AcSia was crucial to defining committed progenitors of pDCs for the first time.

Materials and methods

Animals

8-12-wk-old C57Bl/6 (CD45.2) and B6.SJL-Ptprc^{a}Pepc^{b}/BoyJ (CD45.1) mice used in this study were purchased from Jackson Laboratories and maintained at the animal facility of Massachusetts General Hospital. 10-wk-old mice with the Rag2-GFP knockin fusion gene at the endogenous locus were kindly provided by Duane Weseman (Brigham and Women's Hospital). All animal procedures were approved by the subcommittee on research animal care at Massachusetts General Hospital.

Antibodies, staining, and flow cytometry

The following murine monoclonal antibody conjugates were used: Allophycocyanin (APC)-conjugated 145-2C11 (anti-CD3ε, Armenian hamster IgG), 104 (anti-CD45.2, mouse (SJL) IgG_{2a}, κ), A2F10 (anti-Flt3/CD135, rat IgG_{2a}, κ), N418 (anti-CD11c, Armenian hamster IgG), 927 (anti-CD317/PDCA-1/BST2, rat IgG_{2b}, κ), and 551 (anti-Siglec-H, rat IgG_{1}, κ); APC-Indotricarbocyanine (Cy7)-conjugated A20 (anti-CD45.1, mouse (A.SW) IgG_{2a}, κ), 2B8 (anti-c-Kit/CD117, rat IgG_{2b}, κ), N418 (anti-CD11c, Armenian hamster IgG), and RA3-6B2 (anti-B220/CD45R, rat IgG_{2a}, κ); FITC-conjugated 93 (anti-CD16/32, rat IgG_{2a}, κ), 30-H12 (anti-Thy1.2/CD90.2, rat IgG_{2a}, κ), PK136 (anti-

NK1.1, mouse IgG_{2a} κ), and 551 (anti-Siglec-H, rat IgG_1, κ); Pacific Blue™-conjugated M1/70 (anti-CD11b, rat IgG_{2b}, κ), 6D5 (anti-CD19, rat IgG2a, κ), and D7 (anti-Ly-6A/E (Sca-1), rat IgG_{2a}, κ); r-phycoerythrin (PE)-conjugated 104 (anti-CD45.2, mouse (SJL) IgG_{2a}, κ), 927 (anti-CD317/PDCA-1/BST2, rat IgG_{2b}, κ); peridinin-chlorophyll proteins (PerCP)-Indodicarbocyaninine 5.5 (Cy5.5)-conjugated HM34 (anti-CD34, Armenian hamster IgG), RA3-6B2 (anti-B220/CD45R, rat IgG_{2a}, κ), A734 (anti-IL-7Rα/CD127, rat IgG_{2a}, κ), and 551 (anti-Siglec-H, rat IgG_1, κ); PE-Cy7-conjugated 145-2C11 (anti-CD3ε, Armenian hamster IgG), GK1.5 (anti-CD4, rat IgG_{2b}, κ), 53-6.7 (anti-CD8α, rat IgG_{21}, κ), M1/70 (anti-CD11b, rat IgG_{2b}, κ), N418 (anti-CD11c, Armenian hamster IgG), 6D5 (anti-CD19, rat IgG2a, κ), RA3-6B2 (anti-B220/CD45R, rat IgG_{2a}, κ), A734 (anti-IL-7Rα/CD127, rat IgG_{2a}, κ), RB6-8C5 (anti-Ly-6G/Ly-6C (Gr-1), rat IgG_{2b}, κ), RMM-1 (anti-IgM, rat IgG_{2a}, κ), 1A8 (anti-Ly6G, rat IgG_{2a}, κ), PK136 (anti-NK1.1, mouse IgG_{2a} κ), D7 (anti-Ly-6A/E (Sca-1), rat IgG_{2a}, κ), and TER-119 (anti-TER-119/Erythroid Cells, rat IgG_{2b}, κ), all from BioLegend; APC-eFluor 780 A734 (anti-IL-7Rα/CD127, rat IgG_{2a}, κ); PE-CF™ 594-conjugated 2B8 (anti-c-Kit/CD117, rat IgG_{2b}, κ); PerCP-eFluor® 710 AFS98 (anti-c-fms/CD115, rat IgG_{2a}, κ), all from eBioscience.

Single cell suspensions were made from spleen and bone marrow (two femurs and two tibias) using standard methodology, with procedural modifications to isolate and enrich mouse DCs (Naik et al., 2007; Vremec, 2010).

Spleens were disrupted by gentle teasing with forceps and digested for 25 minutes at 37 °C with mixing in 5 ml PBS and 0.2% bovine serum albumin (PBA) containing collagenase (300 mU/ml; type I and II; Roche) and DNase I (100 μg/ml; Roche). Undigested fibrous material was removed by filtration through 70 μm nylon mesh. Red cells were lysed with 2 ml (spleen) or 1 ml (BM) ACK lysing buffer (Lonza BioWhittaker). The lysing buffer was neutralized by adding 10 ml PBA. Before staining, 1×10^6 cells were reacted with 2.5 ug of 2.4G2 (anti-CD16/CD32 [Fcγ III/II receptor], rat IgG_{2b}, κ; BD Biosciences). Surface staining was performed using appropriate dilutions of antibodies in 12 × 75-mm round-bottom polystyrene tubes in a volume of 200 ul for 30 minutes in the dark at 4 °C.

Multiparameter flow cytometric analysis was performed as previously described (Cariappa et al., 2009) on a BD^{TM} LSR II machine. Unstained cells were used to set voltage and single color positive controls were used for electronic compensation. Viable cells were determined by forward and side scatter characteristics and $3\text{-}5 \times 10^6$ gated events were collected. Analysis was performed with FlowJo software v9.6.4 (TreeStar).

Bone marrow cell populations were gated as follows: LSK hematopoietic stem cells (HSCs): Lin^-(CD3ε, CD4, CD8α, CD19, B220, CD11c, CD11b, NK1.1, Gr.1, TER119)$^-$Sca-1^{Hi}c-Kit^{Hi}; common lymphoid progenitors (CLPs): Lin^-(CD3ε, CD4, CD8α, CD19, B220, CD11c, CD11b, NK1.1, Gr.1, TER119)$^-$ IL-7Rα^+Sca-1^{Lo}c-Kit^{Lo}Thy1.2^-; common myeloid progenitors (CMPs): Lin^-

(CD3ε, CD4, CD8α, IgM, CD19, B220, CD11c, CD11b, NK1.1, Gr.1, TER119)$^-$ IL-7Rα$^-$c-Kit$^+$Sca-1$^-$FcR^{Lo}CD34$^+$; monocyte and dendritic cell progenitors (MDPs): Lin$^-$(CD3ε, CD19, B220, CD11c, CD11b, NK1.1, Gr.1, TER119)$^-$Sca-1$^-$ Flt3$^+$CD115$^+$c-Kit^{Hi}; common cDC and pDC dendritic cell progenitors (CDPs): Lin$^-$(CD3ε, CD19, B220, CD11c, CD11b, NK1.1, Gr.1, TER119)$^-$Sca-1$^-$ Flt3$^+$CD115$^+$c-Kit^{Lo}; CDP-like: Lin$^-$(CD3ε, CD19, B220, CD11c, CD11b, NK1.1, Gr.1, TER119)$^-$Sca-1$^-$Flt3$^+$CD115$^-$c-Kit$^{Lo/-}$IL-7Rα$^-$; pro-plasmacytoid dendritic cells (pro-pDCs): Lin$^-$(CD3ε, CD19, B220, CD11c, CD11b, NK1.1, Gr.1, TER119)$^-$Sca-1^{Lo}9-*O*-AcSia^{Lo}Siglec-H$^-$PDCA-1$^-$Flt3$^+$CD115$^-$IL-7Rα$^-$; pre-plasmacytoid dendritic cells (pre-pDCs): Lin$^-$(CD3ε, CD19, B220, CD11c, CD11b, NK1.1, Gr.1, TER119)$^-$Sca-1^{Lo}9-*O*-AcSia^{Lo}Siglec-H^{Lo}PDCA-1^{Lo}; plasmacytoid dendritic cells (pDCs): Lin$^-$(CD3ε, CD19, NK1.1, Ly6G, TER119)$^-$ CD11c$^{+/Lo}$CD11b$^-$B220$^+$PDCA-1$^+$Siglec-H$^+$; neutrophil (PMN): CD11b$^+$Ly6G$^+$ in the granulocyte gate; FrB/C pro-B: Lin$^-$(CD3ε, IgM, CD11c, CD11b, NK1.1, Gr.1, TER119)$^-$CD19$^+$B220^{Lo}CD43$^+$ in the lymphoid-monocytoid gate (Hardy et al., 1991).

Spleen cell populations were gated as follows: B cells: CD3ε$^-$NK1.1$^-$ Ly6G$^-$TER119$^-$Siglec-H$^-$CD19$^+$ B220$^+$; Red Pulp Macrophages (RPMs): Lin$^-$ (CD3ε, CD19, NK1.1, TER119)$^-$CD11c^{Dim}CD11b^{Dim}F4/80^{Hi}; polymorphonuclear leukocytes (PMNs): Lin$^-$(CD3ε, CD19, NK1.1, TER119)$^-$ CD11c^{Dim}CD11b^{Hi}Ly6G$^+$; Monocytes (Mo): Lin$^-$(CD3ε, CD19, NK1.1, TER119)$^-$

$CD11c^{Dim}CD11b^{Hi}Ly6G^{-}CD115^{+}$; conventional dendritic cells (cDCs): Lin^{-} $(CD3\varepsilon, CD19, NK1.1, Ly6G, TER119)^{-}CD11c^{Hi}B220^{-}PDCA\text{-}1^{-}Siglec\text{-}H^{-}$; plasmacytoid dendritic cells (pDCs): $Lin^{-}(CD3\varepsilon, CD19, NK1.1, Ly6G, TER119)^{-}$ $CD11c^{+/Lo}CD11b^{-}B220^{+}PDCA\text{-}1^{+}Siglec\text{-}H^{+}$.

Ex vivo detection of 9-*O*-AcSia on murine cells

The CHE-FcD probe, a fusion protein composed of the extracellular domains of the influenza C hemagglutinin esterase (CHE) which binds 9-*O*-AcSia, and the Fc portion of human IgG_1 (Fc), treated with diisopropylfluorophosphate (D) was generated as previously described (Cariappa et al., 2009; Krishna and Varki, 1997; Martin et al., 2003). The chimeric CHE-FcD protein was precomplexed with PE-goat anti–human IgG (Fcγ-specific) (Ebioscience; 1.875 µl of a 1:10 dilution of CHE-FcD in PBA with 6 µl of a 1:4 dilution of the secondary antibody in a total volume of 50 µl PBA) for 2 hours at 4 °C in the dark. This pre-complexing step increases the overall avidity of the probe towards 9-*O*-AcSia. 3-5 $\times 10^6$ cells in 100 µl PBA were preincubated for 45 minutes at 37 °C, added to the precomplex, and incubated on ice for an additional 1.5 hours. The cells were washed once with cold PBA, reacted with 2.4G2, an FcγR III/II receptor-blocking antibody, and surface stained as described earlier. To test for specificity of CHE-FcD to bind to 9-*O*-AcSia, cells were treated with the CHE-Fc reagent. CHE-Fc was prepared and precomplexed exactly as CHE-FcD, except without treatment

with D. Following the 45 minute incubation at 37 °C described above, cells were treated first with the CHE-Fc precomplex at the same dilution and with the same conditions as for CHE-FcD. The cells were then washed once with cold PBA, and incubated with the CHE-FcD precomplex as described above, prior to surface staining.

Pre-enrichment of lineage-negative cell fraction from fresh bone marrow

For in vitro differentiation assays and in vivo adoptive transfer assays described below, bone marrow samples were immunomagnetically pre-enriched with a PE-Cy7-conjugated antibody cocktail against lineage antigens (CD3ε, CD19, B220, CD11c, CD11b, Gr.1, NK1.1, TER119) (Biolegend) and Cy7-microbeads (Miltenyi Biotec). Magnetic separation using the QuadroMACS Separator and LS MACS columns (Miltenyi Biotec) according to manufacturer's instructions was used to obtain the lineage-negative cell fraction. Cells were then stained with appropriate mixtures of monoclonal antibodies to identify bone marrow progenitor populations as described above and sorted on the BD^{TM} FACSAria II cell sorter.

In vitro dendritic cell differentiation assay

For the evaluation of cDC and pDC differentiation, 1×10^5 freshly sorted Lin$^-$Sca-1^{Lo}9-*O*-AcSia^{Lo}, Lin$^-$Sca-1^{Lo}9-*O*-AcSia^{Hi} cells, or CDPs were cultured in Iscove's

modified Dulbecco's medium (Gibco) supplemented with 10% (vol/vol) FCS, 2-mercaptoethanol (50 uM), sodium pyruvate (1 mM), penicillin (100 U/ml), streptomycin (100 μg/ml), and 100 ng/ml recombinant murine Flt3-ligand (PeproTech). Half of the medium was replaced every 3 days with medium containing two-fold cytokines (Onai et al., 2007; Onai et al., 2010). After 2, 4, 6, 8, and 10 days of culture, offspring cells were harvested, transferred to 12 × 75-mm round-bottom polystyrene tubes, and centrifuged at 400 × *g* for 5 minutes at 4 °C. Supernatant was aspirated, and cells were stained with appropriate mixtures of monoclonal antibodies to identify pDCs and cDCs using flow cytometry as described above.

In vivo adoptive transfer assay to assess lineage potential

To assess differentiation potential for bone marrow progenitor populations, freshly sorted cells from the bone marrow of 40 10-wk-old CD45.2 donor mice were injected intravenously into 8-wk-old CD45.1 congenic recipient mice that were sublethally irradiated with one dose of 4.5 Gy from a Cesium 137 source. Lethal irradiation was not used as it causes Flt3L upregulation that may favor DC-biased differentiation of transferred cells, and therefore distort the steady-state situation (Chklovskaia et al., 2004). Spleen and BM were harvested at time points ranging from day 4 through 14 post-transfer and donor-derived ($CD45.2^{+}CD45.1^{-}$) and host cells ($CD45.2^{-}CD45.1^{-}$) were assessed using isolation, staining, and

flow cytometry strategies described above. Numbers of cells transferred for each population tested are specified in the order in which they are described:

$Lin^-Sca\text{-}1^{Lo}9\text{-}O\text{-}AcSia^{Lo}Siglec\text{-}H^{Lo}$, 1×10^3

$Lin^-Sca\text{-}1^{Lo}9\text{-}O\text{-}AcSia^{Lo}Siglec\text{-}H^-$, 1×10^3

$Lin^-Sca\text{-}1^{Lo}9\text{-}O\text{-}AcSia^{Lo}Siglec\text{-}H^-Flt3^+CD115^-$, 1×10^4

$Lin^-Sca\text{-}1^{Lo}9\text{-}O\text{-}AcSia^{Lo}Siglec\text{-}H^-Flt3^-CD115^+$, 1×10^4

$Lin^-Sca\text{-}1^{Lo}9\text{-}O\text{-}AcSia^{Lo}Siglec\text{-}H^-Flt3^+CD115^-IL\text{-}7R\alpha^-$, 2×10^3 or 1×10^4

$Lin^-Sca\text{-}1^{Lo}9\text{-}O\text{-}AcSia^{Lo}Siglec\text{-}H^-Flt3^+CD115^-IL\text{-}7R\alpha^+$, 2×10^3

PCR assay for *IgH* gene rearrangements in pro-, pre-, and mature pDCs

Genomic DNA was isolated from freshly sorted cells using the DNAeasy Blood and Tissue Kit (QIAGEN). Primers specific for the D_HQ52 element were used to amplify D_H to J_H (DJ) rearranged and nonrearranged germline (GL) *IgH* loci in a nested PCR approach adapted from that previously described (ten Boekel et al., 1995). Each reaction contained a D_HQ_{52} primer together with a nested 3' J_H4 primer. Primers are listed in **Table 2.1A**. The lengths of the different PCR products are summarized in **Table 2.1B**. The PCRs was carried out over 40 cycles at 95 °C, 30 seconds; 56 °C, 30 seconds; 72 °C, 105 seconds (first round) or 120 seconds (second round). Each PCR reaction was performed in 25 µl. 1 µl of the first round PCR products were used in the second round. 8 µl of the second round PCR products were analyzed on a 1% agarose gel stained with ethidium bromide.

The presence of a GL band and absence of DJ bands in polymorphonuclear cells served as a negative control for DJ rearrangement. The presence of DJ bands in FrB/C pro-B and B cells served as a positive control for DJ rearrangement.

Table 2.1. PCR primers and product lengths used to detect DJ rearrangements at the *IgH* locus.

Table 2.1A

Oligonucleotides used for amplification of rearrangements at the *IgH* locus			
Sequence	**Specificity**	**PCR round**	
		1st	**2nd**
CACAGAGAATTCTCCATAGTTGATAGCTCAG	D_HQ52	+	-
GCCTCAGAATTCCTGTGGTCTCTGACTGGT	D_HQ52	-	+
AGGCTCTGAGATCCCTAGACAG	3' of J_H4	+	-
GGGTCTAGACTCTCAGCCGGCTCCCTCAGGG	3' of J_H4	-	+

Table 2.1B

Approximate PCR product lengths	
Rearrangements	**Product lengths (bp)**
Germline IgH (GL)	2200
D_HQ52J_H (DJ)	1500 (J_H1), 1190 (J_H2), 770 (J_H3), and 240 (J_H4)*

*In Figure 2.18B, DJn reflects rearrangement of D_HQ52 with J_Hn.

Results

9-*O*-AcSia levels define progenitor pools

Most lymphocytes are 9-*O*-AcSia^{Lo}, but levels of cell surface 9-*O*-AcSia on myeloid cells had not been characterized. Flow cytometric analysis (FCA) of wild-type murine splenocytes stained with CHE-FcD showed that CD11c$^{+/Lo}$CD11b^{-}B220^{+}PDCA-1^{+}Siglec-H^{+} pDCs (**Figure 2.1**), like B lymphocytes, exhibit low levels of 9-*O*-AcSia, while CD11c^{Hi} cDCs (**Figure 2.1**) and other myeloid cells (**Figure 2.2**) express high levels of this carbohydrate modification (**Figures 2.3A, B**). (Specificity for the CHE-FcD reagent to recognize 9-*O*-AcSia is depicted in **Figure 2.4**). Further inspection revealed that distinct levels of 9-*O*-AcSia correlate with functionally distinct cDC subsets: cross-presenting CD8α^{+} cDCs stained with lower intensity for CHE-FcD compared to the high levels observed on CD4^{+} and CD4^{-}CD8α^{-} cDCs (**Figure 2.5**).

We considered that low levels of 9-*O*-AcSia on pDCs and lymphoid cells versus high levels observed in myeloid cells including cDCs might reflect their respective origins. Bone marrow progenitor populations were surveyed for levels of 9-*O*-AcSia. CHE-FcD staining of the "LSK" HSC compartment (Lin^{-}Sca-1^{Hi}c-Kit^{Hi}), comprised of long-term HSCs and short-term HSCs with multilineage potential (Wilson and Trumpp, 2006; Yamamoto et al., 2013), revealed intermediate surface levels of 9-*O*-AcSia (**Figures 2.6A** and **2.7A**). In contrast,

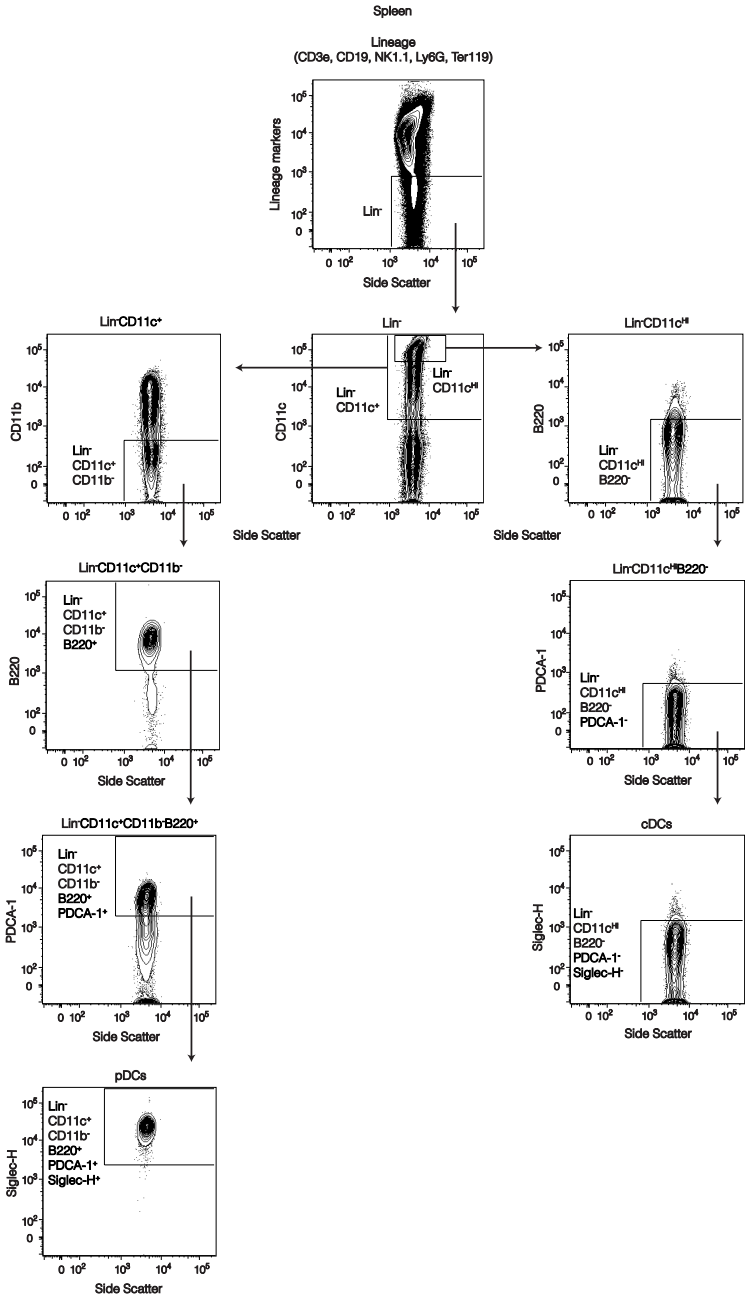

Figure 2.1. Gating strategy to identify pDCs and cDCs in murine spleen Gating strategy for splenic pDCs ($Lin^-CD11c^{+/Lo}CD11b^-B220^+PDCA\text{-}1^+Siglec\text{-}H^+$) and cDCs ($Lin^-CD11c^{Hi}B220^-PDCA\text{-}1^-Siglec\text{-}H^-$). Lin: CD3ε/CD19/NK1.1/Ly6G/Ter119.

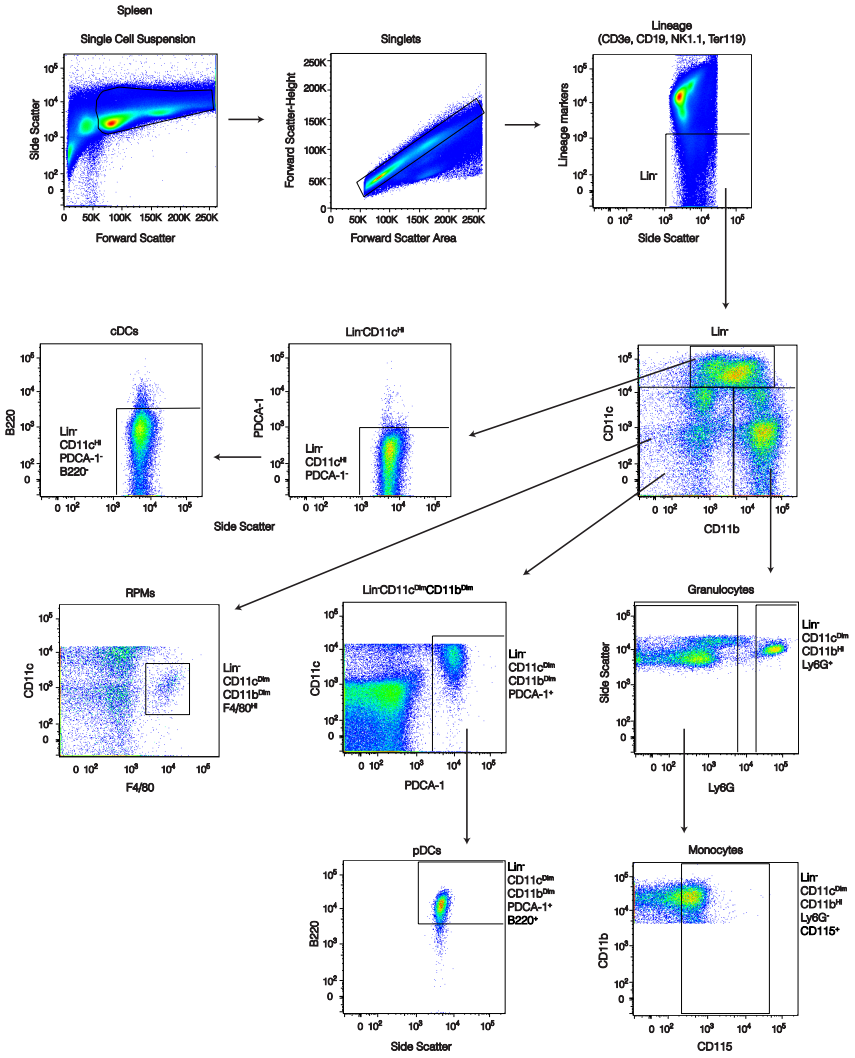

Figure 2.2. Gating strategy to identify myeloid cells in murine spleen. Total splenocytes from 10-wk-old wild type mice were stained with antibody cocktails to identify conventional dendritic cells (cDCs), red pulp macrophages (RPMs), plasmacytoid dendritic cells (pDCs), granulocytes (PMNs), and monocytes [Mo] (Idoyaga et al., 2009). 3×10^6 cells were acquired for each sample. cDCs ($Lin^-CD11c^{Hi}PDCA\text{-}1^-B220^-$) include both $CD11b^+$ and $CD11b^-$ populations; RPMs [$Lin^-CD11c^{Dim}CD11b^{Dim}F4/80^{Hi}$] (Taylor et al., 2005); pDCs ($Lin^-CD11c^{Dim}CD11b^{Dim}PDCA\text{-}1^+B220^+$); PMNs [$Lin^-CD11c^{Dim}CD11b^{Hi}Ly6G^+$] (Daley et al., 2008); Mo ($Lin^-CD11c^{Dim}CD11b^{Hi}Ly6G^-CD115^+$). Lin: CD3ε/CD19/NK1.1/Ter119.

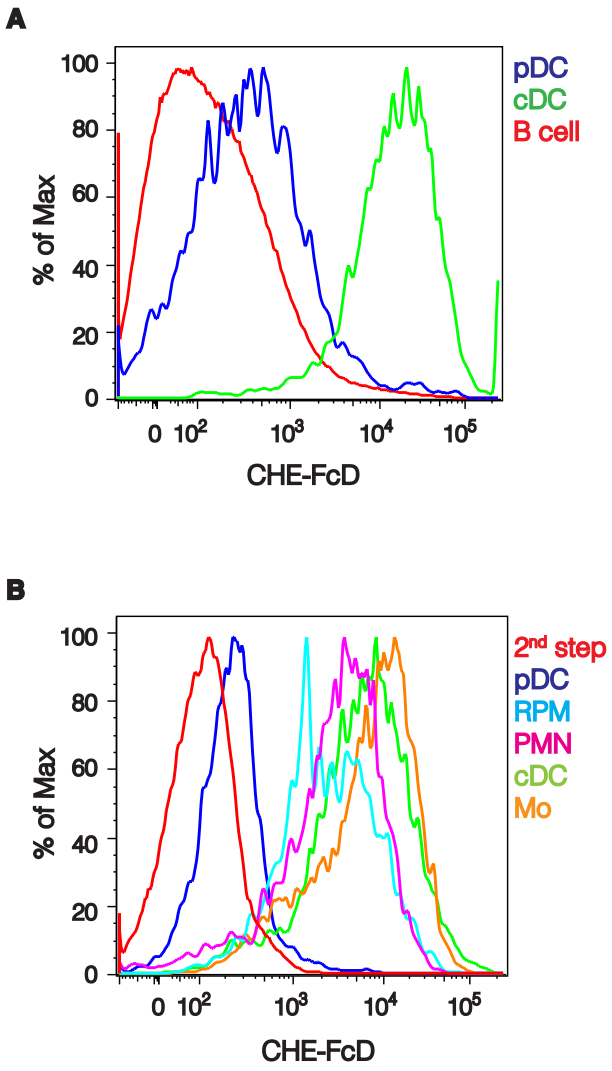

Figure 2.3. Low surface levels of 9-*O*-AcSia distinguish pDCs from cDCs and other myeloid cells. (A-B) Splenocytes and from 10-wk-old wild type mice were stained with CHE-FcD and surface phenotype markers and then examined by flow cytometry.
(A) CHE-FcD profiles of pDCs, cDCs, and B cells. (B) CHE-FcD staining of pDCs and other myeloid cells [Red pulp macrophage (RPM), neutrophil (PMN), monocyte (Mo)].

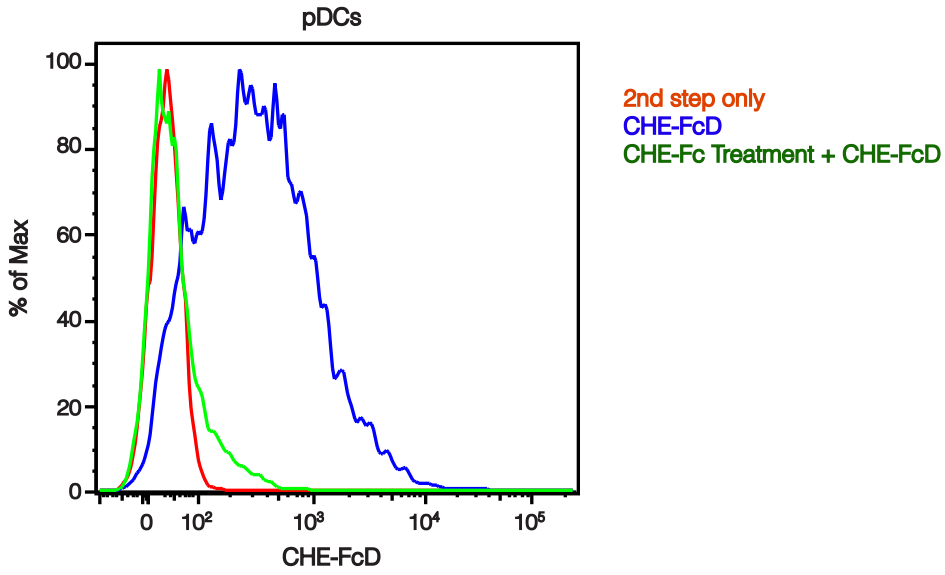

Figure 2.4. Specificity of the CHE-FcD reagent to detect 9-*O*-AcSia. pDCs from 10-wk-old wild type mice were stained with CHE-FcD with or without prior treatment with CHE-Fc and analyzed by flow cytometry.

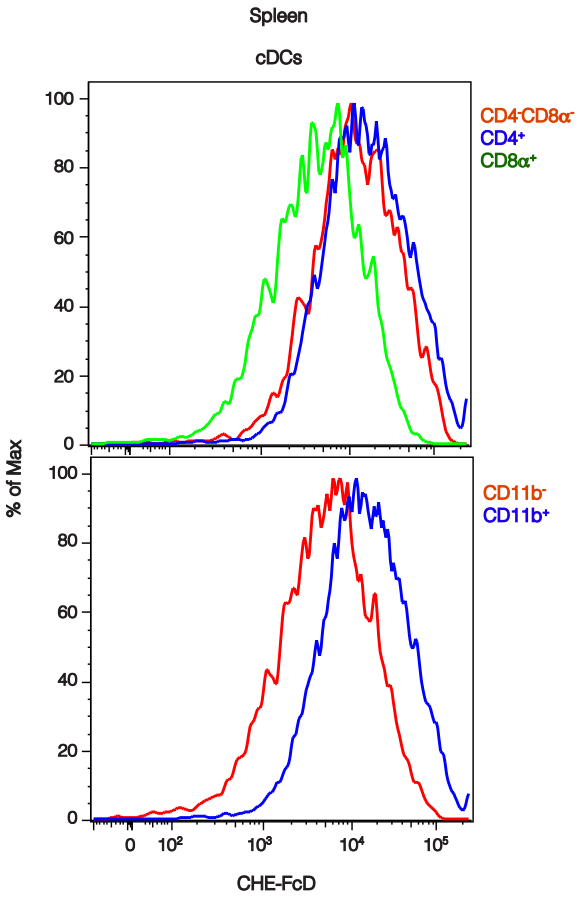

Figure 2.5. Distinct levels of 9-*O*-AcSia characterize functionally distinct cDC subsets. Splenocytes from 10-wk-old wild type mice were treated with the CHE-FcD reagent, stained with surface phenotype markers, and examined by FCA. 3×10^6 cells were acquired for each sample. Data are representative of three independent experiments. (Upper panel) Comparison of CHE-FcD staining in $CD4^+$, $CD4^-$ $CD8\alpha^-$, and cross-presenting $CD8\alpha^+$ cDCs. (Lower panel) CHE-FcD staining in $CD11b^+$cDC pool (that contains $CD4^+$ and $CD4^-$ $CD8\alpha^-$ cDCs) and the $CD11b^-$ cDC pool (that contains $CD8\alpha^+$ cDCs).

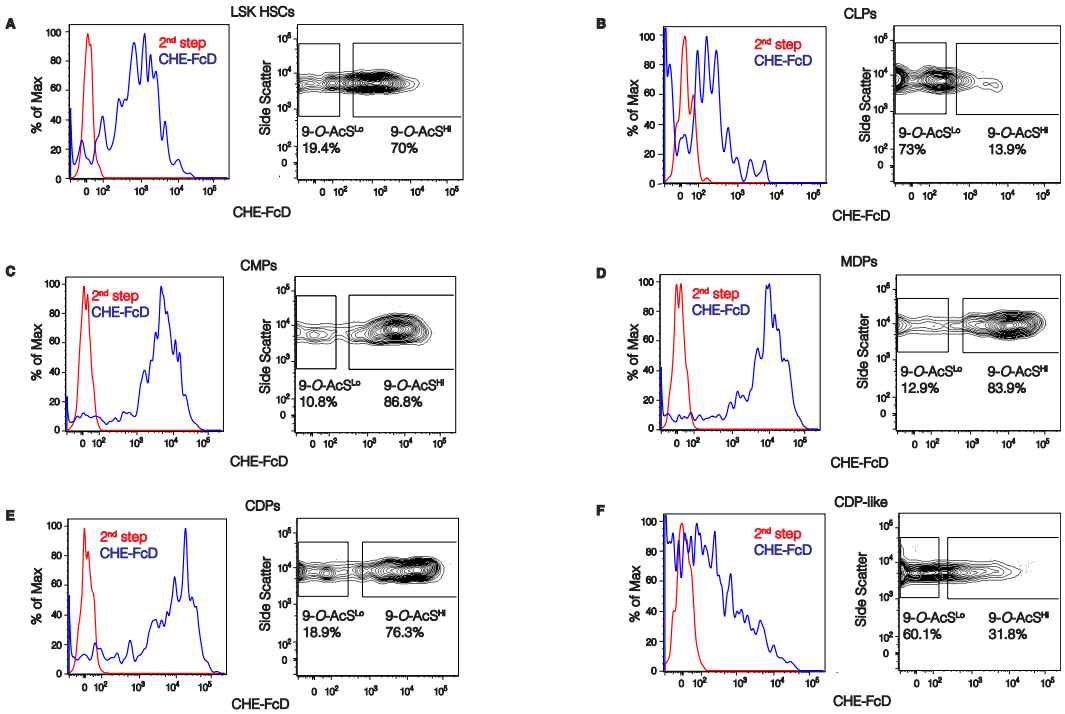

Figure 2.6. Low surface levels of 9-*O*-AcSia separate Lin$^-$ hematopoietic progenitors into distinct pools. (A-E) Bone marrow cells from 10-wk-old wild type mice were stained with CHE-FcD and surface phenotype markers and then examined by flow cytometry. CHE-FcD staining profiles of bone marrow progenitors [(A) LSK HSCs (B) CLPs (C) CMPs (D) MDPs (E) CDPs (F) CDP-like cells].

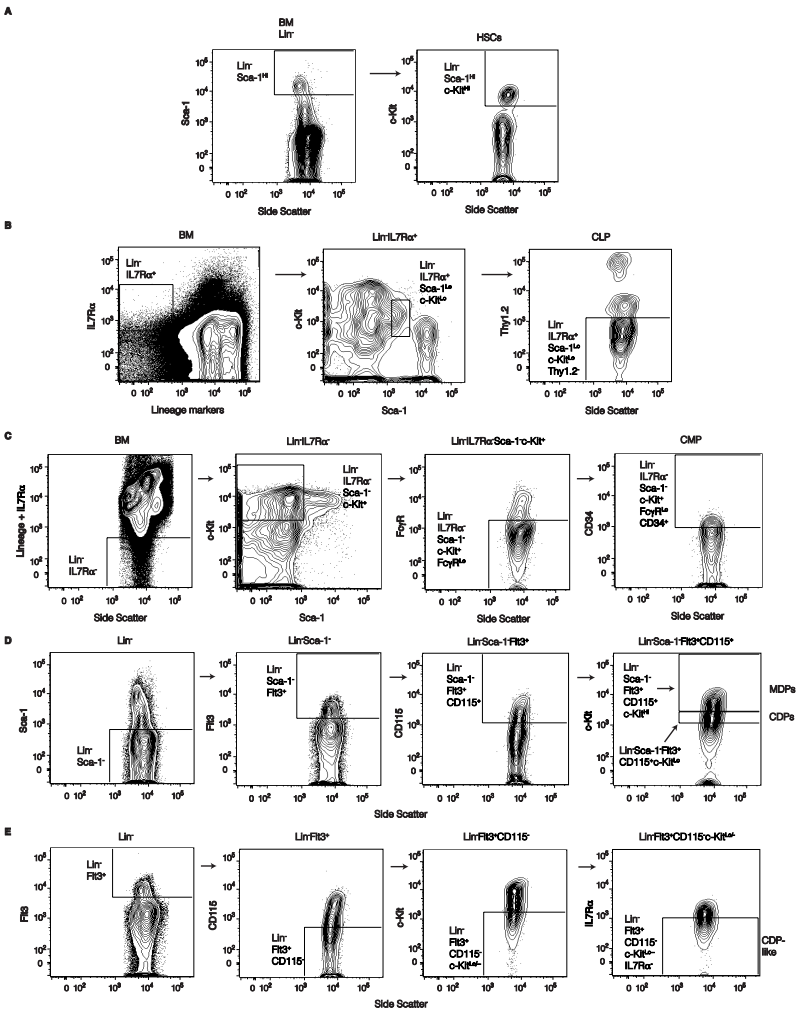

Figure 2.7. Gating strategy to identify early bone marrow progenitor populations. Bone marrow cells from 10-wk-old wild type mice were stained with surface phenotype markers and examined by flow cytometry. 3×10^6 cells were acquired for each sample.
(A**)** LSK fraction of HSCs ($Lin^-Sca\text{-}1^{Hi}c\text{-}Kit^{Hi}$); this population is comprised of long-term HSCs (LT-HSCs; $Flt3^-CD34^-$) and short-term HSCs with multilineage potential [ST-HSCs or MPPs; $Flt3^{int}CD34^+$ and LMPPs; $Flt3^+CD34^+$] (Wilson and Trumpp, 2006); Yamamoto et al., 2013). **(**B**)** CLPs [$Lin^-IL7R\alpha^+Sca\text{-}1^{Lo}c\text{-}Kit^{Lo}Thy1.2^-$] (Kondo et al., 1997). **(**C**)** CMPs [$Lin^-IL7R\alpha^-Sca\text{-}1^-c\text{-}Kit^+Fc\gamma R^{Lo}CD34^+$] (Akashi et al., 2000). **(**D**)** MDP [$Lin^-Sca\text{-}1^-Flt3^+CD115^+c\text{-}Kit^{Hi}$] (Liu et al., 2009) and CDP [$Lin^-Sca\text{-}1^-Flt3^+CD115^+c\text{-}Kit^{Lo}$] (Onai et al., 2007; Naik et al., 2007). **(**E**)** CDP-like [$Lin^-Flt3^+CD115^-c\text{-}Kit^{Lo/-}IL7R\alpha^-$] (Onai et al., 2013). For **(**A-B**)**, **(**D-F**)**: Lin: CD3ε/CD4/ CD8α/CD19/B220/NK1.1/CD11c/CD11b/Gr.1/Ter119. For **(**C**)**: Lin: CD3ε/CD4/ CD8α/CD19/B220/IgM/NK1.1/CD11c/CD11b/Gr.1/Ter119.

the vast majority of CLPs expressed low levels of 9-*O*-AcSia, similar to those observed on their B cell progeny and pDCs (**Figures 2.6B** and **2.7B**). Most CMPs, on the other hand, resembled their myeloid progeny including cDCs, and exhibited robust levels of 9-*O*-AcSia (**Figures 2.6C** and **2.7C**). Furthermore, the majority of MDPs that are immediate descendants of CMPs (Fogg et al., 2006), as well as most CDPs, which derive directly from MDPs (Liu et al., 2009), maintained these high levels (**Figures 2.6D, E** and **2.7D**). The similar CHE-FcD staining of MDPs and CDPs is consistent with their highly overlapping phenotypes that differ only in the degree of c-Kit expression (Auffray et al., 2009). A sizable fraction of CDP-like cells defined by Onai et al. (2013) had high levels of 9-*O*-AcSia consistent with the considerable cDC potential that remains in this pool, (**Figures 2.6F** and **2.7E**). Although these progenitor pools are heterogeneous with respect to 9-*O*-AcSia levels and developmental potential, there appears to be a correspondence between the relative proportion of cells with low 9-*O*-AcSia levels and pDC potential.

We wished to determine if bone marrow progenitors with low levels of 9-*O*-AcSia might be predisposed to pDC development. Since our studies above involved only individual progenitor types, we first examined the entire pool of early bone marrow progenitors, i.e., all potential pDC progenitors, to see if it could be divided based on 9-*O*-AcSia levels. This pool was defined as $Lin^{-}Sca\text{-}1^{Lo}$ and was designed to exclude LSK HSCs, whose multipotency might mask distinct

developmental potentials based on differing 9-*O*-AcSia levels. CHE-FcD staining of the Lin$^-$Sca-1^{Lo} pool revealed clearly distinguishable 9-*O*-AcSia^{Lo} and 9-*O*-AcSia^{Hi} cells (**Figure 2.8A**). To test if the Lin$^-$Sca-1^{Lo}9-*O*-AcSia^{Lo} cells contained progenitors that preferentially gave rise to pDCs, we used fluorescent activated cell sorting to isolate these cells from the bone marrow and examined their differentiation potential. Of note, this pool includes CLPs and the minor group of CMPs with low 9-*O*-AcSia. The cells were cultured in vitro with Flt3L, a cytokine critical for DC development, and with which supplementation of bone marrow cultures generates only pDCs and cDCs (Onai et al., 2007). As shown in **Figure 2.8B**, the Lin$^-$Sca-1^{Lo}9-*O*-AcSia^{Lo} bone marrow progenitors differentiated substantially into pDCs. CD11c$^+$ cells from parallel cultures of Lin$^-$Sca-1^{Lo}9-*O*-AcSia^{Hi} cells, however, were almost exclusively cDCs, and CDPs generated four times fewer pDCs than the Lin$^-$Sca-1^{Lo}9-*O*-AcSia^{Lo} cells (**Figures 2.9A, B**). Taken together, the data suggest that exclusive precursors of pDCs might exist in the Lin$^-$Sca-1^{Lo}9-*O*-AcSia^{Lo} bone marrow progenitor pool.

Identifying exclusive precursors of pDCs

We considered that the Lin$^-$Sca-1^{Lo}9-*O*-AcSia^{Lo} pool might be enriched for a spectrum of pDC progenitors, since all of its members lacked lineage markers including B220 and CD11c, which are found on mature pDCs. We reasoned that fully committed precursors of pDCs in this pool might express low levels of the

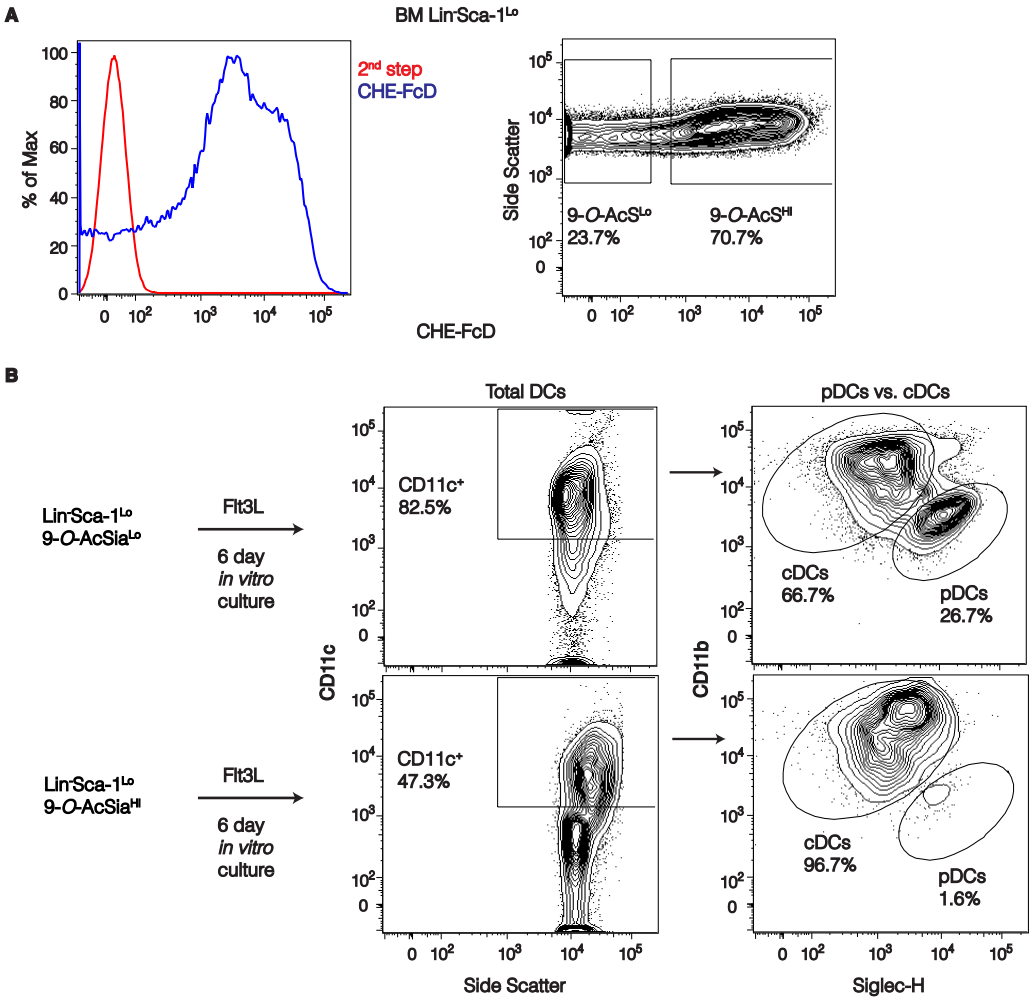

Figure 2.8 The 9-*O*-AcSia^{Lo}Lin^{-}Sca-1^{Lo} progenitor pool is enriched for pDC developmental potential. **(**A**)** CHE-FcD staining of the total pool of non-HSC early bone marrow progenitors (Lin^{-}Sca-1^{Lo}). **(**B**)** In vitro DC differentiation from sorted 9-*O*-AcSia^{Lo} and 9-*O*-AcSia^{Hi}Lin^{-}Sca-1^{Lo} cells. Data is shown at time of peak pDC differentiation (day 6). Data are representative of three independent experiments.

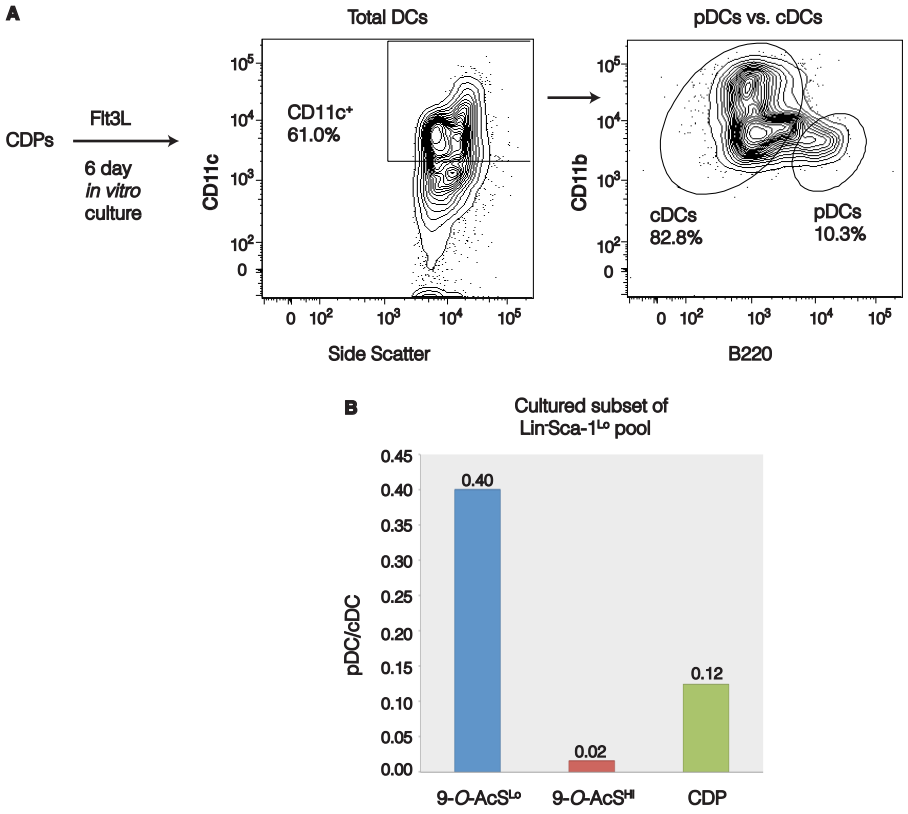

Figure 2.9. CDPs have less pDC developmental potential than Lin$^-$Sca-1^{Lo}9-*O*-AcSia^{Lo} bone marrow progenitors. **(**A**)** In vitro DC differentiation from sorted CDPs. Cells (1×10^5) were cultured with murine Flt3L (100 ng/ml) and absolute numbers of DCs were determined on day 2, 4, 6, 8, and 10. Data is shown at time of peak pDC differentiation (day 6). Data are representative of three independent experiments. **(**B**)** Summary of data in **(**A**)** and Figure 2.8B showing pDC versus cDC generation from cultured progenitors.

pDC-specific markers, Siglec-H (Blasius et al., 2004; Blasius et al., 2006a; Zhang et al., 2006) and PDCA-1 (Blasius et al., 2006b). Siglec-H is found only on the surface of murine pDCs; PDCA-1, however, has been described on certain B cell subsets (Bao et al., 2011; Vinay et al., 2012), limiting its use to discriminating pDCs from cDCs.

Our strategy to identify committed pDC progenitors was to interrogate expression of Siglec-H and PDCA-1, in conjunction with 9-*O*-AcSia levels in the $Lin^{-}Sca\text{-}1^{Lo}$ bone marrow progenitor pool. FCA revealed a small group of cells that co-expressed low levels of both Siglec-H and PDCA-1 among progenitors with the lowest 9-*O*-AcSia levels (**Figure 2.10A**). Comparison of Siglec-H and PDCA-1 levels between these cells and mature bone marrow pDCs confirmed that they were distinct populations (**Figure 2.10B**). We next investigated whether these Siglec-H^{Lo}PDCA-1^{Lo} cells represented a fully committed pDC precursor population.

We injected freshly sorted $Lin^{-}Sca\text{-}1^{Lo}$9-*O*-$AcSia^{Lo}Siglec\text{-}H^{Lo}$ bone marrow cells (**Figure 2.11**) from CD45.2 donor mice into sublethally irradiated CD45.1 recipients and analyzed all transferred cells 9-10 days later. We found that the transferred Siglec-H^{Lo} cells gave rise exclusively to pDCs (**Figure 2.11 upper panel**). Donor cells did not give rise to $B220^{-}CD11c^{Hi}$ cDCs, although these were clearly identified among host cells (**Figure 2.11 middle panel**). Markers used to identify pDCs included B220, which is not found on cDCs, and

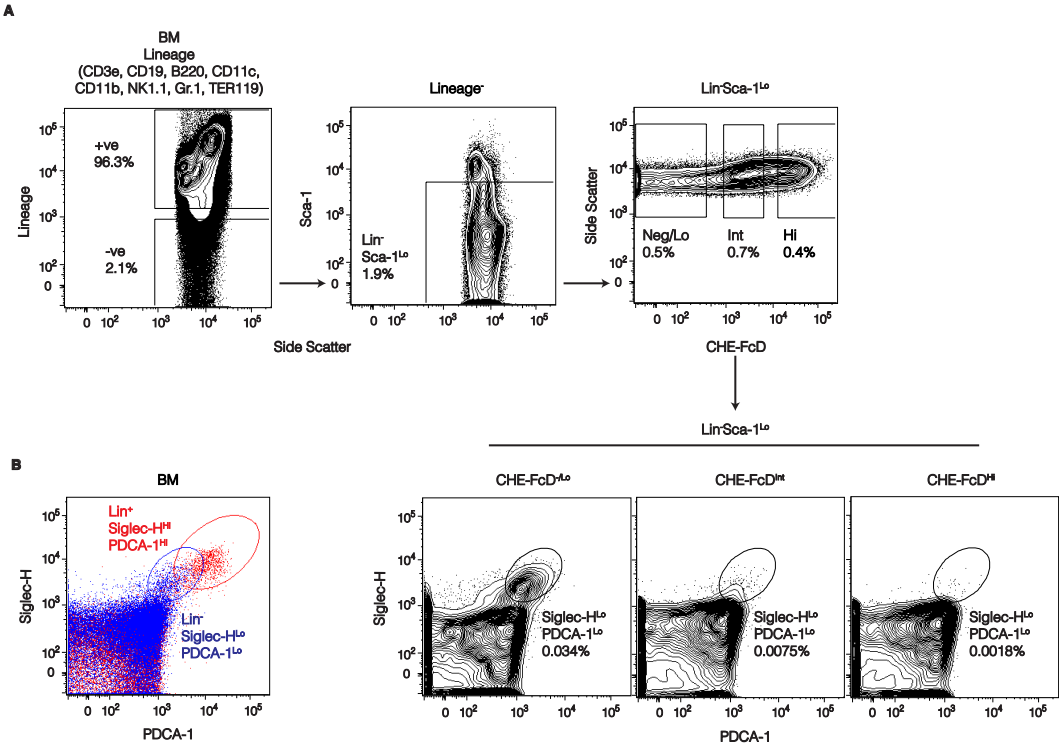

Figure. 2.10. Identification of Siglec-H^{Lo}PDCA-1^{Lo} putative pDC progenitors in the Lin^{-}Sca-1^{Lo}9-*O*-AcSia^{Lo} bone marrow pool. **(**A**)** Flow cytometric analysis for co-expression of Siglec-H and PDCA-1 among Lin^{-}Sca-1^{Lo} bone marrow cells stratified by 9-*O*-AcSia levels. **(**B**)** Siglec-H and PDCA-1 staining of total Lin^{-} cells and of mature pDCs.

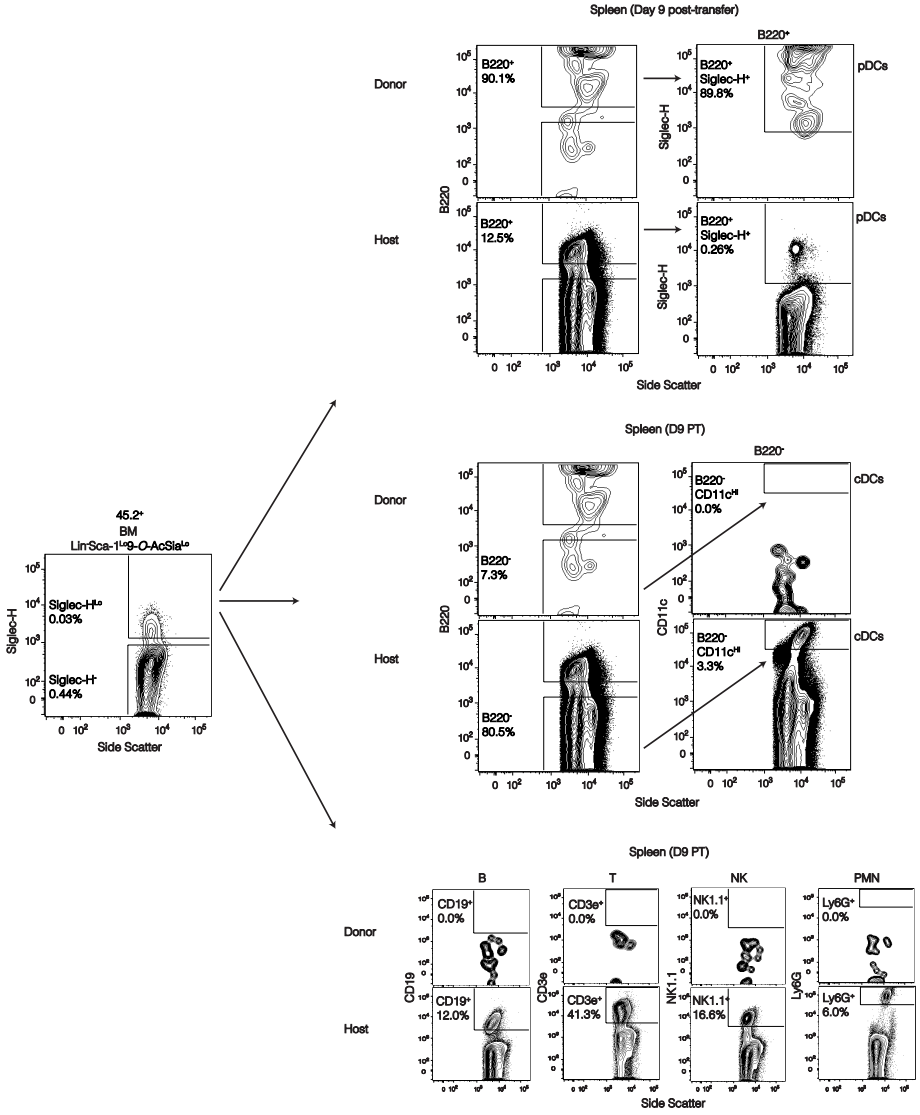

Figure. 2.11. Lin$^-$Sca-1^{Lo}9-*O*-AcSia^{Lo}Siglec-H^{Lo} bone marrow cells represent pre-pDCs — exclusive precursors of pDCs. 1×10^3 sorted Lin$^-$Sca-1^{Lo}9-*O*-AcSia^{Lo}Siglec-H^{Lo} cells from the bone marrow of CD45.2$^+$ mice were intravenously injected into sublethally irradiated CD45.1$^+$mice and donor-derived cells were examined at time points between 4 and 14 days. Flow cytometric analysis of (upper panel) pDCs, (middle panel) cDCs, and (lower panel) non-DC cell types among donor- and host-derived cells. Data is shown in the spleen for day 9 when the number of progeny cells peaked. Percentages are of donor- (CD45.2$^+$CD45.1$^-$) or host-derived (CD45.2$^-$CD45.1$^+$) cells. Data are representative of two independent experiments.

Siglec-H, which is thought to be expressed exclusively on pDCs. Further analyses failed to reveal other myeloid or lymphoid cells among any of the donor-derived cells in the spleen (**Figure 2.11 lower panel**). Markers not found on pDCs were used to identify other lineages. Ly6G was used to identify granulocytes, as antibodies to the commonly used Gr.1 marker also cross-react with Ly6C, a known marker of pDCs (Asselin-Paturel et al., 2001; Dalod et al., 2002; Wrammert et al., 2002). These studies demonstrate that $Lin^{-}Sca\text{-}1^{Lo}9\text{-}O\text{-}AcSia^{Lo}Siglec\text{-}H^{Lo}$ bone marrow cells represent a novel precursor-pDC (pre-pDC) population that is fully committed to pDC development.

PDC progenitors lack myeloid potential

We identified pre-pDCs as cells exclusively committed to pDC development that expressed low levels of Siglec-H in the pool of early bone marrow progenitors with low levels of 9-*O*-AcSia. We reasoned that the larger Siglec-H^{-} fraction of this pool (**Figure 2.12A**) might also contain a progenitor pDC population from which fully committed pre-pDCs arise. To investigate the pDC potential of the Siglec-H^{-} subset, we performed in vivo transfers with these cells. Freshly sorted $Lin^{-}Sca\text{-}1^{Lo}9\text{-}O\text{-}AcSia^{Lo}Siglec\text{-}H^{-}$ from CD45.2 mice were injected into CD45.1 recipients, and donor cells were analyzed. Siglec-H^{Lo} pre-pDCs were identified among donor-derived progeny in the BM at d 4 post-transfer (**Figure 2.12B**). Further examination of the bone marrow and the spleen revealed that transferred

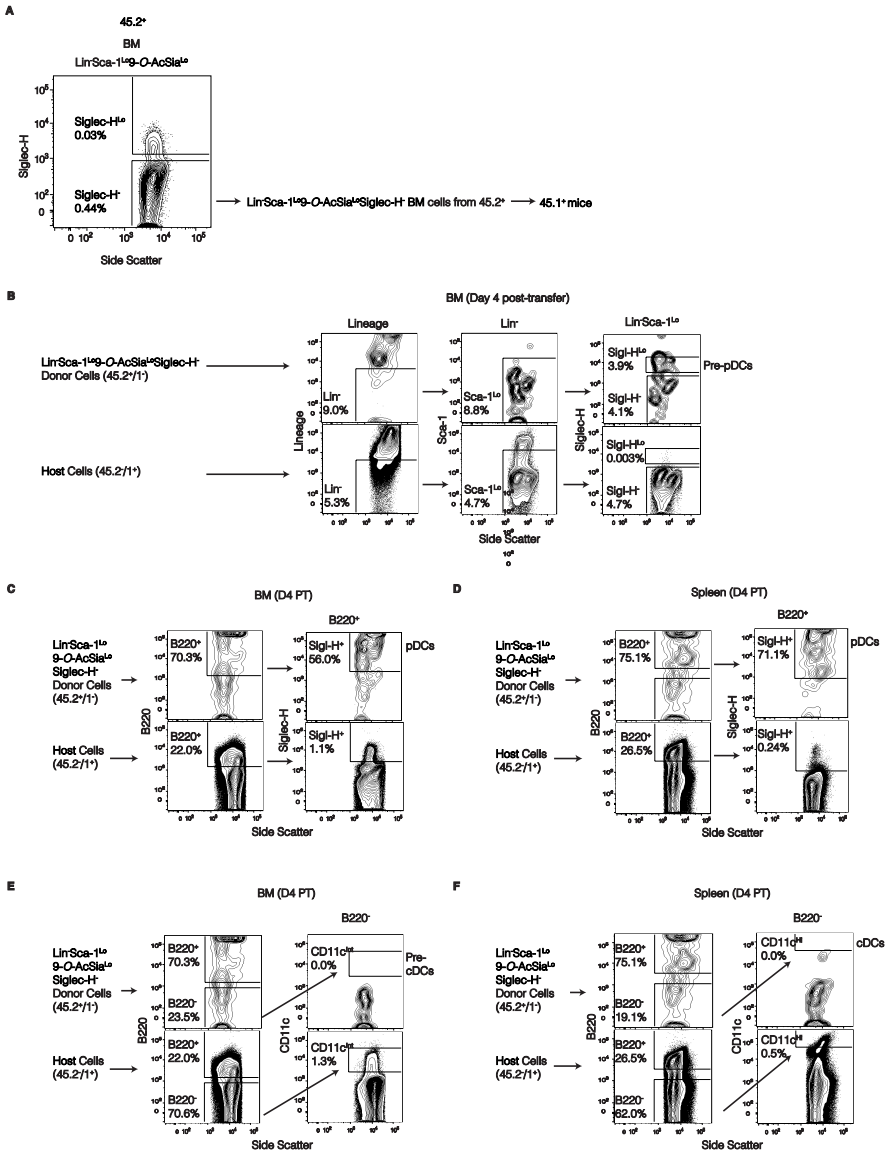

Figure. 2.12. Lin$^-$Sca-1^{Lo}9-*O*-AcSia^{Lo}Siglec-H$^-$ cells give rise to pre-pDCs and pDCs. (A) 1×10^3 sorted Lin$^-$Sca-1^{Lo}9-*O*-AcSia^{Lo}Siglec-H$^-$ cells from the bone marrow of B6 mice (CD45.2$^+$) were intravenously injected into sublethally irradiated B6.SJL mice (CD45.1$^+$) and donor derived cells were examined at time points between 4 and 14 days. Percentages are of donor- (CD45.2$^+$CD45.1$^-$) or host- (CD45.2$^-$CD45.1$^+$) derived cells. Data are representative of two independent experiments. (B) pre-pDC potential of Lin$^-$Sca-1^{Lo}9-*O*-AcSia^{Lo}Siglec-H$^-$ donor cells in the bone marrow. (C-D) pDC potential of Lin$^-$Sca-1^{Lo}9-*O*-AcSia^{Lo}Siglec-H$^-$ donor cells at early time points in the (C) bone marrow and (D) spleen. (E) Examination of Lin$^-$Sca-1^{Lo}9-*O*-AcSia^{Lo}Siglec-H$^-$ donor progeny for exclusive precursors of cDCs (pre-cDCs). (F) cDC potential of Lin$^-$Sca-1^{Lo}9-*O*-AcSia^{Lo}Siglec-H$^-$ donor cells.

cells differentiated preferentially into mature pDCs (**Figures 2.12C, D**) that had low 9-*O*-AcSia levels similar to their endogenous counterparts (**Figure 2.13**). The Siglec-H$^-$ cells did not give rise to pre-cDCs (**Figure 2.12E**) or cDCs (**Figure 2.12F**). These data indicate that the Siglec-H$^-$ fraction of the Lin$^-$Sca-1^{Lo}9-*O*-AcSia^{Lo} bone marrow pool contains progenitors of Siglec-H^{Lo} pre-pDCs that further differentiate into mature pDCs.

Evaluation at later time points (d 8) revealed that donor cells still differentiated preferentially into pDCs (**Figure 2.14A**), but also into other myeloid and lymphoid cells, including cDCs (**Figure 2.14B**), NK cells, and T cells (**Figure 2.14C**). Lin$^-$Sca-1^{Lo}9-*O*-AcSia^{Lo}Siglec-H$^-$ cells are thus a heterogeneous pool that is biased toward pDC development.

We devised an approach to exclude the residual cDC potential from the Lin$^-$Sca-1^{Lo}9-*O*-AcSia^{Lo}Siglec-H$^-$ progenitor pool (**Figure 2.14B**). Our strategy was based on the distinct cytokine requirements for pDC versus cDC development and our phenotypic analysis of pre-pDCs. Flt3L and its receptor Flt3 are essential for cDC and pDC development, DC potential is restricted to the Flt3$^+$ fractions of CLPs and CMPs in transfer experiments, and Flt3L supplementation of BM cultures drives differentiation of pDCs and cDCs only (Schmid et al., 2010). In addition to the role of Flt3, there is a presumed dependence of cDC and myeloid cell development on the M-CSFR [CD115] (Onai et al., 2007; Naik et al., 2007). Injected bone marrow Lin$^-$CD115$^+$ cells

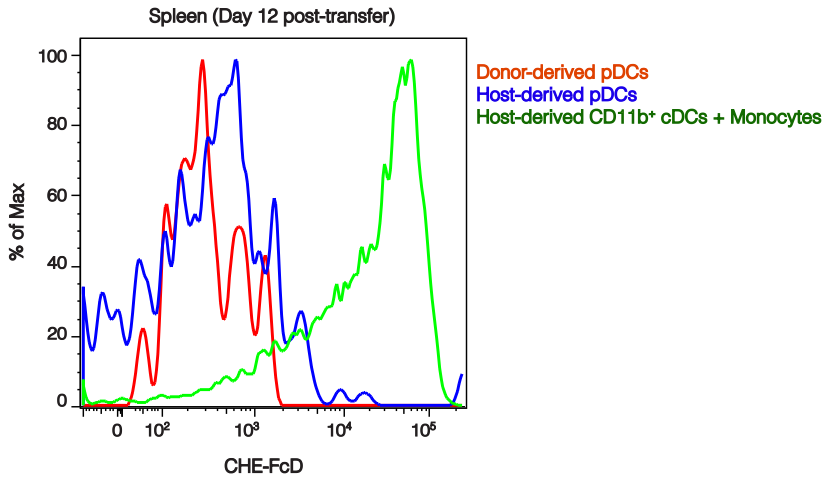

Figure. 2.13. pDCs derived from Lin$^-$Sca-1^{Lo}9-*O*-AcSia^{Lo}Siglec-H$^-$ progenitors and endogenous pDCs have similar low levels of 9-*O*-AcSia. Comparison of CHE-FcD staining in the spleen for pDCs derived from transferred Lin$^-$Sca-1^{Lo}9-*O*-AcSia^{Lo}Siglec-H$^-$ cells and host-derived pDCs and myeloid cells. Data is shown for day 12 post-transfer for experiment described in Figure 2.12.

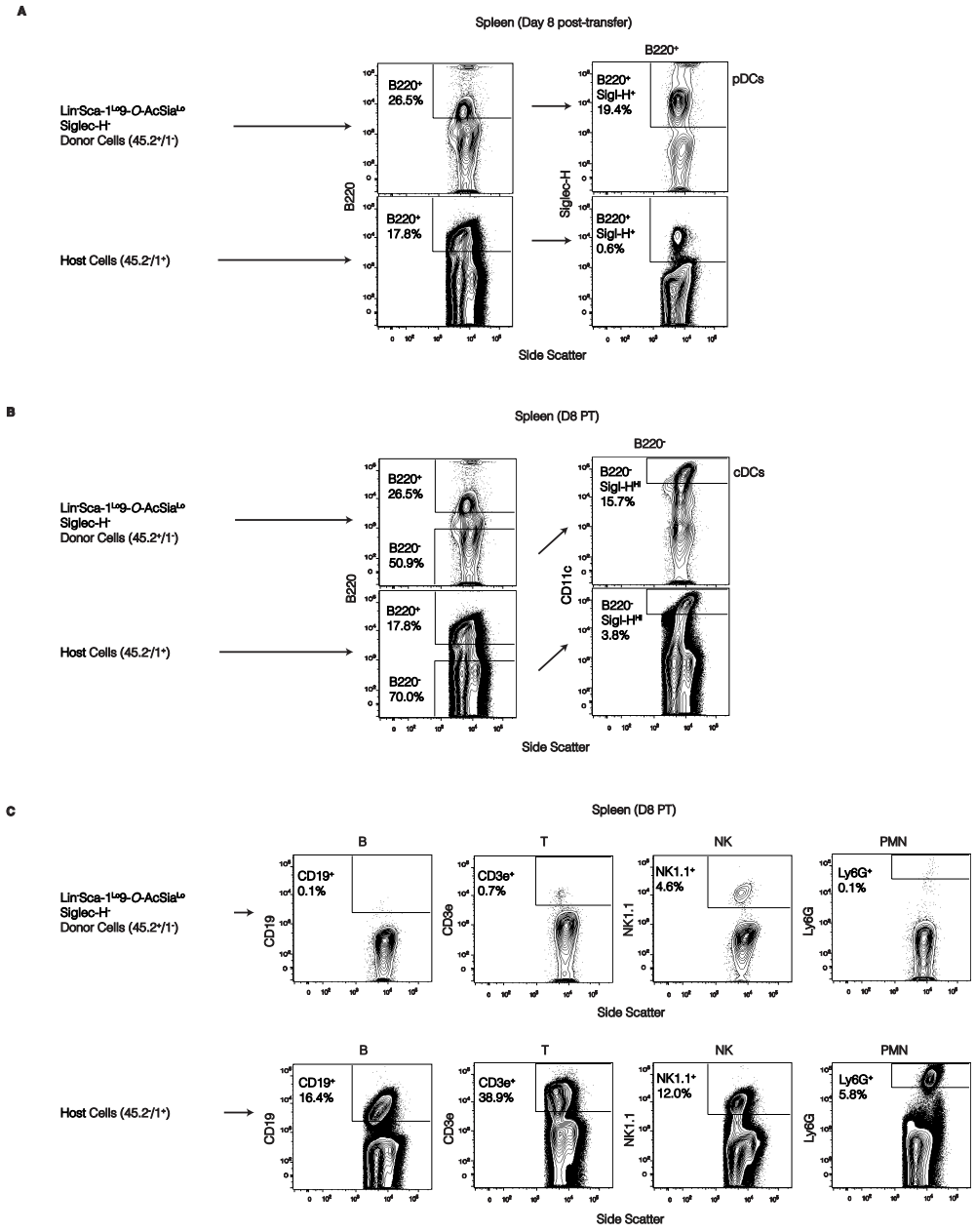

Figure 2.14. Lin$^-$Sca-1^{Lo}9-*O*-AcSia^{Lo}Siglec-H$^-$ cells have non-pDC potential. Data is shown for day 8 post-transfer in the spleen for experiment described in Figure 2.12. Percentages are of donor- (CD45.2$^+$CD45.1$^-$) or host- (CD45.2$^-$CD45.1$^+$) derived cells. Data are representative of two independent experiments. **(**A-B**) (**A**)** pDC and (B) cDC potential of Lin$^-$Sca-1^{Lo}9-*O*-AcSia^{Lo}Siglec-H$^-$ donor cells. (C) Analysis of Lin$^-$Sca-1^{Lo}9-*O*-AcSia^{Lo}Siglec-H$^-$ donor progeny for non-DC cell types.

gave rise to spleen cDCs and marginal zone macrophages, but not to pDCs (Waskow et al., 2008).

Our analysis revealed that most Siglec-H^{Lo} pre-pDCs express Flt3, but not CD115 (**Figure 2.15**), the majority of Lin$^-$Sca-1^{Lo}9-*O*-AcSia^{Lo}Siglec-H$^-$ cells express only Flt3 or CD115 (**Figure 2.16A**), and cDCs express much higher levels of CD115 than pDCs (**Figure 2.16B**). Based on these findings, we reasoned that the Flt3$^+$CD115$^-$ fraction of the Lin$^-$Sca-1^{Lo}9-*O*-AcSia^{Lo}Siglec-H$^-$ bone marrow progenitor pool might contain pDC progenitors that are precursors of pre-pDCs and devoid of cDC potential. We transferred freshly sorted Flt3$^+$CD115$^-$ or Flt3$^-$CD115$^+$ cells from the Lin$^-$Sca-1^{Lo}9-*O*-AcSia^{Lo}Siglec-H$^-$ pool of CD45.2 mice into CD45.1 recipients. Donor cells were analyzed to compare the ability of Flt3$^+$CD115$^-$ and Flt3$^-$CD115$^+$ cells to generate pre-pDCs and pDCs. At early time points in the bone marrow (d 4), we found that Flt3$^+$CD115$^-$ cells were far more effective at giving rise to pre-pDCs than their Flt3$^-$CD115$^+$ counterparts (**Figure 2.17A**). In line with this data, Flt3$^+$CD115$^-$ cells gave rise exclusively to pDCs, but not to cDCs (**Figure 2.17B**) at later time points (d 8) in the spleen. In contrast, Flt3$^-$CD115$^+$ cells lacked pDC potential (**Figure 2.17B**). Analysis of the Flt3$^+$CD115$^-$ cells for non-DC lineage potential demonstrated that over time (d10-d14), these cells maintained the ability of the broader Lin$^-$Sca-1^{Lo}9-*O*-AcSia^{Lo}Siglec-H$^-$ pool to give rise to NK, B, and T cells, but lacked any myeloid potential (**Figures 2.14C** and **2.17C**).

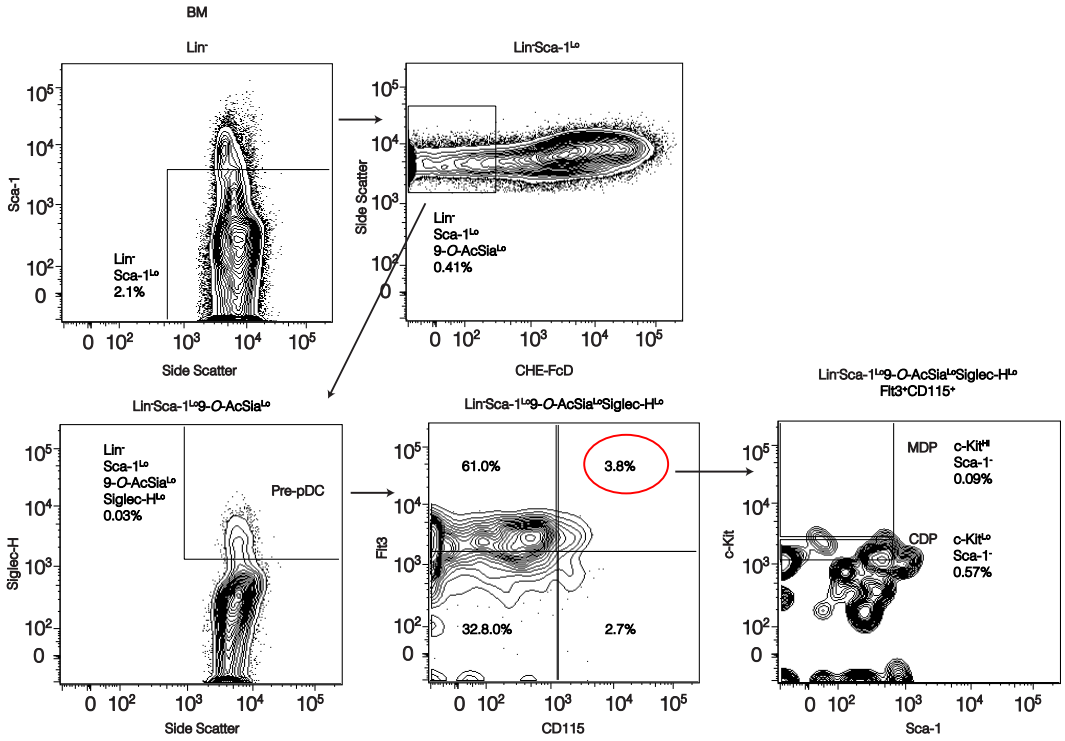

Figure 2.15. Occurrence of MDPs and CDPs among pre-pDCs. The fraction of $Flt3^{+}CD115^{+}$ pre-pDCs was analyzed by flow cytometry for high and low levels of c-Kit to screen for the presence of MDPs and CDPs, respectively.

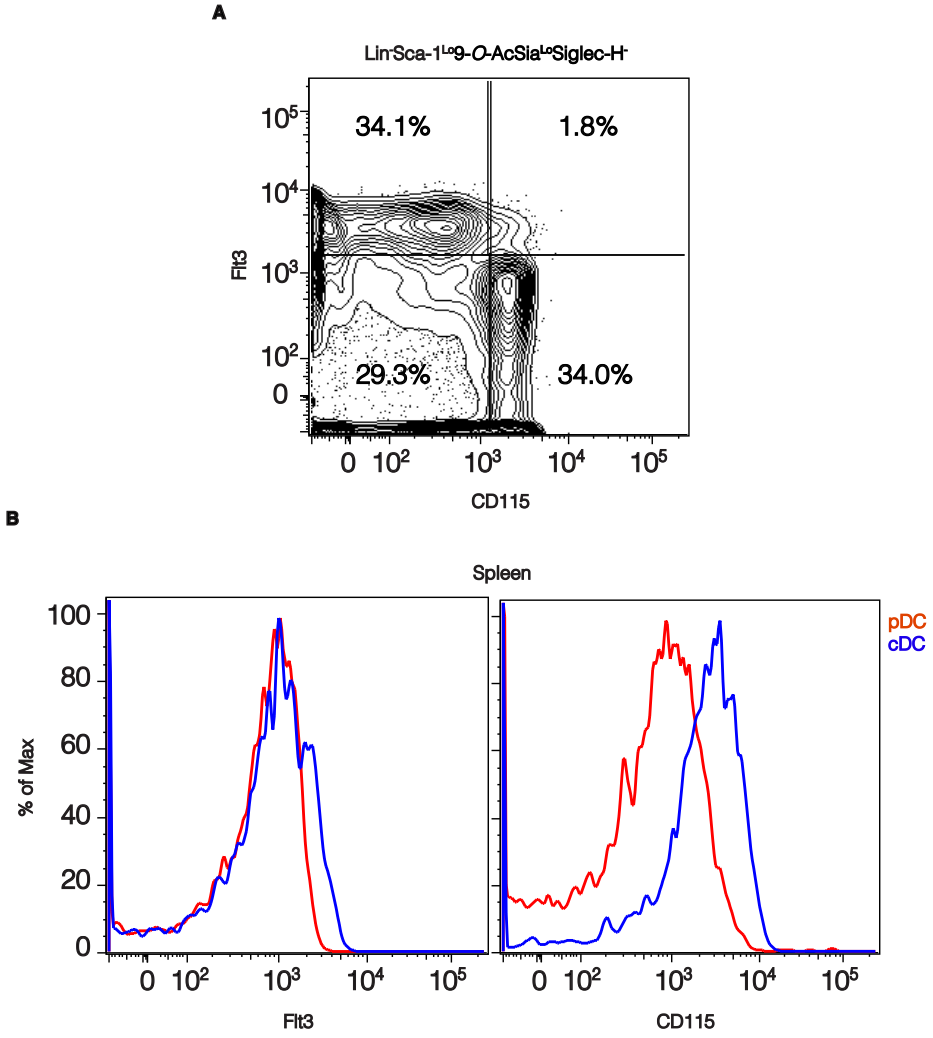

Figure 2.16. Cytokine receptor expression on DCs and their progenitors. **(**A**)** Surface staining for Flt3 and CD115 (M-CSFR) in bone marrow Lin$^-$Sca-1^{Lo}9-*O*-AcSia^{Lo}Siglec-H$^-$ cells. **(**B**)** Comparison of Flt3 and CD115 levels in splenic pDCs and cDCs.

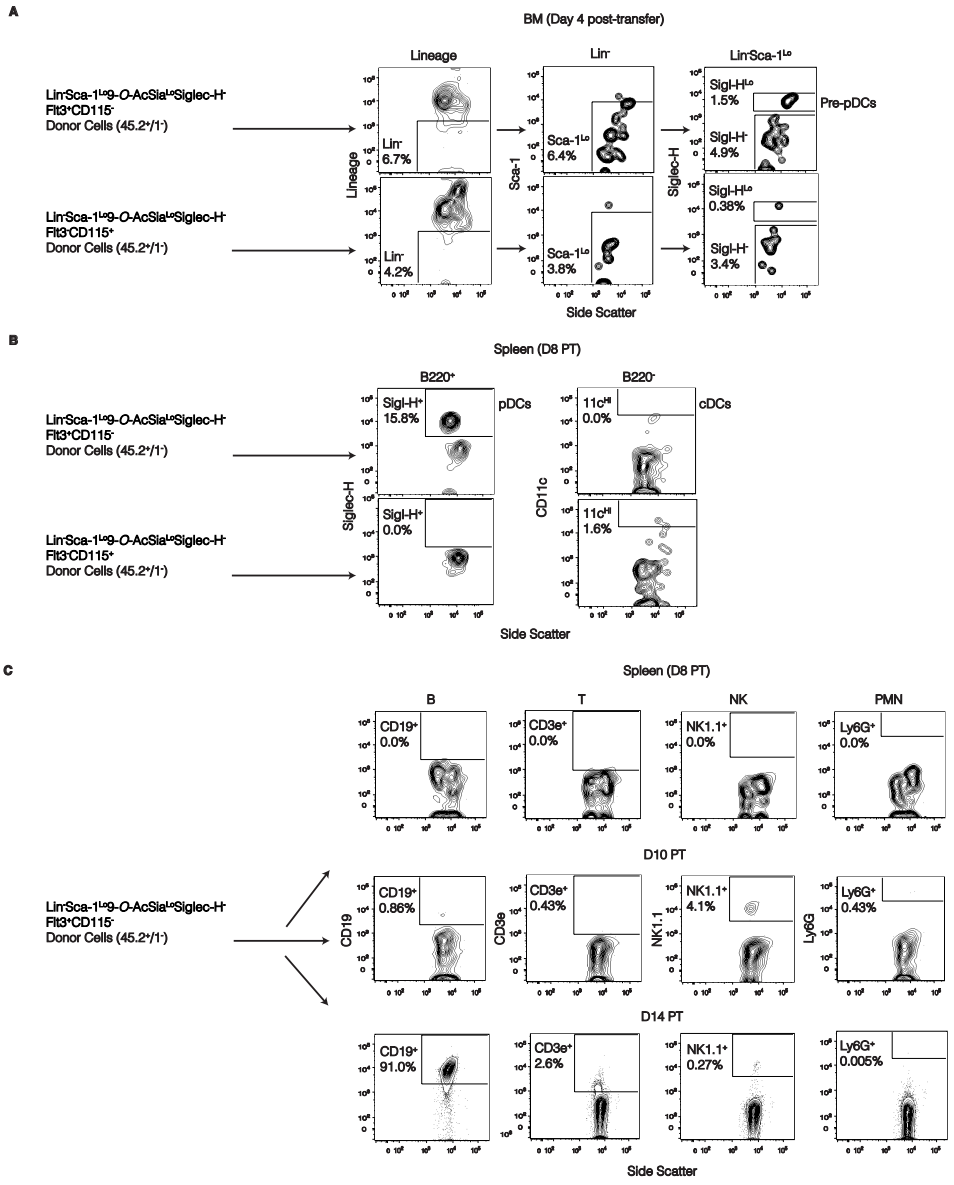

Figure 2.17. Lin$^-$Sca-1^{Lo}9-*O*-AcSia^{Lo}Siglec-H$^-$Flt3$^+$CD115$^-$ bone marrow cells give rise to pre-pDCs and to pDCs, but not to cDCs or any other myeloid cells. 1×10^4 sorted Flt3$^+$CD115$^-$ or Flt3$^-$CD115$^+$ cells from the Lin$^-$Sca-1^{Lo}9-*O*-AcSia^{Lo}Siglec-H$^-$ bone marrow of CD45.2$^+$ mice were intravenously injected into CD45.1$^+$ recipients and donor-derived cells were examined at time points between 2 and 14 days. Percentages are of donor-derived cells. Data are representative of two independent experiments. **(**A-B**)** Donor-derived cells examined for **(**A**)** pre-pDCs in the bone marrow (day 4) and **(**B**)** pDCs and cDCs in the spleen (day 8) of recipients. **(**C**)** Donor-derived cells assessed for non-DC lineage potential in animals receiving Flt3$^+$CD115$^-$ cells.

These findings indicate that the Flt3^{+}CD115^{-} members of the Lin^{-}Sca-1^{Lo}9-*O*-AcSia^{Lo}Siglec-H^{-} bone marrow pool are progenitors of pre-pDCs and mature pDCs that lack potential for cDCs or any other myeloid cells. Previous attempts to separate pDC from cDC development have exploited disparate expression patterns of growth factor receptors but have been unsuccessful at identifying committed pDC progenitors (Onai et al., 2013). Our data reveal, however, that identification of commitment to the pDC lineage and the concomitant absence of cDC potential requires stratifying BM progenitors by levels of 9-*O*-AcSia.

PDC and lymphoid progenitors are distinct

We identified Siglec-H^{-}Flt3^{+}CD115^{-} cells in the 9-*O*-AcSia^{Lo} bone marrow progenitor pool devoid of cDC and myeloid potential, but these cells were still a heterogeneous group that gave rise to lymphoid cells (**Figure 2.17C**). This result was not unexpected since most CLPs are 9-*O*-AcSia^{Lo} (**Figure 2.6B**) and would be expected to overlap with this pool. IL-7R-mediated signals play a non-redundant role in murine T and B cell development, and IL-7R expression was a key marker in the original studies that identified CLPs (Kondo et al., 1997). IL-7 signaling is not required for pDC development or maintenance as demonstrated in IL-7R$\alpha^{-/-}$ and IL-7$^{-/-}$ mice (Yang et al., 2005; Vogt et al., 2009), and IL-7R$\alpha^{-/-}$ and

WT donor cells reconstitute the pDC compartment equally well in sublethally irradiated mice (Takeuchi and Katz, 2006).

We noted that most Lin$^-$Sca-1^{Lo}9-*O*-AcSia^{Lo}Siglec-H$^-$Flt3$^+$CD115$^-$ cells, as well as pre-pDCs and mature pDCs, do not express IL-7Rα (**Figures 2.18A** and **2.19A**), and wished to determine whether pDC developmental potential could be ascribed to a more circumscribed pool of progenitors distinct from IL-7Rα$^+$ CLPs. We used adoptive transfers to compare the lineage potential of IL-7Rα$^-$ and IL-7Rα$^+$ Lin$^-$Sca-1^{Lo}9-*O*-AcSia^{Lo}Siglec-H$^-$Flt3$^+$CD115$^-$ cells, in which CLPs would be restricted to the latter group of cells. Inspection of donor-derived progeny revealed that IL-7Rα$^-$ cells maintained the characteristics of the broader Lin$^-$Sca-1^{Lo}9-*O*-AcSia^{Lo}Siglec-H$^-$Flt3$^+$CD115$^-$ pool and gave rise to pre-pDCs at early time points (**Figure 2.18A upper panel**) and to pDCs at later time points (**Figures 2.18A lower panel** and **2.19B**), without giving rise to cDCs (**Figure 2.19D**). In contrast, their IL-7Rα$^+$ counterparts lacked the ability to give rise to pDCs (**Figure 2.18A lower panel**). Additional analyses revealed that IL- 7Rα$^-$ cells continued to show robust pDC potential at later time points (**Figure 2.19C**). This data suggests that pDC potential can be attributed to the IL-7Rα$^-$ group of Lin$^-$Sca-1^{Lo}9-*O*-AcSia^{Lo}Siglec-H$^-$Flt3$^+$CD115$^-$ cells that is completely distinct from conventionally defined IL-7Rα$^+$ CLPs.

Assessment for other lineage potential, however, revealed that at the time of maximum pDC potential (d 8), IL-7Rα$^-$ cells also gave rise to a small

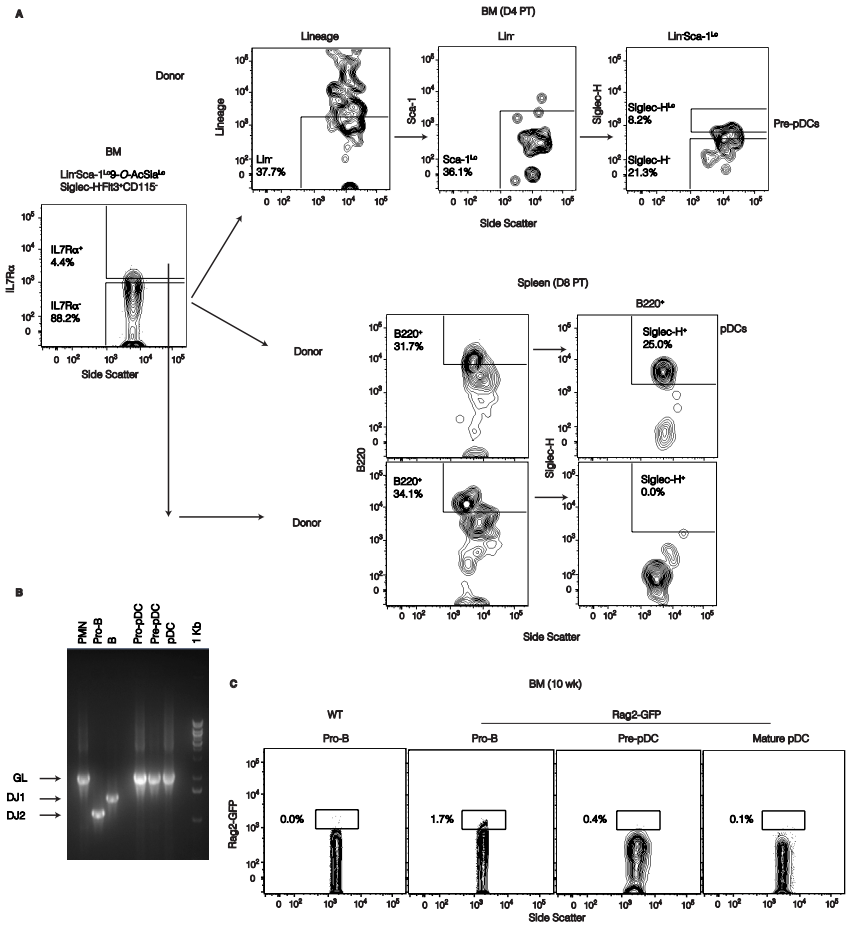

Figure 2.18. Separate progenitors develop into pDCs and lymphocytes. (A**)** IL-7Rα$^-$ or IL-7Rα$^+$ cells from the Lin$^-$Sca-1^{Lo}9-*O*-AcSia^{Lo}Siglec-H$^-$ Flt3$^+$CD115$^-$ bone marrow pool of CD45.2$^+$ mice were injected into CD45.1$^+$ recipients and donor progeny were examined. Percentages are of donor cells. Data are representative of two independent experiments. (Upper panel) Recipients of IL-7Rα$^-$ cells were examined for pre-pDCs. (Lower panel) IL-7Rα$^-$ and IL-7Rα$^+$ donor progeny examined for pDCs. **(**B**)** D-J rearrangement of the *IgH* gene assessed by genomic PCR in pDCs and their progenitors. PMNs served as a negative control and pro-B and B cells served as positive controls. **(**C**)** Rag2 expression in pDCs and their progenitors in Rag2-GFP mice. Pro-B cells served as a positive control for Rag2 expression. GFP levels in pro-B cells from wild-type animals are representative of background staining in all populations shown.

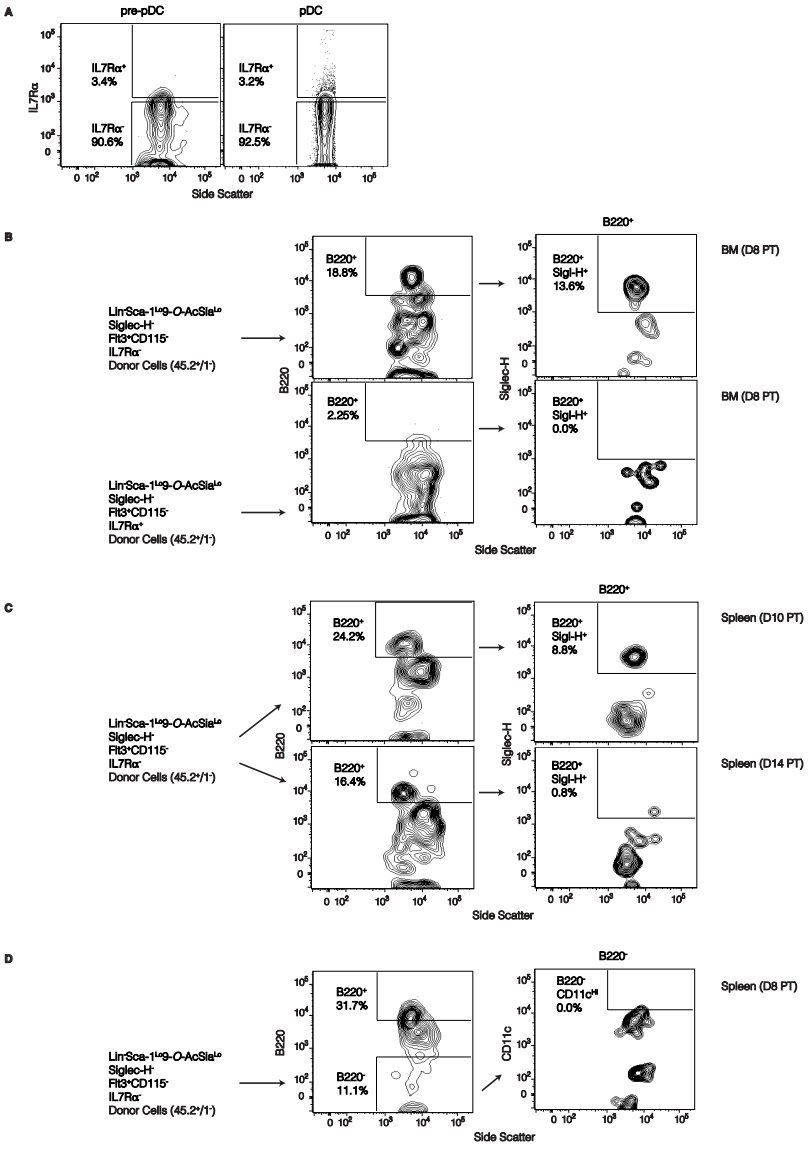

Figure 2.19. Lin$^-$Sca-1^{Lo}9-*O*-AcSia^{Lo}Siglec-H$^-$Flt3$^+$CD115$^-$IL-7Rα$^-$ cells are progenitor-pDCs, distinct from CLPs. (A) Comparison of IL-7Rα$^-$ expression in bone marrow pre-pDCs and mature pDCs. (B-D) 1×10^4 sorted IL-7Rα$^-$ or 2×10^3 IL-7Rα$^+$ cells from the Lin$^-$Sca-1^{Lo}9-*O*-AcSia^{Lo}Siglec-H$^-$ Flt3$^+$CD115$^-$ pool from the bone marrow of CD45.2$^+$ mice were intravenously injected into sublethally irradiated CD45.1$^+$ recipients and donor-derived cells were examined at time points between 2 and 14 days. Percentages are of donor-derived (CD45.2$^+$CD45.1$^-$) cells. Data are representative of two independent experiments. (B) IL-7Rα$^-$ and IL-7Rα$^+$ donor progeny examined for pDC potential in the bone marrow (day 8). (C) pDC potential of IL-7Rα$^-$ donor cells at later time points in the spleen. (D) cDC potential of IL-7Rα$^-$ donor cells.

population of NK cells, while IL- 7Rα^{+} cells had differentiated into B and T lymphocytes (**Figure 2.20A**). The latter is consistent with the CLP potential of the IL-7Rα^{+} transferred pool. Several days later, IL-7Rα^{-} cells gave rise to B and T lymphocytes (**Figure 2.20B**), potentially by traversing an intermediate IL- 7Rα^{+} CLP stage. Based on these results, we term this heterogeneous pool of Lin^{-}Sca-1^{Lo}9-*O*-AcSia^{Lo}Siglec-H^{-}Flt3^{+}CD115^{-}IL-7Rα^{-} cells that is broadly committed to pDC development and separate from conventionally defined IL-7Rα^{+} CLPs, as progenitor-pDCs (pro-pDCs).

These adoptive transfer studies demonstrate separate cellular origins for pDCs and lymphoid cells. We aimed to determine, however, if these developmental pathways might be differentiated at a molecular level. B lymphocyte differentiation absolutely requires the introduction of indelible genetic rearrangements through the process of VDJ recombination at the *IgH* locus. Examination of pDCs revealed the occurrence of D-J rearrangements at the *IgH* locus in a minority of these cells (Corcoran et al., 2003; Shigematsu et al., 2004; Onai et al., 2013; Harman et al., 2006) lending support to a lymphoid affiliation. Complete VDJ events necessary to create a complete antigen receptor heavy chain are never observed, however, bringing into question the potential function of this type of recombination in pDCs, which are innate immune cells. Moreover, D-J rearrangements cannot always be demonstrated in mature pDCs (Pelayo et al., 2005; Sathe et al., 2013; Schlitzer et al., 2011). These

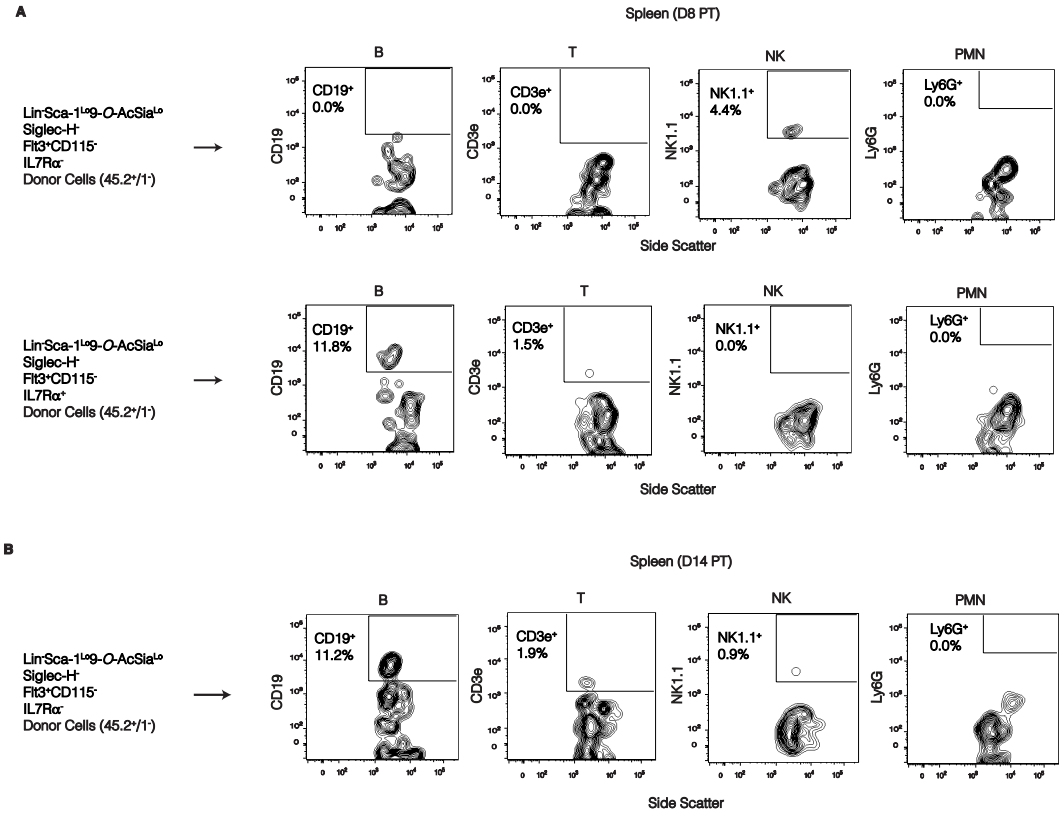

Figure 2.20. Lin$^-$Sca-1^{Lo}9-*O*-AcSia^{Lo}Siglec-H$^-$Flt3$^+$CD115$^-$IL-7Rα$^-$ cells exhibit lymphoid potential at late time periods after transfer. Data is shown for the experiment described in Figure 2.19. (A) Analysis of IL-7Rα$^-$ and IL-7Rα$^+$ donor progeny for non-DC cell types at early time points in the periphery. (B) Examination of IL-7Rα$^-$ donor progeny for non-DC lineages at a later time points.

inconsistencies are likely due to the difficulty in isolating pure pDCs. While B220, PDCA-1, and CD11c are all markers used routinely in pDC purification schemes, each is also found on B cells (Bao et al., 2011; Vinay et al., 2012; Coffman and Weissman, 1981); Rubstov et al., 2011).

We examined pro-, pre-, and mature pDCs (purified using low 9-*O*-AcSia as an additional marker for stringency) and found that these cells lacked D-J rearrangements that were clearly detectable in both pro-B and mature B cells and absent from neutrophils (**Figure 2.18B**). We also studied Rag2-GFP mice and confirmed that Rag-2 is expressed in pro-B cells but not in pre-pDCs or pDCs (**Figure 2.18C**). These results also suggest that the pDC and lymphoid pathways of development are distinct. They also emphasize that the tight definition of pDCs using low levels of Sia 9-*O*-acetylation in combination with Siglec-H expression unequivocally establishes that pDCs are not of lymphoid origin.

Discussion

Our studies underscore the value of separating bone marrow progenitors into two broad pools, one in which cell surface 9-*O*-AcSia levels are low and the other in which they are high. This separation facilitates the delineation of progenitors with distinct developmental potentials. An initial stratification based on 9-*O*-AcSia levels complements and enhances prevalent cell segregation strategies that rely largely on selective expression of distinct growth factor receptors on the cell surface.

Segregating progenitors using levels of 9-*O*-AcSia was a critical step in identifying progenitors of pDCs. While the use of antibodies to growth factor receptors does contribute to the process of defining specific progenitors, their use alone has previously failed to eliminate cDC potential (Onai et al., 2007; Naik et al., 2007; Liu et al., 2009; Onai et al., 2013). Focusing on cells with low levels of 9-*O*-AcSia not only facilitated the categorization of progenitor populations, but also permitted the stringent definition of pDCs, eliminating some of the long-standing ambiguities about the origins and functions of these cells.

We have established the existence of two sequential progenitor populations in the 9-*O*-AcSia^{Lo} pool of Lin^{-} hematopoietic cells that comprise the bone marrow stages in the pathway of pDC development. These studies identified unique pro-pDCs that are distinct from myeloid or lymphoid progenitors, and which differentiate into precursors that we call pre-pDCs. These

pre-pDCs are wholly committed to the pDC lineage and have no potential for any other cell types, including cDCs. This cellular pathway is schematically described in **Figure 2.21**. Our findings taken together support a distinct pathway for pDC development whose inception occurs in the pool of bone marrow progenitors with the lowest levels of 9-*O*-AcSia, and in which the earliest progenitors, broadly committed pro-pDCs, are distinct from CLPs and CMPs. These data also suggest that the pDC potential reported among previously defined progenitor pools likely reflects their contamination by 9-*O*-AcSia^{Lo} pro-, pre-, and mature pDCs themselves.

By revealing that pro-pDCs are indeed distinct from CLPs and any progenitors with myeloid potential these data reinforce the notion developed in recent studies that early hematopoietic progenitors may commit to distinct lineages (Naik et al., 2013; Yamamoto et al., 2013), suggesting that "common" progenitors may not be obligate cellular intermediates during the ontogeny of hematopoietic cells.

Our studies also raise a number of issues unrelated to the developmental pathway outlined above, but that are currently being addressed. Do low 9-*O*-AcSia levels on pDCs have a functional role, perhaps in mediating Siglec dependent attenuation of signaling in pDCs, and conversely, do the high levels seen in cDCs have a functional role in development? What are the glycoconjugates in pDCs and cDCs that exhibit these low and high levels of 9-*O*-

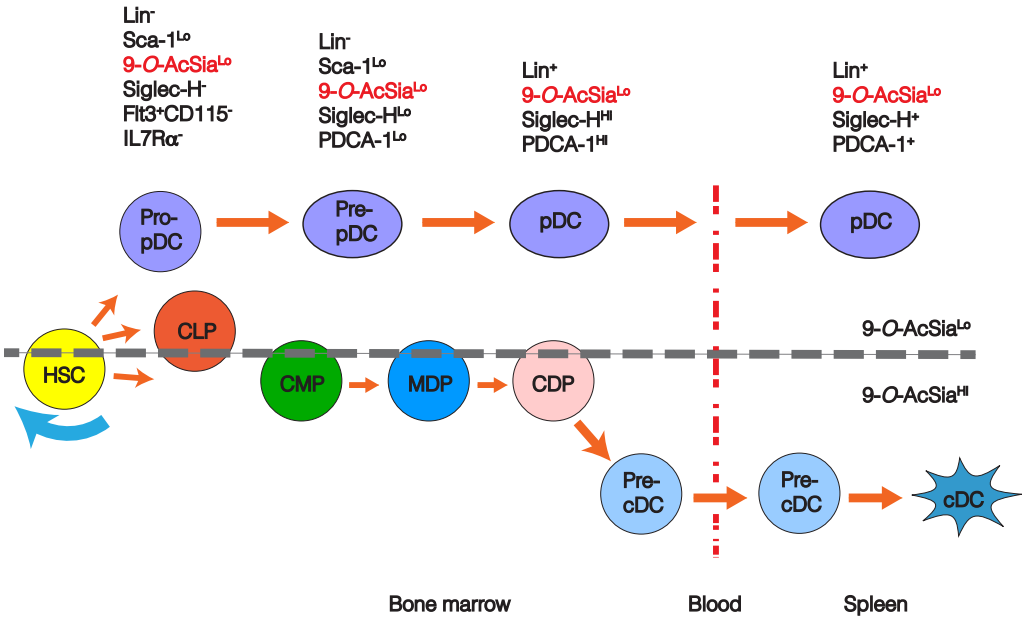

Figure 2.21. The pathway of pDC development. In this model, distinct levels of 9-*O*-AcSia segregate early bone marrow progenitors into two large pools. Progenitors with low levels of this modification include the majority of CLPs, while the pool with high levels includes most CMPs. A three-step cellular sequence for pDC differentiation, distinct from the lymphoid and myeloid streams, can be delineated within the 9-*O*-AcSia^{Lo} pool. This pathway originates from post-HSC pro-pDCs that are broadly committed to the pDC lineage, but are distinct from CLPs and CMPs. Pro-pDCs give rise to pre-pDCs that are committed to pDC development. Pre-pDCs differentiate exclusively into mature pDCs that maintain the low 9-*O*-AcSia levels of their progenitors.

acetylation on Sia moieties, respectively, and do they play a role in cell specification?

We believe that important information about hematopoiesis, that goes beyond the segregation of progenitors and the delineation of the cellular pathway of pDC development, will likely be revealed if increased attention is paid to the *O*-acetylation and deacetylation of Sia moieties on hematopoietic cells.

Chapter 3:

Characterization of pre-plasmacytoid dendritic cells

Introduction

Developmental potential for pDCs has been identified along several routes involving precursors from both myeloid and lymphoid streams, although commitment to this lineage had not been identified previously. In contrast, pre-cDCs, progenitors that exclusively give rise to cDCs have been characterized downstream of a well-described myeloid pathway. In the preceding chapter, our studies of a particular carbohydrate modification, 9-*O*-AcSia, on the surface of bone marrow cells in combination with adoptive transfer approaches helped define pre-pDCs completely committed to pDC development in the steady-state. Pre-pDCs were identified among a lineage negative pool of bone marrow progenitors that like mature pDCs express low levels of 9-*O*-AcSia. These cells additionally express low levels of pDC specific markers, Siglec-H and PDCA-1, and derive from pro-pDCs that lack myeloid and lymphoid potential, and are themselves members of the 9-*O*-AcSia^{Lo} progenitor pool.

In this section, we report on the additional characterization of pre-pDCs, comparing and contrasting these cells with both their mature counterparts and other known progenitors with pDC and cDC potential. Specific topics examined include a further delineation of their phenotype, an exploration of their functional properties, and a description of their migratory behavior.

Materials and methods

Morphological analysis by transmission electron microscopy

Transmission electron microscopy was performed as follows: 2×10^3 freshly sorted pre-pDCs were pelleted at 300 × g in 5 ml PBS for 5 minutes in a 12 × 75-mm round-bottom polystyrene tube and resuspended in 150 µl PBS. Cells were transferred to a 1.5 ml microcentrifuge tube to which 0.5 ml human RBCs were added. The combined cell mixture was pelleted at 300 × g for 5 minutes. Pelleting the small numbers of pre-pDCs with bright red human RBCs "marked" the pellet to enhance its visualization. Importantly, the RBCs could be distinguished from pre-pDCs based on their red color and and lack of nucleus. The combined pellet was then fixed in 2.0% glutaraldehyde in 0.1 M sodium cacodylate buffer, pH 7.4 (Electron Microscopy Sciences, Hatfield, PA) overnight at 4 °C. The pellets were rinsed in the same 0.1 M cacodylate buffer, post-fixed in 1.0% osmium tetroxide in cacodylate buffer for 1 hour at RT, rinsed in the same buffer, and stabilized with a small amount of 2% agarose in PBS to hold them together. They were then dehydrated through a graded series of ethanol dilutions in water to 100% ethanol, followed by propylene oxide, 100%. They were infiltrated with Epon resin (Ted Pella, Redding, CA) in a 1:1 solution of Epon:propylene oxide overnight while being rocked overnight at room temperature. The following day they were placed in fresh Epon for several hours and then embedded in Epon overnight at 60 °C. Thin sections were cut on a Leica

EM UC7 ultramicrotome, collected on formvar-coated grids, stained with uranyl acetate and lead citrate, and examined in a JEOL JEM 1011 transmission electron microscope at 80 kV. Images were collected using an AMT digital imaging system (Advanced Microscopy Techniques, Danvers, MA).

Induction of Type I IFN production by in vivo treatment with TLR ligands

10-wk-old mice were intravenously injected with 200 μl of PBS or resiquimod (R-848, 5 μg in 200 μl of PBS; Invivogen) using an approach adapted from a previously described method (Asselin-Paturel et al., 2005). Splenocytes were harvested 1 hour after injection and initial processing and surface staining was performed as described above, but with the addition of Brefeldin A (10 μg/ml; Sigma-Aldrich) to PBA to enable the detection of intracellular IFN-α. Cells were subsequently processed with the Fix & Perm kit (BD Biosciences) according to the manufacturer's instructions and then stained with a FITC-conjugated rat anti-mouse anti-IFN-α mAb (RMMA-1; PBL InterferonSource) in an excess of rat IgG (Sigma-Aldrich). Stained cells were analyzed by flow cytometry in Chapter 2.

Additional materials and methods are as described in Chapter 2.

Results

Pre-pDCs are distinct from defined DC progenitors

PDCs have been identified among the progeny of CDPs and MDPs, although these progenitors are far more effective at generating cDCs (Onai et al., 2007; Naik et al., 2007; Liu et al., 2009; Auffray et al., 2009). We searched for CDPs and MDPs within the pre-pDC population to confirm that the latter is a distinct cell type unrelated to these cDC progenitors. MDPs and CDPs are rigorously defined to coexpress Flt3 and M-CSFR; only a small minority of pre-pDCs expressed both of these, of which an even smaller fraction expressed c-Kit at levels found on these progenitors (**Figure 2.15**). This result is consistent with the robust 9-*O*-AcSia levels found on most myeloid progenitors (**Figures 2.6C-E**), which are minimally represented in the 9-*O*-AcSia^{Lo} pool that includes pre-pDCs. Similar to CDP-like cells that have greater pDC potential and lower levels of 9-*O*-AcSia than CDPs (**Figure 2.6F**), the majority of pre-pDCs express Flt3, but not CD115. Nevertheless, Siglec-H^{Lo} pre-pDCs are clearly distinct from these cells that lack expression of Siglec-H (Naik et al., 2006).

While the majority of pre-pDCs lack expression of CCR9 (**Figure 3.1**) similar to CCR9^{-} pDC-like progenitors that derive from CDPs (Schlitzer et al., 2001; Schlitzer et al., 2012), the two cell types have very different phenotypes and in vivo pDC differentiation capacity. The latter cells express CD11c and similar high levels of Siglec-H and PDCA-1 as found on mature pDCs; in contrast,

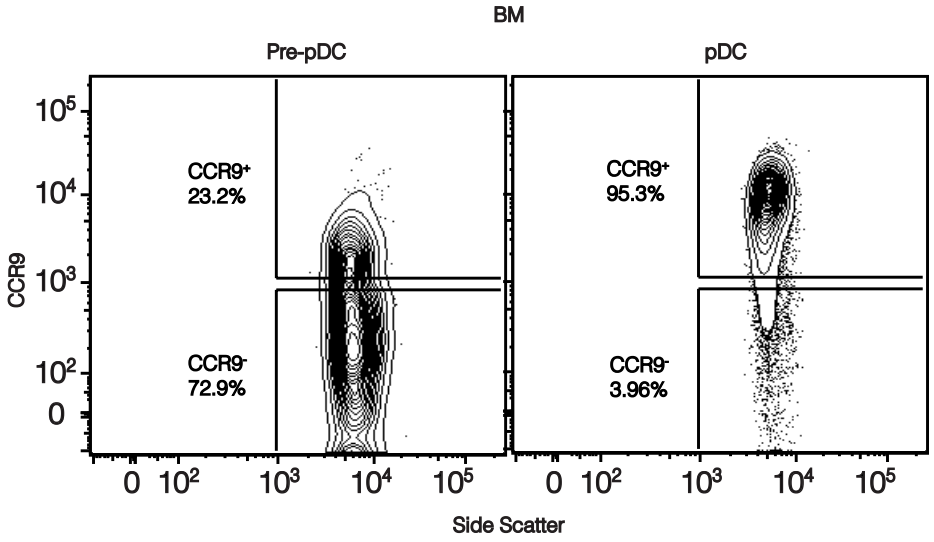

Figure 3.1. Expression of CCR9 on bone marrow pre-pDCs and mature pDCs. Bone marrow pre-pDCs and pDCs from 10-wk-old wild type mice were stained for expression of CCR9 and examined by flow cytometry.

CD11c$^-$ pre-pDCs express lower levels of Siglec-H and PDCA-1 than their mature counterparts. In addition, the majority of CCR9$^-$ progenitors obtained from Flt3L treated animals developed into far more cDCs than pDCs in the spleen on transfer (Schlitzer et al., 2011; Schlitzer et al., 2012), and only into cDCs in Flt3L cultures (O'Keeffe et al., 2012); pre-pDCs, however, develop exclusively into mature pDCs (**Figure 2.11**). The expression of low levels of CCR9 on a minor fraction of pre-pDCs may reflect members of this pool that are closer to becoming mature CCR9$^+$ pDCs (**Figure 3.1**).

MDPs, CDPs, CDP-like cells, and CCR9$^-$ pDC-like common DC progenitors are multipotent progenitors capable of generating cDCs and pDCs, and we wanted to determine if pre-pDCs might share any characteristics with pre-cDCs, which are committed to cDC development. Pre-pDCs were defined in the Lin$^-$ bone marrow fraction that lacks CD11c expression, and are therefore distinct from CD11c^{int} pre-cDCs that are committed cDC precursors (Diao et al., 2006; Liu et al., 2009; Naik et al., 2006). Moreover, while pre-cDCs, which are derived from CDPs in the bone marrow, circulate through the blood to secondary lymphoid organs prior to differentiating into mature cDCs, cells with the pre-pDC phenotype could not be found in the spleen (**Figure 3.2**). Instead, pre-pDCs appear to complete their development into functional pDCs within the bone marrow itself. Taken together, the data suggest that commitment to the pDC lineage is distinct from the myeloid process of cDC development.

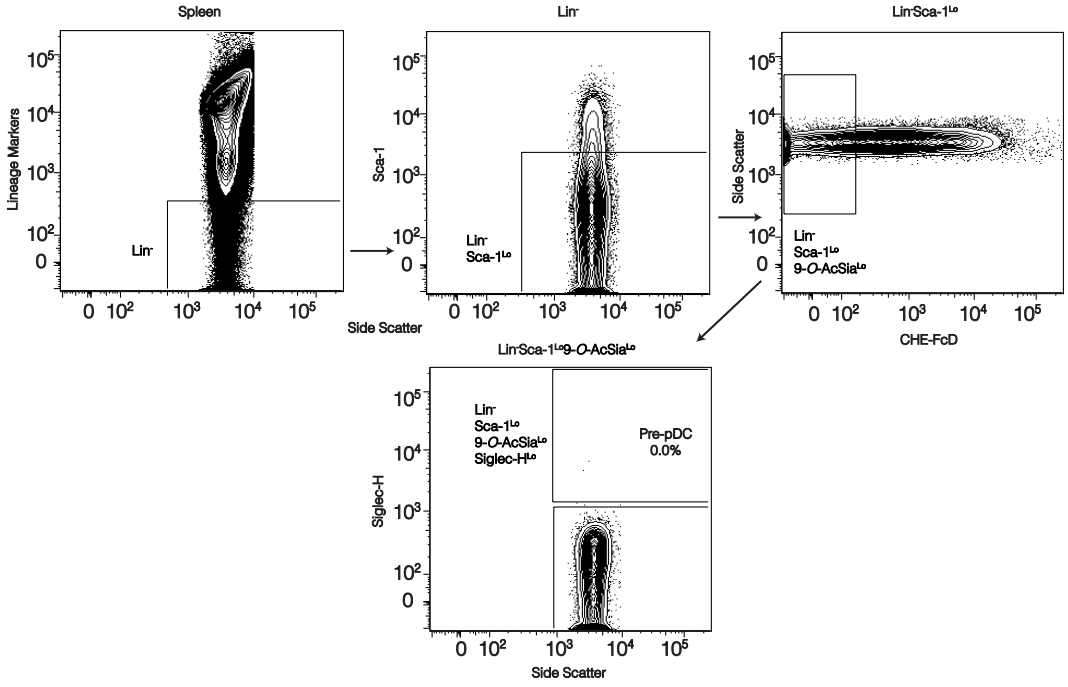

Figure 3.2. Examination of peripheral lymphoid organs for presence of pre-pDCs. Splenocytes from 10-wk-old wild type mice were stained with surface phenotype markers to identify pre-pDCs and examined by flow cytometry.

Pre-pDCs are distinct from mature pDCs

Pre-pDCs are phenotypically distinct from mature pDCs based in part on levels of staining for the pDC markers Siglec-H and PDCA-1 (**Figure 2.10**), but we sought to determine if they exhibited other defining features of pDCs. A functional hallmark of pDCs is their rapid and massive production of Type I IFN when triggered through nucleic-acid sensing TLRs such as TLR7 and TLR9 (Asselin-Paturel et al., 2005; Barchet et al., 2002; Cao and Liu, 2007). We compared the ability of bone marrow pre-pDCs and mature pDCs to make Type I IFN in vivo in response to intravenous injection with resiquimod (R-848), a TLR7 agonist. Intracellular staining for IFN-α was observed in pDCs but not in pre-pDCs underscoring that the latter have not yet acquired the full functional capacity of mature pDCs (**Figure 3.3**). This is in contrast to previously defined pDC progenitors (but which retain cDC potential) that secrete even larger amounts of IFN-α than mature pDCs in response to endosomal TLR stimulation (Schlitzer et al., 2011; O'Keeffe et al., 2012). Electron microscopy revealed that pre-pDCs contain large numbers of cytoplasmic vacuoles as opposed to the extensive rough endoplasmic reticulum (**Figure 3.4**) that is a characteristic morphological adaptation of mature pDCs (Liu, 2005). Similar to pDCs, however, pre-pDCs are spherical and contain nuclei with marginal heterochromatin. Taken together, these studies suggest that pre-pDCs and mature

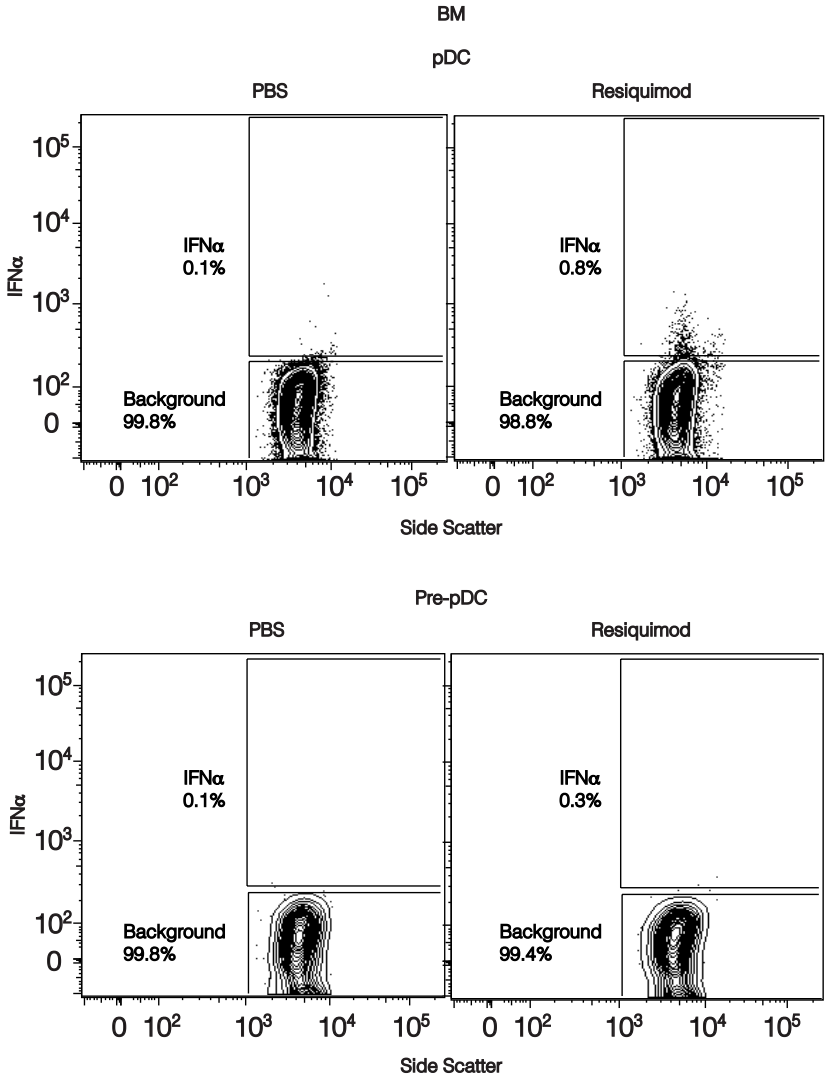

Figure 3.3. Functional characterization of pre-pDCs. In vivo production of Type I IFN by pre-pDCs in response to TLR7 stimulation was assessed. Bone marrow cells from 10-wk-old wild type C57BL/6 mice were collected 1 hour after intravenous injection with PBS or resiquimod (R-848), and stained with surface markers to identify pre-pDCs and pDCs and intracellularly for IFN-α. The background gate was set according to staining for IFN-α in samples from PBS-treated animals. An optimized treatment regime for resiquimod (dose: 5 μg; time point: 1 hour) that elicited the maximal pDC IFN-α production (data not shown), consistent with previous reports was used (Asselin-Paturel et al., 2005). Data are representative of three independent experiments.

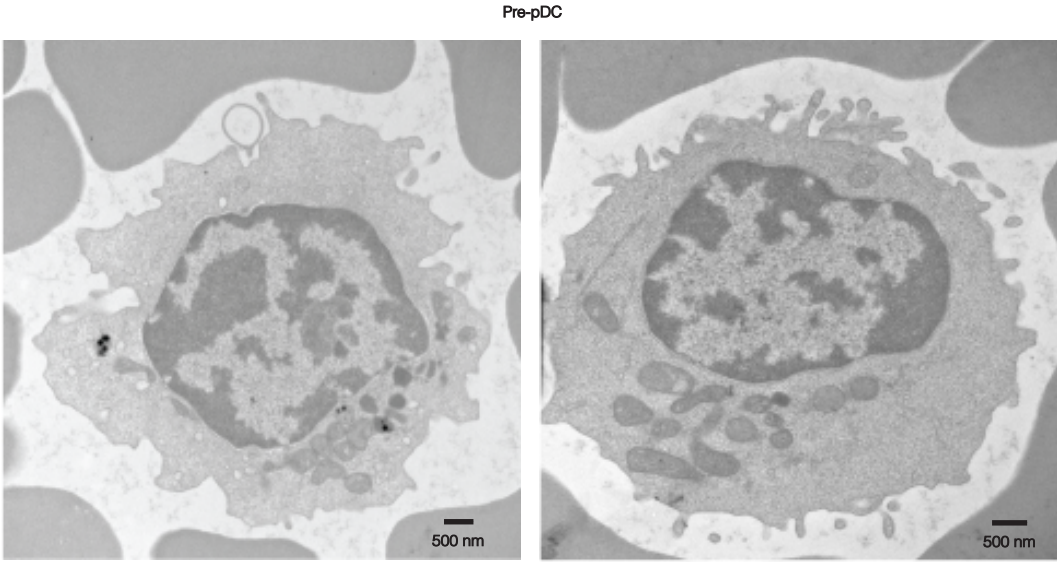

Figure 3.4. Morphology of pre-pDCs. Transmission electron microscopy of bone marrow pre-pDCs from 10-wk-old wild type mice.

pDCs are discrete cells with distinct phenotypic, functional, and structural attributes.

Discussion

The interrogation of pre-pDCs presented here raises a number of issues. In contrast to mature pDCs, pre-pDCs did not produce IFN-α in response to TLR7 stimulation, in keeping with their immature state, but the underlying molecular mechanistic reasons for this difference remain unclear. Perhaps pre-pDCs do not express TLR7 itself or downstream adapter molecules and transcription factors such as MyD88 and IRF7 that are required for pDC Type I IFN secretion in response to all endosomal TLR stimulation (Kerkmann et al., 2003; Izaguirre et al., 2003; Honda et al., 2005), but many other molecular differences could potentially be responsible for this difference. The fractional activation of mature pDCs that we see in these studies is consistent with similar published studies on the in vivo activation of TLR7 in pDCs (Asselin-Paturel et al., 2005). Investigating the pre-pDC response to CpG oligonucleotides that engage TLR9 in addition to determining the expression levels of key genes involved in the Type I IFN response may provide a more complete picture.

Our adoptive transfer data suggests that pre-pDCs complete their differentiation into mature pDCs in the bone marrow and we could not identify pre-pDCs in the spleen. It remains to be determined, however, if pre-pDCs migrate through the blood to other tissues where mature pDCs have been identified. These include the gut (Iwasaki, 2007), where pDCs have been shown to induce T cell-independent IgA production by B cells (Tezuka et al., 2011) and

the thymus (Li et al., 2009), where pDCs promote central tolerance through transport of peripheral antigens and subsequent deletion of antigen-reactive thymocytes (Hadeiba et al., 2012).

In addition to these more direct inferences that may be drawn based on the presented data, pre-pDCs may be utilized as a tool to facilitate definitive studies aimed at clarifying and expanding on several aspects of pDC biology and function. In contrast to cDCs and lymphocytes, which proliferate in situ, little to no proliferation occurs among mature pDCs (Waskow et al., 2008; Liu et al., 2007). While all of DC development depends on signaling through the Flt3L-Flt3 axis, Flt3L administration expands CDPs, pre-cDCs, and cDCs to a far greater extent than pDCs (Vollstedt et al., 2004; Liu et al., 2007) and BrdU incorporation by *Flt3*$^{-/-}$ pDCs is no different than by their wild type counterparts (Waskow et al., 2008). The apparent permanent quiescence of pDCs contributes to the technical challenge of artificially increasing their numbers in vivo. It also impedes an understanding of how the development of pDCs may be boosted in certain physiological contexts that would benefit from their massive and rapid type I IFN secretion, for example, viral infection. The size of the total pDC pool and its generation may not be regulated at the level of the terminally differentiated cell, but at the level of its progenitors, and a careful study of the proliferation and half-life of pre-pDCs and their parent pro-pDCs may prove informative.

While cDCs are considered to be superior stimulators of naïve T cells and pDCs to be the key producers of type I IFNs in response to viral infection, the true functional distinctions between these cells remain ambiguous. This is due in large part to a paucity of pDC specific markers and subsequent difficulty in successfully purifying pDC populations devoid of contamination from other cell types including cDCs. Both cDCs and pDCs have been demonstrated to drive Th_1 polarization, prime and cross-prime $CD8^+$ T cell responses, and induce Treg differentiation (Reizis et al., 2011). Studies using pre-pDCs may help uncover the true roles of pDCs and cDCs in immune responses.

Upregulation of the bHLH transcription factor, E2-2, is required for pDC development in both mice and humans (Cisse et al., 2008). While E2-2 itself activates other transcription factors essential for pDC development including IRF8 and SpiB, the exact cellular stage of and signals for E2-2 induction remain unknown. This gap in our knowledge has prevented the complete elucidation of the molecular networks that drive pDC differentiation. In addition to comparative gene expression profiling of pre-pDCs and pDCs, the ability to purify pre-pDCs from different knockout mice and to transfer them into wild type recipients will allow the examination of the cell intrinsic role of many genes in pDC development and function.

Pre-pDCs may also serve to better enable a determination of the fundamental epigenetic events that govern commitment to the pDC lineage.

Previously described pDC progenitor cells have the potential to differentiate into other myeloid and lymphoid cell types, and therefore may well have a number of genes in a bivalent chromatin state, many of which would eventually be turned "on" or "off" in a mature pDC (Bernstein et al., 2006; Mikkelsen et al., 2007). Pre-pDCs that are already committed to a specific state, however, may already have subsets of genes that will later be expressed in pDCs, already available in a poised "pre-activated" chromatin state, while genes that will not be expressed may be in a "pre-repressed" state. ChIP studies using antibodies to specific histone marks including trimethylated H3K4 (a mark of gene activation) and trimethylated H3K27 (a mark of repression) of pre-pDCs should reveal several key pDC genes in a preactivated state. An analysis of prerepressed genes in pre-pDCs will simultaneously shed light on pathways that may prevent pDC development, and may drive commitment to other lineages.

Given the growing evidence for the importance of type I IFN production in all aspects of immunity, as well as the recently ascribed roles for pDCs in antigen presentation and induction of tolerance, pDCs are emerging as prime targets for immunotherapy. Controlled enhancement of pDC function in chronic viral infections or immunodeficiency may be beneficial. Conversely, autoimmune diseases such as lupus and psoriasis may be treated by targeted inhibition of chronic pDC activation. Insight garnered from investigations with

pre-pDCs may fuel translational research and pave the way to novel pDC-targeted immunotherapies.

Chapter 4:

Investigating the role of 9-*O*-acetylated sialic acid in the development and function of plasmacytoid dendritic cells

Introduction

Prior studies to determine the origins of pDCs searched for developmental potential among classically defined myeloid or lymphoid progenitor pools, but were unable to identify exclusive commitment to this lineage. The previous two chapters demonstrate that classifying bone marrow progenitors not by myeloid versus lymphoid boundaries, but instead by distinct levels of 9-*O*-AcSia played a key role in defining the cellular stages of pDC development (**Figure 2.21**). Importantly, this pathway was distinct from the myeloid and lymphoid streams, both phenotypically and in terms of differentiation potential.

Bone marrow pro-pDCs, their progeny pre-pDCs that are committed to pDC development, and mature pDCs all express low levels of 9-*O*-AcSia, a characteristic maintained by pDCs in the periphery. In contrast, cDCs, cells that are considered to be the closest relatives of pDCs, and their progenitors, all express high levels of 9-*O*-AcSia. The use of a revised phenotypic definition of pDCs to include low levels of 9-*O*-AcSia also helped clarify that these cells do not contain D-J rearrangements at the *IgH* locus, a phenomenon identified inconsistently in previous investigations. In this section, we examine whether low levels of 9-*O*-AcSia, which served as an important marker to decipher the origin of pDCs, are also required for pDC development. The potential relevance of this carbohydrate modification in the function of pDCs is also considered.

Materials and methods

Animals

8-12-wk-old C57Bl/6 and *Cmah* knockout mice that lack exon 6 of the *Cmah* gene and are maintained on a C57Bl/6 background (Hedlund et al., 2007) were used in this study and were purchased from Jackson Laboratories. 8-12-wk-old *Siae* knockout mice that lack exon 2 and are maintained on a C57Bl/6 were described previously (Cariappa et al., 2009). All mice were maintained at the animal facility of Massachusetts General Hospital and all animal procedures were approved by the subcommittee on research animal care at Massachusetts General Hospital.

Gene expression analysis

RNA preparation: $Lin^{-}Sca\text{-}1^{Lo}9\text{-}O\text{-}AcSia^{Lo}$ and $Lin^{-}Sca\text{-}1^{Lo}9\text{-}O\text{-}AcSia^{Hi}$ bone marrow progenitors were isolated from 10-wk-old C57Bl/6 mice as described under Materials and Methods in Chapter 2. RNA was isolated using an RNAeasy micro kit (Qiagen) according to the manufacturer's instructions. RNA integrity was verified by visualization of the 28S and 18S ribosomal RNA bands using RNA 6000 Nano Labchips in an Agilent 2100 Bioanalyzer (Agilent Technologies). Results represent data from three independent pools.

Gene microarray hybridization: All RNA samples for microarray analysis were prepared and hybridized to Affymetrix Mouse ST v1.0. GeneChips (Affymetrix)

containing probes for over 28000 well-annotated genes according to the manufacturer's instructions at the Bauer Core of the FAS Center for Systems Biology of Harvard University. Briefly, total RNA (300 ng/sample) was labeled using the Affymetrix GeneChip cDNA Synthesis and Amplification kit protocol and hybridized to the arrays as described by the manufacturer.

Microarray data analysis: Arrays were scanned on an Affymetrix GeneChip Scanner 3000 7G. GeneChip Operating Software supplied by Affymetrix was used to generate initial data (.CEL) files that were subsequently analyzed and statistically filtered using the BioConductor Suite (http://www.bioconductor.org). Input files were normalized using the Robust Multichip Analysis (RMA) algorithm (Irizarry et al., 2003) and independently using the Model Based Expression Index (MBEI; dChip) algorithm (Li and Wong, 2001). The correlation between the rankings generated by the two algorithms was 0.8. The ranking from each algorithm was considered independently and a combined ranking was also computed. Only probes with at least one significant detection value were included in the analysis. Multiple probes of genes were collapsed to the probe with the highest mean expression value. Statistically significant genes were identified using mixed model analysis of variance with a false discovery rate (Benjamini–Hochberg test) of $P<0.05$ (Benjamini and Hochberg, 1995). Genes with $\log_2$(fold change) < |±2.5| were not considered.

Ex vivo detection of Neu5Gc on murine cells

The blocking solution used for all analysis, manipulations, and dilutions was Neu5Gc-free 0.5% cold water fish skin gelatin in PBS, pH 7.3 containing 1 mM EDTA (Sialix) and all staining reactions were performed at 4 °C. Single-cell suspensions from murine spleen and BM were prepared with blocking buffer as described in Chapter 2. 3-5 × 10^6 cells in 100 µl were stained for 1 hour on ice with polyclonal chicken anti-Neu5Gc IgY (Sialix) or chicken IgY isotype (Sialix) control diluted at 1:400 in blocking solution, similar to previously described approaches (Diaz et al., 2009; Bergfeld et al., 2012). The cells were washed with 5 ml of blocking buffer, mixed gently, and pelleted at 500 ×g for 5 minutes. The cells were then suspended in 100 ul of PE-conjugated Donkey-anti-chicken IgY antibody (Jackson ImmunoResearch), diluted 1:200 in blocking buffer, incubated on ice for 1 hour, and washed as above. Stained cells were then reacted with 2.4G2, an FcγR III/II receptor-blocking antibody, surface stained, and multiparameter flow cytometric analysis was performed as described in Chapter 2.

Additional materials and methods are as described in Chapters 2 and 3.

Results

PDCs maintain low levels of 9-*O*-AcSia in the absence of *Siae*

CD22 is a prominent inhibitory receptor of the Siglec family that is expressed at high levels on murine B lymphocytes. Upon antigen-receptor ligation, it is recruited to the BCR, upon which phosphorylation by the Src family tyrosine kinase, Lyn, of CD22 ITIM tyrosine residues and the subsequent recruitment and activation of the SHP-1 phosphatase ensues. CD22 function is highly dependent on its recognition of α2, 6-linked Sia moieties on N-glycans, and if the latter contain 9-*O*-AcSia, CD22 binding fails (Sjoberg et al., 1994).

SIAE is an enzyme that removes 9-*O*-acetyl moieties from 9-*O*-AcSia (Guimaraes et al., 1996; Takematsu et al., 1999). Originally thought to be lysosomal in location, this enzyme can enter the secretory pathway and can access glycosylated membrane proteins that are ligands of CD22 in a post-Golgi vesicular compartment (Cariappa et al., 2009). Although overexpressed SIAE is secreted, secretion does not occur in vivo (Chellappa et al., 2013). In mice lacking SIAE, we have demonstrated previously that there is enhancement of 9-*O*-acetylation on B cells and a significant reduction in BCR-induced tyrosine phosphorylation of CD22 and of SHP-1 recruitment (Cariappa et al., 2009). In line with these findings, *Siae*$^{-/-}$ mice also exhibit enhanced BCR signaling on calcium flux assays, have impaired development of marginal zone B cells, and a marked reduction in recirculating bone marrow perisinusoidal B cells.

Interestingly, these animals have a stronger autoimmune phenotype than *Cd22*-deficient mice. They spontaneously develop anti-DNA and antichromatin antibodies at an earlier age and develop immune complex glomerulonephritis not found in the latter (Cariappa et al., 2009). It is therefore possible that the phenotype in *Siae*-null animals might reflect a role for this enzyme that extends beyond B lymphocytes, to other cell types including innate immune effector cells, such as pDCs.

Since we had demonstrated that pDCs and their progenitors express low levels of 9-*O*-AcSia that are similar to the levels observed on B cells (**Figures 2.3A** and **2.10**) and given the importance of enzymatic modulation of levels of 9-*O*-AcSia by SIAE in regulating B cell behavior, we sought to determine whether SIAE might also influence the development and function of pDCs. As an initial step, we compiled microarray data provided by the ImmGen Consortium to assess how expression of *Siae* in pDCs compared to that in B cells and myeloid cell populations (Heng et al., 2008). As shown in **Figure 4.1**, pDCs express higher mRNA levels of *Siae* than B cells, and our expectation was that levels of 9-*O*-AcSia on these cells would increase in the absence of *Siae*. While CHE-FcD staining in $Siae^{-/-}$ B cells increased slightly as previously described (**Figure 4.2B)**, it did not change in $Siae^{-/-}$ splenic pDCs, which maintained low levels of surface 9-*O*-AcSia (**Figure 4.2A**). Bone marrow pre-pDCs and pDCs also continued to demonstrate low levels of CHE-FcD staining in the absence of *Siae* (**Figure 4.3)**.

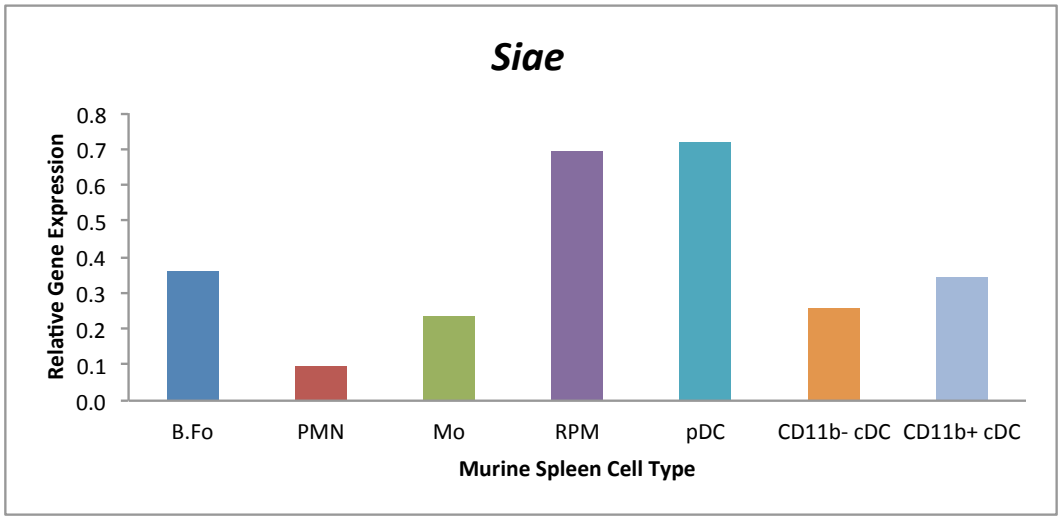

Figure 4.1. pDCs express high levels of *Siae*. Shown are values of relative gene expression that are normalized to maximum expression of *Siae* across all cell types (represented in ImmGen data) and presented in a linear scale. B.Fo, Follicular B cell; PMN, polymorphonuclear leukocyte; Mo, monocyte; RPM, red pulp macrophage; pDC, plasmacytoid dendritic cell; $CD11b^-$ cDC, $CD11b^-$ conventional dendritic cell; $CD11b^+$ cDC, $CD11b^+$ conventional dendritic cell. This figure is based on data assembled by the ImmGen Consortium (Heng et al., 2008).

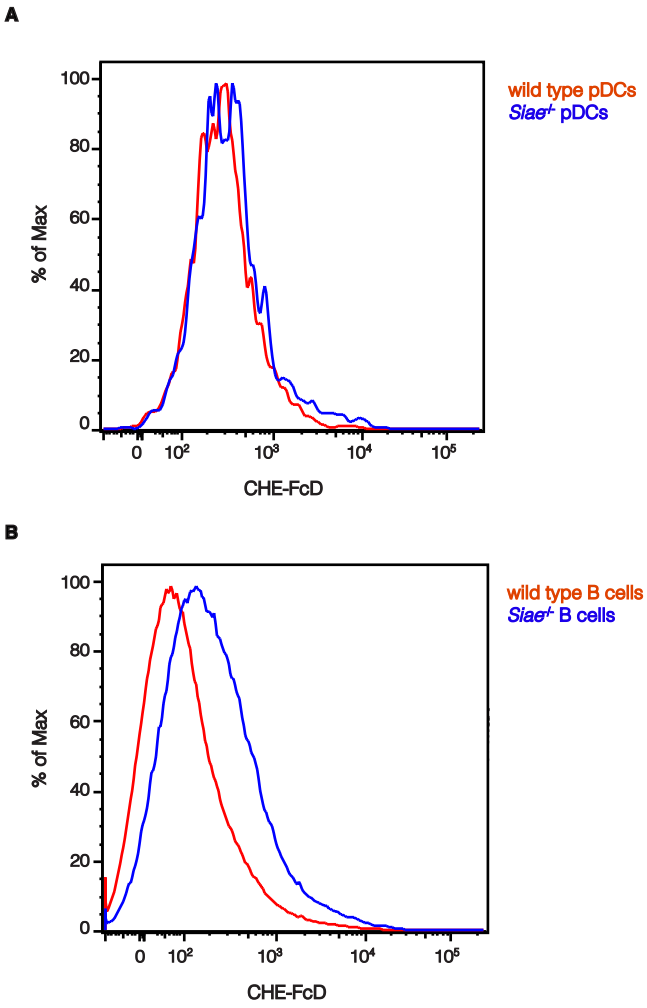

Figure 4.2. Surface levels of 9-*O*-AcSia on pDCs and B cells from *Siae*$^{-/-}$ animals. CHE-FcD staining of (A) pDCs and (B) B cells from the spleens of 10-wk-old wild type and *Siae*$^{-/-}$ mice.

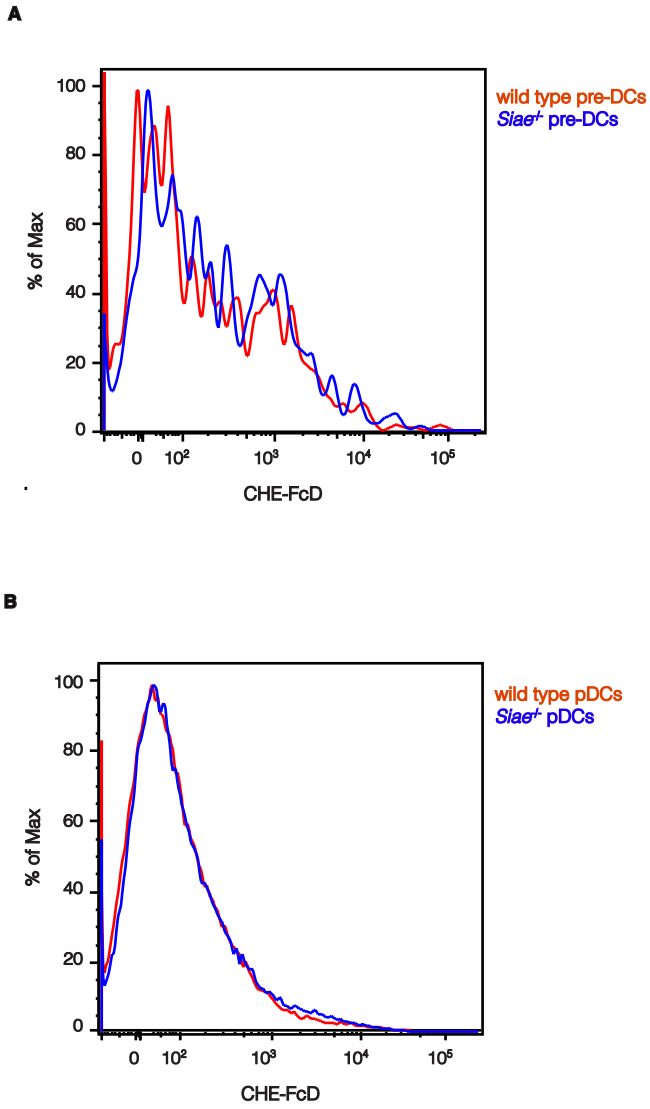

Figure 4.3. 9-*O*-AcSia levels on bone marrow *Siae*-null pre-pDCs and mature pDCs. CHE-FcD staining of pre-pDCs and pDCs from the bone marrows of 10-wk-old wild type and *Siae*$^{-/-}$ mice.

Based on this data, a direct role for *Siae* in regulating levels of 9-*O*-AcSia on pDCs and their progenitors is not apparent.

Altered patterns of surface 9-*O*-AcSia on myeloid cells in the absence of *Siae*

As described earlier, while overall CHE-FcD staining in the total splenic $CD11c^{Hi}$ cDC compartment is high (**Figure 2.3**), discrete levels of 9-*O*-AcSia correlate with functionally distinct cDC subsets. Specifically, $CD8\alpha^+$ cDCs can clearly be distinguished by lower intensity staining for CHE-FcD from the $CD4^-CD8\alpha^-$ and $CD4^+$ subsets, which express similar high levels (**Figure 2.5**). In *Siae*$^{-/-}$ animals, levels of 9-*O*-AcSia on $CD8\alpha^+$ cDCs increased to those found on $CD4^-CD8\alpha^-$ and $CD4^+$ cDCs, while the levels of 9-*O*-AcSia on the latter cell types did not change (**Figure 4.4**). Interestingly, *Siae* mRNA expression in cDC subsets is similar to that in B cells (**Figure 4.1**) and increases in CHE-FcD staining in *Siae*$^{-/-}$ animals might have been expected, although more so in $CD4^-CD8\alpha^-$ and $CD4^+$ cDCs in which *Siae* expression was higher than in the $CD8\alpha^+$ cDC subset.

Examination of non-DC myeloid cell types that have robust surface 9-*O*-AcSia (**Figure 2.3B**) also yielded notable results. Consistent with their high level *Siae* expression (**Figure 4.1**), 9-*O*-AcSia levels increased on red pulp macrophages in the absence of *Siae* (**Figure 4.5A)**. High level CHE-FcD staining remained unchanged on neutrophils (**Figure 4.5B**), which was predictable since they had the lowest levels of *Siae* expression among members of the myeloid

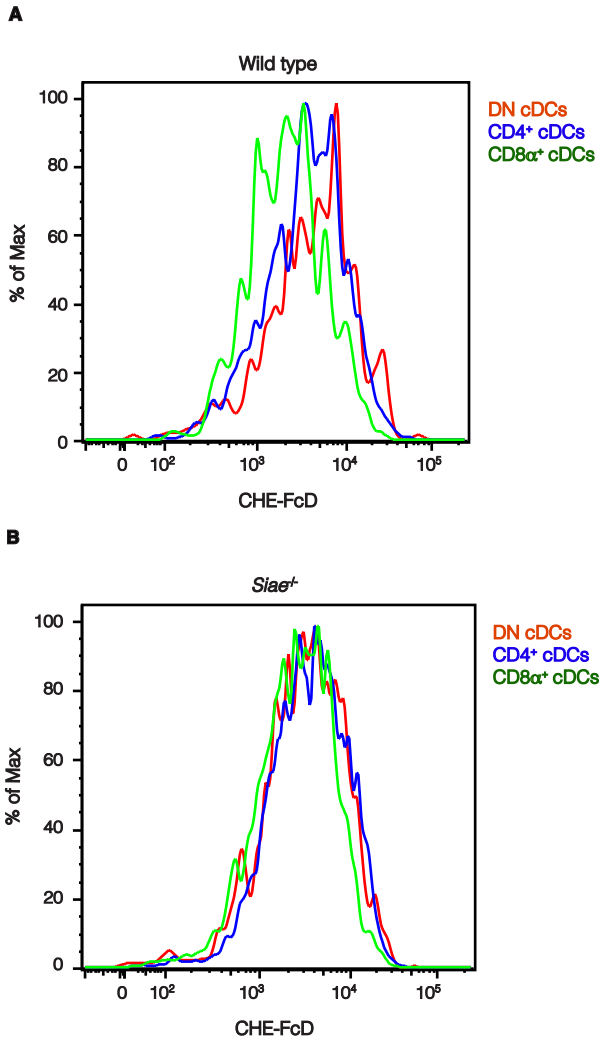

Figure 4.4. Patterns of 9-*O*-AcSia on cDC subsets in the absence of *Siae*$^{-/-}$. CHE-FcD staining of double-negative (CD4$^-$CD8α$^-$; DN), CD4$^+$, and CD8α$^-$ conventional dendritic cells (cDCs) from spleens of 10-wk-old (A) wild type and (B) wild *Siae*$^{-/-}$ mice.

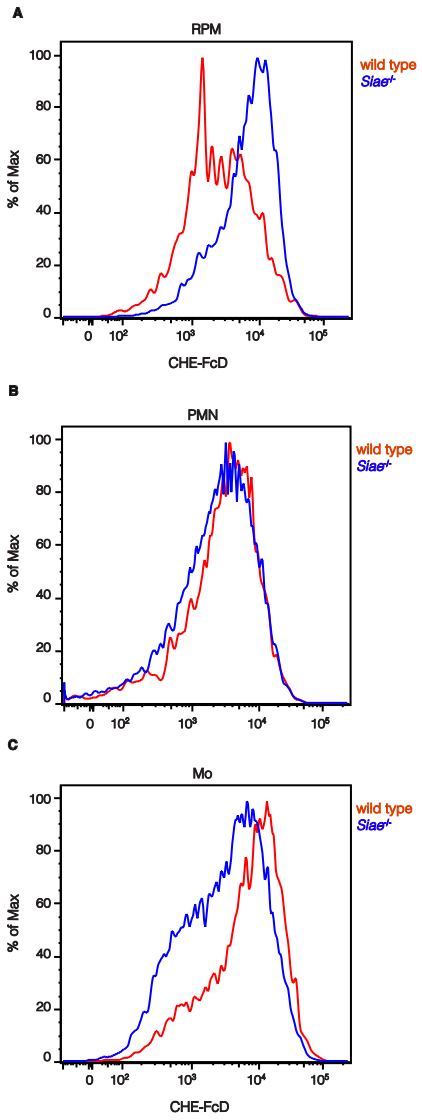

Figure 4.5. 9-*O*-AcSia levels on non-DC myeloid cells in *Siae*$^{-/-}$ mice. CHE-FcD staining on (A) red pulp macrophages (RPM), (B) polymorphonuclear leukocytes (PMN) and (C) monocyes (Mo) from spleens of 10-wk-old *Siae*$^{-/-}$ mice.

compartment (**Figure 4.1**). Interestingly, monocytes that have modest levels of *Siae* expression (**Figure 4.1**) demonstrated reduced levels of 9-*O*-AcSia in *Siae*$^{-/-}$ mice (**Figure 4.5C)**. This alteration may reflect cell-extrinsic effects of *Siae*, although the mechanism is not obvious.

PDCs are significantly reduced in the periphery of *Siae*-deficient animals

To further characterize potential effects of the absence of *Siae* in pDCs, I examined their absolute numbers in addition to those of myeloid cells in the spleens of *Siae*$^{-/-}$ mice. We have previously shown that these animals have a dramatic leukopenia that is characterized in the spleen by a striking decrease in marginal zone B cells (Cariappa et al., 2009). As shown in **Table 4.1A**, a comparison of total white blood cell counts in wild type and *Siae*$^{-/-}$ mice confirmed this leukopenia. Among the myeloid cells, there were significant changes in absolute numbers of almost all cell types, including a greater than two-fold increase in granulocytes and three-fold increase in red pulp macrophages. The most outstanding finding by far, however, was the seven-fold reduction in the total number of pDCs.

Bone marrow production of pDCs is unimpaired in *Siae*$^{-/-}$ mice

To determine if this reduction in pDCs was due to their reduced production in the bone marrow, we next assessed the numbers of pDCs and their progenitors in the

Table 4.1. Absolute numbers of pDCs and their progenitors in wild type and *Siae*$^{-/-}$ mice.

Table 4.1A

Absolute numbers of pDCs and myeloid cells in the spleen of *Siae*$^{-/-}$ mice			
Population	**C57BL/6***	***Siae*$^{-/-}$***	**Fold Change**
pDCs	42 (1.9)	6 (0.3)	-7.0
cDCs	151 (2.3)	101 (0.4)	-1.5
RPMs	6 (0.7)	20 (1.3)	+3.3
PMNs	26 (0.9)	54 (1.2)	+2.1
Monocytes	59 (1.5)	38 (0.7)	-1.6
Total cell count	11167 (371)	2984 (352)	-3.7

*, mean (SD) x 10^4; n = 8 mice per group

Table 4.1B

Absolute numbers of pDCs and B cells in the bone marrow of *Siae*$^{-/-}$ mice			
Population	**C57BL/6***	***Siae*$^{-/-}$***	**Fold Change**
pDCs	9.5 (0.6)	12 (1.2)	+1.3
B cells	230 (3.7)	166 (2.5)	-1.4
Granulocytes	37 (0.9)	86 (1.7)	+2.3
Total cell count	1543 (428)	1889 (519)	+1.2

*, mean (SD) x 10^4; n = 3 mice per group

Table 4.1C

Absolute numbers of pDC progenitors in the bone marrow of *Siae*$^{-/-}$ mice			
Population	**C57BL/6***	***Siae*$^{-/-}$***	**Fold Change**
pro-pDCs	1.2 (0.3)	1.4 (0.4)	-1.1
pre-pDCs	.23 (0.02)	.22 (0.01)	+1.2
Total cell count	1543 (428)	1889 (519)	+1.2

*, mean (SD) x 10^4; n = 3 mice per group

BM. As shown in **Table 4.1B**, the total white cell count in the bone marrow in *Siae*-deficient animals is similar to that of wild type counterparts, and there is a decrease in B lymphocytes, consistent with a selective loss of recirculating perisinusodal B cells as previously noted (Cariappa et al., 2009). Interestingly, we observed a greater than two-fold expansion among granulocytes that may be the basis for their increase in the spleen (**Table 4.1A**). A corresponding "swelling" in the SSC^{Hi} granulocyte gate of $Siae^{-/-}$ mice could easily be identified (**Figure 4.6**). Absolute numbers of pDCs as well as of their parent pro- and pre-pDCs in the bone marrow of wild type and $Siae^{-/-}$ mice, however, were similar (**Table 4.1C**), indicating that the development of this lineage was not compromised. It is formally possible that the severe pDC deficit observed in the periphery could be due to their retention in the bone marrow, but this is unlikely since the bone marrow pDC compartment was not enlarged.

Selective loss of pDCs in the absence of Siae cannot be explained by pDC to cDC conversion

As described in Chapter 1, there is evidence to support the view that activated pDCs undergo a conversion into $CD11c^{Hi}$ cDCs. When bone marrow pDCs from LCMV infected animals were transferred into congenic naïve recipients, they generated cDCs with characteristic dendrites and increased expression of costimulatory MHC class II molecules to levels observed on cDCs of recipient

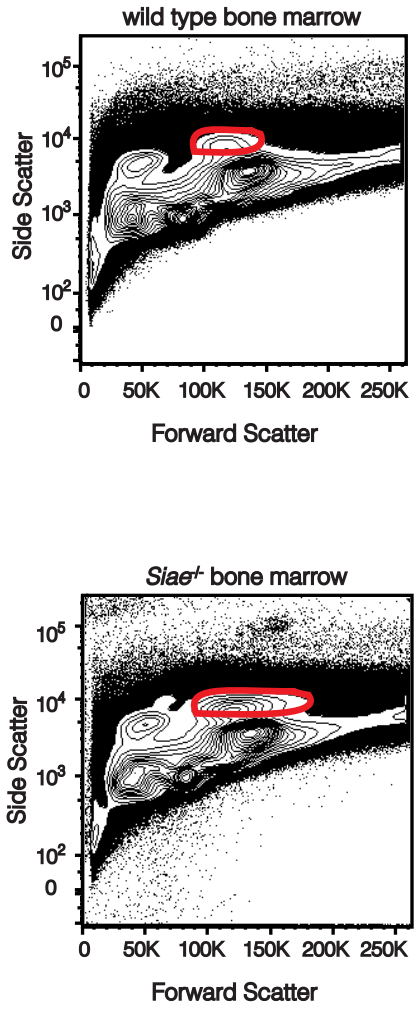

Figure 4.6. A comparison of the forward versus side scatter characteristics of bone marrow cells from wild type and *Siae*$^{-/-}$ mice. Cells with high side scatter (including granulocytes) from 10-wk-old (Upper panel) wild type and (Lower panel) *Siae*$^{-/-}$ mice are outlined in red.

origin (Liou et al., 2008; Zuniga et al., 2004). Furthermore, these pDC-derived cDCs could prime LCMV-specific T cells as well as endogenous cDCs from LCMV-infected mice. In another study, deletion of E2-2, a transcription factor required for pDC development, from mature pDCs caused their spontaneous differentiation into cDC-like cells that had acquired a cDC phenotype, morphology, and antigen-presentation capacity (Zuniga et al., 2004).

To address if *Siae*$^{-/-}$ pDCs might be converting into cDCs, we examined their expression profiles of key pDC lineage markers. As shown in **Figure 4.7**, in the absence of *Siae*, levels of pDC-specific markers, Siglec-H and PDCA-1, did not change. In addition, staining intensity of B220, which is a pDC-defining marker within the DC compartment, was also maintained on *Siae*-deficient pDCs (**Figure 4.7**). In the presence of conversion, reduced expression of all of these markers would have been expected. Staining for CD11c, which is found at much higher levels on cDCs than on pDCs, was also indistinguishable between *Siae*$^{-/-}$ and wild type pDCs (**Figure 4.7**). Expression of costimulatory molecules CD80 and CD86 as well as CD40, all of which are characteristically higher on cDCs than on pDCs, also was not different on *Siae*$^{-/-}$ pDCs **(Figure 4.8**). Furthermore, levels of MHC class II which are higher on cDCs than on pDCs, presumably because of the greater antigen-presentation capabilities of the former, decreased on pDCs in the absence of *Siae* (**Figure 4.8**). Taken together, this data suggests that pDCs are not undergoing conversion into cDCs in the absence of *Siae*. That

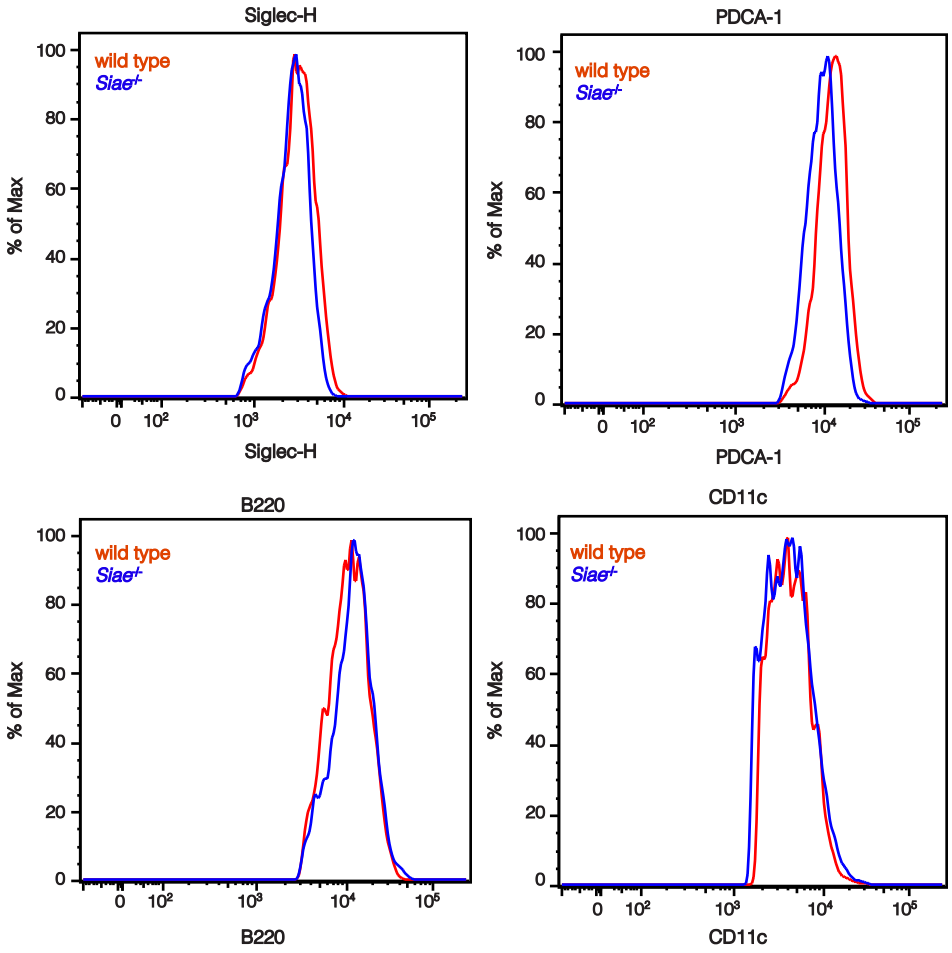

Figure 4.7. Expression of lineage-defining markers on *Siae*$^{-/-}$ pDCs. Wild type and *Siae*$^{-/-}$ pDCs from spleens of 10-wk-old animals were stained for expression of pDC-specific (Siglec-H and PDCA-1) and pDC-characteristic (B220 and CD11c) markers and analyzed by flow cytometry.

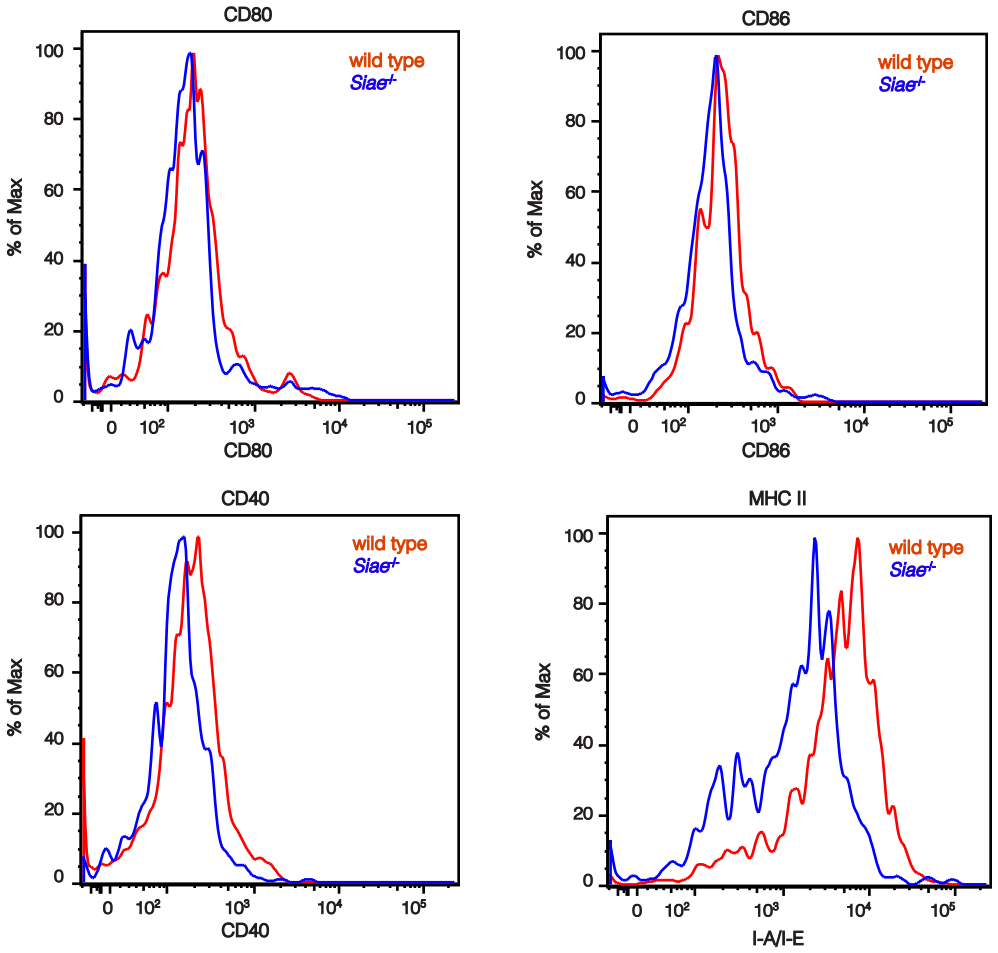

Figure 4.8. Expression of activation markers on *Siae*$^{-/-}$ pDCs. Wild type and *Siae*$^{-/-}$ pDCs from spleens of 10-wk-old animals were stained for expression of co-stimulatory markers (CD80 and CD86) as well as CD40 and MHC Class II (I-A/I-E) and analyzed by flow cytometry.

CHE-FcD staining on pDCs from *Siae*-null mice (**Figure 4.2**) does not rise to levels observed on cDCs (**Figure 4.4**) and an increase in cDC numbers in the periphery to account for converting pDCs is not observed (**Table 4.1A**), also support this interpretation.

The cause of the dramatic reduction of the peripheral pDC compartment in the absence of *Siae* is not clear from these studies, and potential investigations that may yield insights are outlined in the Discussion section below. What is apparent, however, is that the esterase activity of SIAE does not regulate the low levels of 9-*O*-AcSia on pDCs and their progenitors.

Cmah is expressed at higher levels in the pool of 9-*O*-AcSia^{Lo} versus 9-*O*-AcSia^{Hi} bone marrow progenitors

To further address the relevance of the low levels of 9-*O*-AcSia on pDCs and their precursors, we considered that early bone marrow progenitors could be divided into pools based on low versus high levels of 9-*O*-AcSia (**Figure 2.8**) and reasoned that insights regarding the mechanisms responsible for this dichotomy might be obtained from searching for differentially expressed genes between these populations. Genome-wide expression profiles of the Lin$^-$Sca-1^{Lo}9-*O*-AcSia^{Lo} and Lin$^-$Sca-1^{Lo}9-*O*-AcSia^{Hi} cells from murine bone marrows of C57Bl/6 mice were compared using both the RMA and dChip algorithms. Only genes that were differentially expressed at levels > |±2.5| between the two populations were

considered, and highest priority was given to those that were among the top twenty hits in both the RMA and dChip rankings (**Table 4.2**). In order to determine which of these genes might be associated with the distinct patterns of 9-*O*-AcSia, we looked for genes involved in Sia biochemistry. The best candidate to emerge from these microarray studies was CMAH, which was expressed at higher levels in the 9-*O*-AcSia^{Lo} progenitors.

Neu5Ac and Neu5Gc are the two most commonly occurring mammalian Sias. CMAH is the enzyme that converts Neu5Ac to Neu5Gc in an irreversible reaction. Specifically, it catalyzes the hydroxylation of CMP-Neu5Ac to CMP-Neu5Gc (Hedlund et al., 2007). Although abundant in many mammals including the chimpanzee and great apes (our closest evolutionary relatives), Neu5Gc is difficult to detect in human tissues (Varki, 2001), although it is found in some human tumors and fetal samples (Devine et al., 1991; Higashi et al., 1985; Hirabayashi et al., 1987; Kawachi et al., 1988; Malykh et al., 2001; Miyoshi et al., 1986; Varki, 2001) and was originally assumed to be an "oncofetal" antigen whose expression is the result of a gene being expressed in tumors and fetuses, but not in adults. An exon deletion/frameshift mutation in the human *CMAH* gene was discovered shortly thereafter (Chou et al., 1998; Irie et al., 1998; Varki, 2001) that not only markedly truncated the length of the final protein encoded by the human gene (Chou et al., 1998), but specifically eliminated amino acids known to be critical for the activity of the enzyme itself (Schlenzka et al., 1996).

Table 4.2. Genes differentially expressed between bone marrow progenitors categorized by levels of 9-*O*-AcSia as determined by gene expression analysis. Genes with $\log_2$(fold change) ≥|±2.5| that were among the top 20 hits as determined by both Robust Multichip Analysis and the dChip algorithm are shown.

Table 4.2A

Genes significantly overexpressed in 9-*O*-AcSia^{Lo} versus 9-*O*-AcSia^{Hi} progenitors	
Gene Symbol	**Fold Change**
Dntt	5.5
Hbb-b1	4.7
Il2rb	4.3
Gimap6	4.2
Hba-a2	3.9
Gm4759	3.8
Cmah	3.6
Il7r	3.5
Nr4a1	3.5

Table 4.2B

Genes significantly overexpressed in 9-*O*-AcSia^{Hi} versus 9-*O*-AcSia^{Lo} progenitors	
Gene Symbol	**Fold Change**
Prss34	5.6
Mcpt8	5.5
Elane	5.0
Il6	4.6
F13a1	4.6
Ms4a3	4.5
Gstm1	3.6
Lyz2	3.6
Tfec	3.6
Dstn	3.5

More sensitive chemical assays subsequently demonstrated small amounts of Neu5Gc in normal human tissue (Tangvoranuntakul et al., 2003), raising the possibility of an alternate pathway for its biosynthesis (Malykh et al., 2001). Existing biochemical pathways, however, allow exogenous Neu5Gc to be metabolically incorporated into cultured human cells (Bardor et al., 2005) and it was subsequently found that Neu5Gc in normal human tissues, tumors, and fetuses originates from dietary sources (Tangvoranuntakul et al., 2003; Diaz et al., 2009; Bergfeld et al., 2012), such as red meat and milk products. Moreover, Neu5Gc could not be detected in the tissues of *Cmah*$^{-/-}$ mice maintained on a long-term Neu5Gc-free diet (Hedlund et al., 2007), arguing against a second mammalian biosynthetic pathway.

PDCs express robust surface levels of Neu5Gc

Few investigations have dealt with the potential immune consequences of the absence of CMAH and therefore Neu5Gc in humans. *Cmah*-null mice have distinct neurological abnormalities including a diminished acoustic startle response and also show delayed skin wound healing (Hedlund et al., 2007). Interestingly, the absence of Neu5Gc in *Cmah*$^{-/-}$ mice harboring the human-like deletion resulted in increased 9-*O*-acetylation of Neu5Ac in plasma and erythrocytes, as well as in tissues, including the liver and lungs (Hedlund et al., 2007). The reasons for this phenomenon in null mice is unknown, but it is of note

that it appears to mimic the human condition, as increased *O*-acetylated Neu5Ac was also demonstrated in human samples versus those of great apes (Altheide et al., 2006).

It is known that certain Siglecs preferentially bind Neu5Gc- or Neu5Ac-containing structures even though these structures differ by only the presence of a single additional oxygen atom in the former (Varki, 2001). Murine CD22, unlike human CD22 for example, has a markedly higher affinity for Neu5Gc (Blixt et al., 2003; Brinkman-Van der Linden et al., 2000; Kelm et al., 1998; Collins et al., 2002). Our study demonstrated that B cells from *Cmah* mutant mice exhibit an enhanced proliferative response to BCR cross-linking (Naito et al., 2007). The same study revealed that activated B cells also exhibit a poorly understood down-regulation of *Cmah* and *Siae* expression (Naito et al., 2007). Furthermore, our work revealed that the B cells from both *Cmah*-null animals and *Cmah*/*Siae* double mutant mice have higher levels of 9-*O*-AcSia. In addition, both types of mutant mice present with enhanced BCR activation as well as marked reductions in MZ B cells and perisinusoidal B cells (Cariappa et al., 2009). Thus, a combination of two changes in the structure of Sia (i.e., absence of Gc and increased 9-*O*-acetylation) results in a phenotype that is similar to that seen in *Siae*$^{-/-}$ mice, which have only enhanced 9-*O*-AcSia.

With the exception of the studies performed in B cells, potential functions of CMAH in other immune cells have not been explored. To determine if CMAH

and its production of Neu5Gc might be relevant to the low levels of 9-*O*-AcSia on pDCs and their progenitors, we first investigated if the selectively high *Cmah* expression found among total 9-*O*-AcSia^{Lo} early bone marrow progenitors was maintained in pDCs. Microarray data provided by the ImmGen Consortium showed that pDCs express the highest *Cmah* mRNA levels among all cell types represented (Heng et al., 2008). These levels were slightly greater than those observed in B cells, and significantly higher than the minimal expression observed in cDCs, as depicted in **Figure 4.9**. Based on this data, our expectation was that Neu5Gc would be the predominant Sia species on pDCs and B cells, but not in cDCs.

To address this possibility, we used a recently developed polyclonal chicken IgY that binds specifically to Neu5Gc regardless of the underlying glycan structure (Diaz et al., 2009) in flow cytometry studies to determine the levels of Neu5Gc on murine splenocytes. As shown in **Figure 4.10**, pDCs and B cells expressed high levels of Neu5Gc. Staining intensity in cDCs had a wider distribution, although the majority of these cells had less surface Neu5Gc than found on either B cells or pDCs.

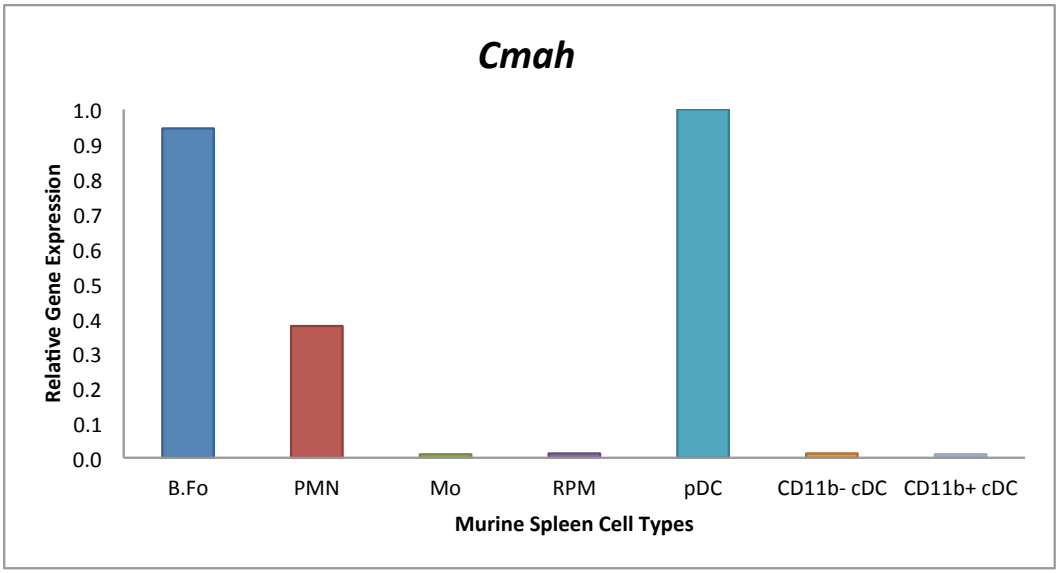

Figure 4.9. pDCs express high levels of *Cmah*. Shown are values of relative gene expression that are normalized to maximum expression of *Cmah* across all cell types (represented in ImmGen data) and presented in a linear scale. B.Fo, Follicular B cell; PMN, polymorphonuclear leukocyte; Mo, monocyte; RPM, red pulp macrophage; pDC, plasmacytoid dendritic cell; $CD11b^-$ cDC, $CD11b^-$ conventional dendritic cell; $CD11b^+$ cDC, $CD11b^+$ conventional dendritic cell. This figure is based on data assembled by the ImmGen Consortium (Heng et al., 2008).

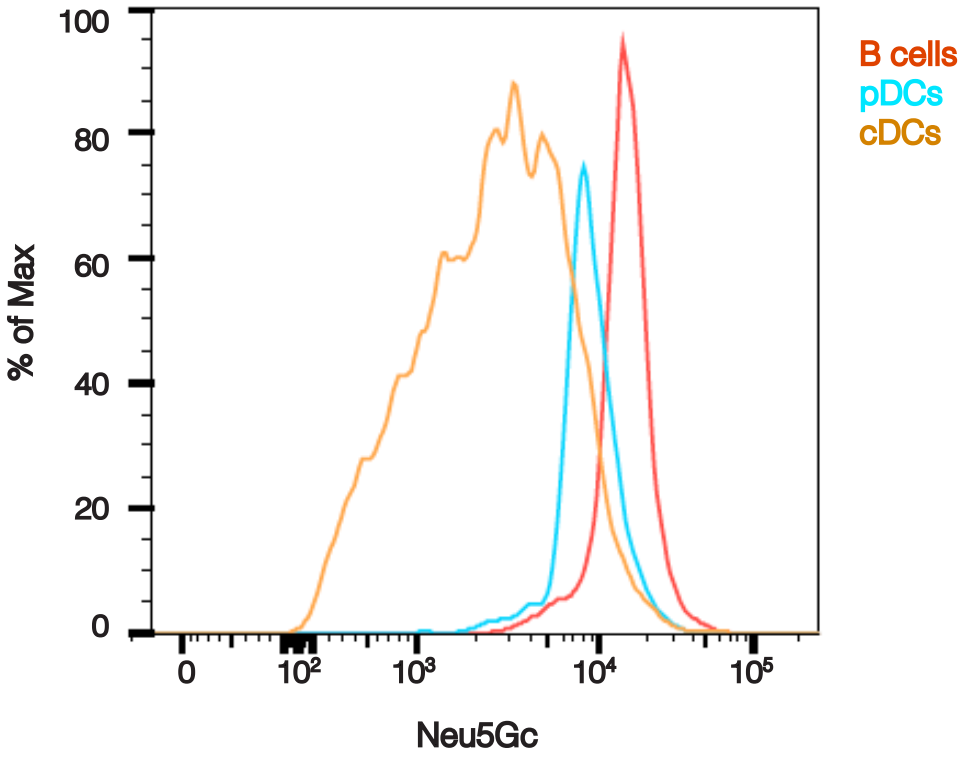

Figure 4.10. Neu5Gc levels on B cells, pDCs, and cDCs. B cells, pDCs, and cDCs from spleens of10-wk-old wild type mice were stained for surface Neu5Gc expression and analyzed by flow cytometry.

9-*O*-AcSia levels are markedly increased on *Cmah*$^{-/-}$ pDCs and their progenitors

In order to determine if the high levels of Neu5Gc found on wild type pDCs might be linked to their low surface 9-*O*-AcSia, we examined pDCs from *Cmah*$^{-/-}$ mice. Our expectation was that the absence of Neu5Gc would result in increased 9-*O*-AcSia levels on pDCs, which would only contain Neu5Ac. As demonstrated in **Figure 4.11**, staining with CHE-FcD revealed higher surface levels of 9-*O*-AcSia on both pDCs and B cells from *Cmah*-null mice compared with those from wild type controls (**Figures 4.11A, B)**. In contrast, cDCs from these animals maintained the robust 9-*O*-AcSia staining found on wild type cDCs (**Figure 4.11C)**, and were indistinguishable from the latter. Of note, the most dramatic increase in 9-*O*-AcSia levels was on *Cmah*$^{-/-}$ pDCs, whose CHE-FcD levels approached those on cDCs (**Figure 4.11C**).

Based on these data, we next sought to assess if pDC progenitors in the bone marrow, which are also characterized by low levels of 9-*O*-AcSia, would be impacted by the absence of Neu5Gc in *Cmah*$^{-/-}$ mice. CHE-FcD staining of mature pDCs in the bone marrow of *Cmah*$^{-/-}$ mice revealed an increase in 9-*O*-AcSia levels (**Figure 4.12**) that was similar to what was observed in their splenic counterparts (**Figure 4.11B**). 9-*O*-AcSia staining in *Cmah*-null pre-pDCs was also enhanced (**Figure 4.12**), although not to the extent observed on mature pDCs.

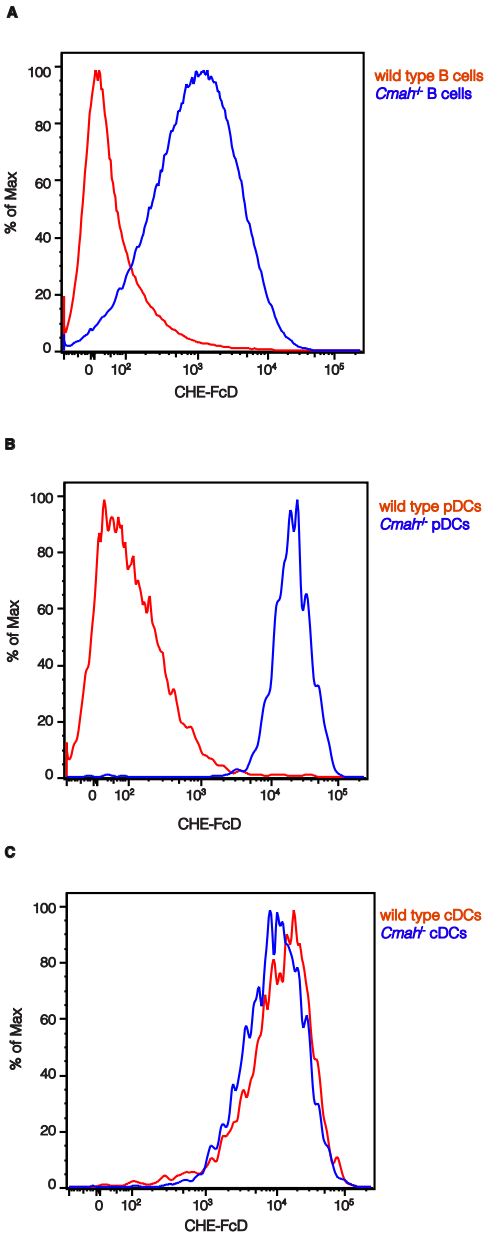

Figure 4.11. Surface levels of 9-*O*-AcSia on pDCs, B cells, and cDCs from Cmah$^{-/-}$ animals. CHE-FcD staining of (A) pDCs, (B) B cells, and (C) cDCs from the spleens of 10-wk-old wild type and *Cmah*$^{-/-}$ mice.

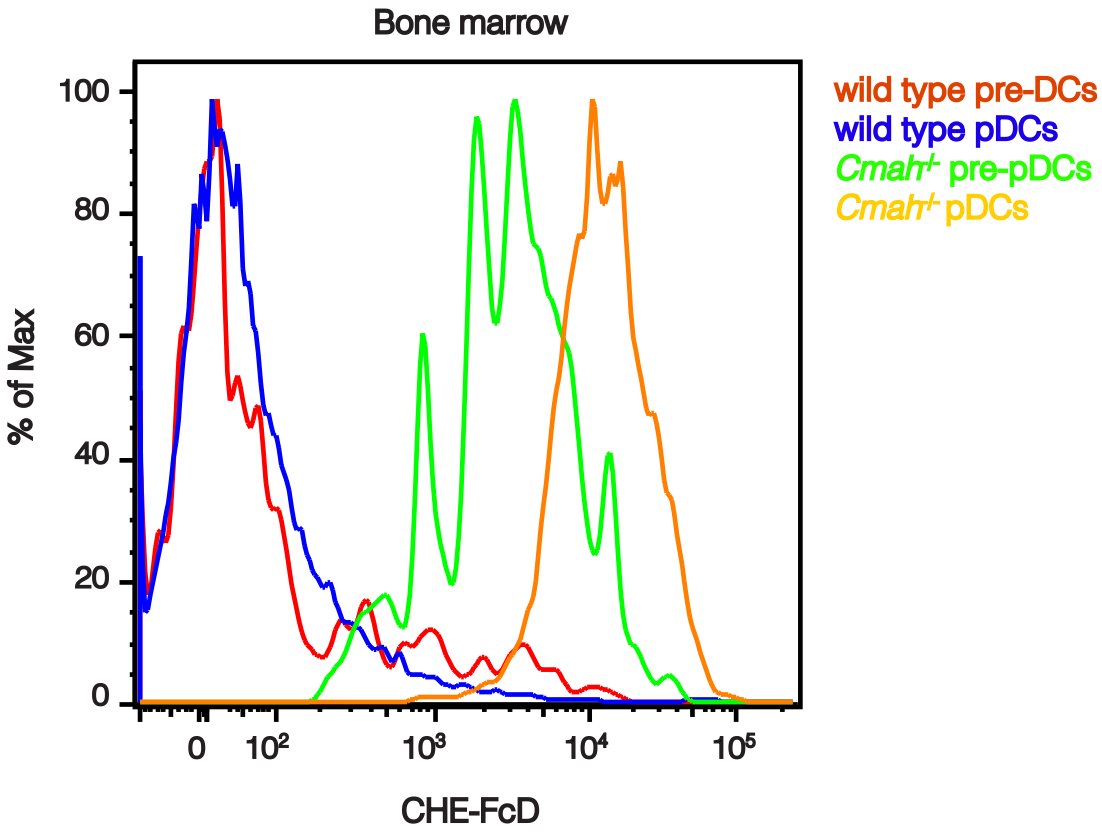

Figure 4.12. 9-*O*-AcSia levels on bone marrow *Cmah*-null pre-pDCs and mature pDCs. CHE-FcD staining of pre-pDCs and pDCs from the bone marrows of 10-wk-old wild type and *Cmah*$^{-/-}$ mice.

Bone marrow production of pDCs is unimpaired in *Cmah*$^{-/-}$ mice

Given the substantial increase in 9-*O*-AcSia levels on pDCs and their committed progenitors in the absence of *Cmah*, we considered that the development of pDCs might be impacted in these animals. We therefore compared absolute numbers of bone marrow pre-pDCs and pDCs between *Cmah*$^{-/-}$ mice and their wild type counterparts. Total white cells counts, as well as numbers of pre-pDCs and mature pDCs in *Cmah*-null and wild type animals were similar. A slight reduction in B lymphocytes was observed, consistent with the loss of perisinusoidal B cells that we had noted previously in these animals (**Table 4.3A** and Cariappa et al., 2009). Taken together, the data indicate that although there is an increase in levels of 9-*O*-AcSia on pDCs and their progenitors, development of this lineage is not compromised in the absence of *Cmah*. Interestingly, the overall cell numbers and conclusions regarding pDC development made in *Cmah*$^{-/-}$ mice are similar to those arrived at in *Siae*$^{-/-}$ animals.

PDCs are reduced in the periphery of *Cmah*$^{-/-}$ mice

Our experiments indicated that maintaining low surface levels of 9-*O*-AcSia was not necessary for pDC development. We considered, however, that additional roles for this specific carbohydrate modification and for *Cmah* expression in pDCs might exist, and sought to further characterize the phenotype of pDCs in *Cmah*-null animals. The pDC compartment in the bone marrow of *Cmah*$^{-/-}$ mice

Table 4.3. Absolute numbers of pDCs and their progenitors in wild type and *Cmah*$^{-/-}$ mice.

Table 4.3A

Absolute numbers of pDC progenitors in the bone marrow of *Cmah*$^{-/-}$ mice			
Population	**C57BL/6***	***Cmah*$^{-/-}$***	**Fold Change**
pre-DCs	.27 (0.06)	.29 (0.03)	+1.1
pDCs	9.2 (0.4)	10.6 (0.9)	+1.2
B cells	196 (3.2)	134 (1.7)	-1.5
Total cell count	1421 (279)	1378 (214)	-1.0

*, mean (SD) x 10^4; n = 3 mice per group

Table 4.3B

Absolute numbers of DCs in the spleen of *Cmah*$^{-/-}$mice			
Population	**C57BL/6***	***Cmah*$^{-/-}$***	**Fold Change**
pDCs	59 (1.3)	6 (0.7)	-9.8
cDCs	175 (1.8)	161 (2.3)	-1.1
B cells	6036 (192)	1304 (39)	-4.8
Total cell count	12843 (426)	3345 (289)	-3.8

*, mean (SD) x 10^4; n = 8 mice per group

was conserved, but to develop a more complete view of the pDC compartment in the periphery, we compared absolute numbers of pDCs in these animals and wild type controls. Analysis of splenocytes revealed a close to four-fold reduction in total white cells in *Cmah*-deficient animals (**Table 4.3B**). Numbers of cDCs were relatively preserved and there was a decrease in B lymphocytes consistent with the loss of marginal zone B cells previously reported in the absence of *Cmah* (Cariappa et al., 2009). These changes were similar to those in *Siae*$^{-/-}$ mice. The most striking finding in *Cmah*-null animals, however, was the selective, almost ten-fold reduction in pDC numbers (**Table 4.3B**) that was larger than what was observed in the absence of *Siae* (**Table 4.1A**).

We considered the possibility that the selective loss of pDCs, as well as their increased surface 9-*O*-AcSia in *Cmah*-deficient animals reflected their conversion into cDCs. An analysis of expression levels of other pDC and cDC characteristic markers on *Cmah*$^{-/-}$ pDCs, however, did not convincingly support this possibility. PDCs from *Cmah*$^{-/-}$ mice had lower surface levels of CD11c and B220 levels, and slightly higher levels of Siglec-H than their wild type counterparts (**Figure 4.13**). The lack of an increase in splenic cDC numbers in *Cmah*-null animals provides further evidence that pDC to cDC conversion is most likely not occurring.

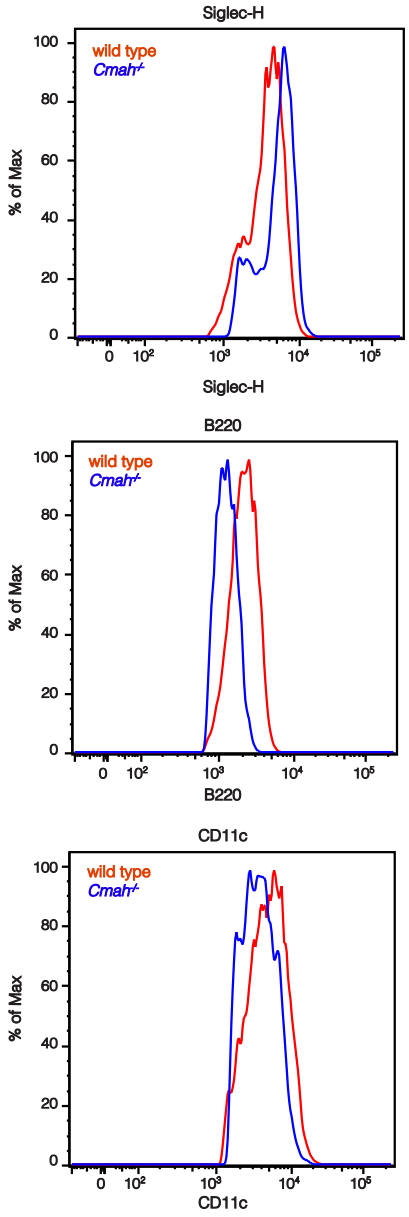

Figure 4.13. Expression of lineage-defining markers on *Cmah*$^{-/-}$ pDCs. Wild type and *Cmah*$^{-/-}$ pDCs from spleens of 10-wk-old animals were stained for expression of pDC-specific (Siglec-H) and pDC-characteristic (B220 and CD11c) markers and analyzed by flow cytometry.

Cmah$^{-/-}$ pDCs demonstrate an enhanced response to endosomal TLR stimulation

The 9-*O*-acetylation of Sia prevents ligation and subsequent function of certain inhibitory receptors, including CD22 on B cells, as described above (Sjoberg et al., 1994). We reasoned that increased 9-*O*-AcSia on pDCs in *Cmah*$^{-/-}$ mice might impair inhibitory receptor signaling in these cells and that the dramatic reduction in peripheral pDC numbers in these animals may indicate their hyperactivation and enhanced turnover. We therefore compared the ability of *Cmah*-null and wild type pDCs to make type I IFN in vivo in response to intravenous injection with resiquimod, a TLR7 agonist, as described in Chapter 3. Intracellular staining for IFN-α was greater in *Cmah*$^{-/-}$ versus wild type pDCs (**Figure 4.14B**). Of note, similar to their wild type counterparts, *Cmah*$^{-/-}$ pre-pDCs subject to the same stimulation did not produce IFN-α (**Figures 4.14A** and **3.3)**. Taken together, the data suggests that pDCs might become hyperactivated in the absence of *Cmah*, but only after commitment to the lineage has occurred.

PDCs express inhibitory receptors impacted by levels of 9-*O*-AcSia

We considered that the increased production of IFN-α in *Cmah*$^{-/-}$ pDCs might be related to the lack of function of inhibitory receptors. Specifically, we thought that pDCs might express Siglecs that engage Sia-containing ligands only when they are not 9-*O*-acetylated, and that the increased surface 9-*O*-AcSia on pDCs in

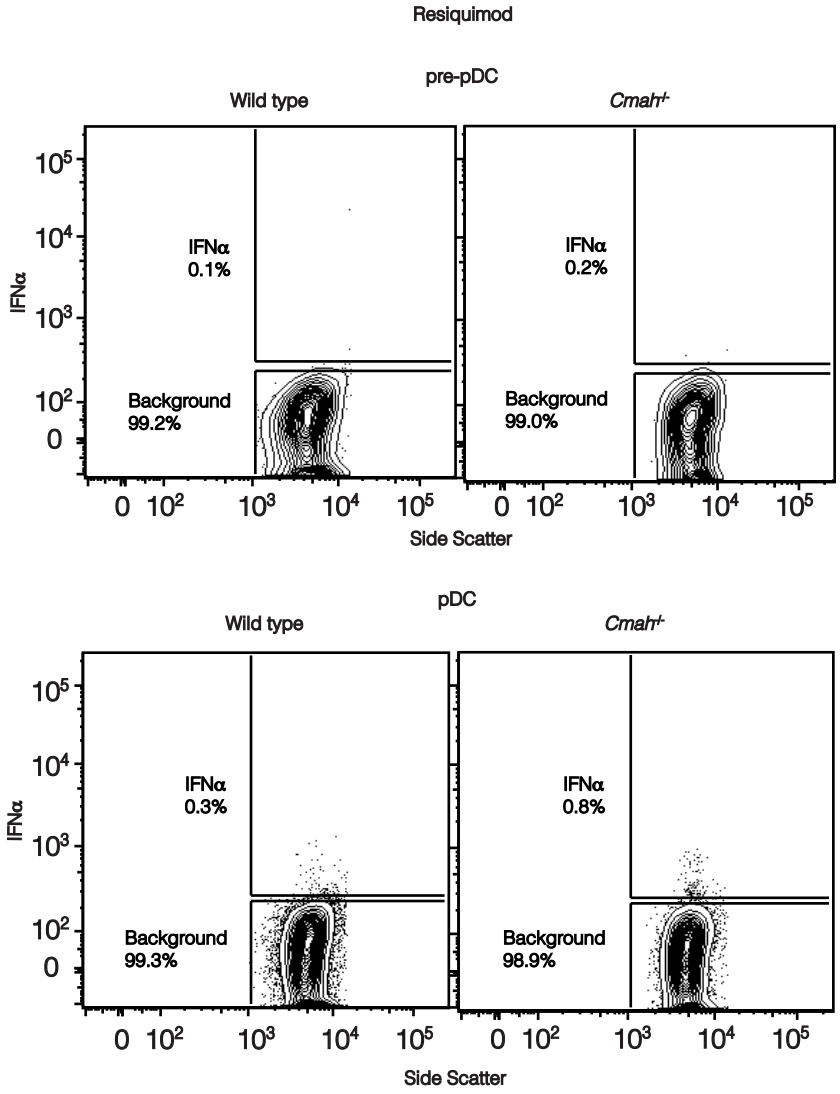

Figure 4.14. In vivo production of Type I IFN by *Cmah*$^{-/-}$ pre-pDCs and mature pDCs in response to TLR7 stimulation. Bone marrow cells from 10-wk-old wild-type and *Cmah*$^{-/-}$ mice were collected 1 hour after intravenous injection with PBS or resiquimod (R-848), and stained with surface markers to identify pre-pDCs and pDCs and intracellularly for IFN-α. Background gate is set according to staining for IFN-α in samples from PBS-treated animals. An optimized treatment regime for resiqumod (dose: 5 μg; time point: 1 hour) that elicited the maximal pDC IFN-α production (data not shown), consistent with previous reports was used (Asselin-Paturel et al., 2005). Data are representative of three independent experiments.

the absence of *Cmah* might compromise the inhibitory function of one or more of these Siglecs. In addition to CD22, 9-*O*-acetylation of Sia impairs the ability of other Siglecs, CD33 and sialoadhesin, to engage their ligands (Sjoberg et al., 1994). Sialoadhesin expression is restricted to macrophages (Pillai et al., 2012). We found, however, that pDCs do express CD22, although at much lower levels than on B cells (**Figure 4.15A)**. In addition, CD33 expression could also be discerned on pDCs, although this was significantly less than that observed on neutrophils **(Figure 4.15B**), which are known to express the highest levels of this Siglec (Pillai et al., 2012). The expression of CD22 and CD33 had not been described previously on pDCs. The pDC compartment has not been interrogated in prior studies of *Cd22* knockout animals (Otipoby et al., 1996; Sato et al., 1996; Nitschke et al., 1997) and *Cd33*-null mice do not have an obvious phenotype (Brinkman-Van der Linden et al., 2003), although again, pDCs were not specifically investigated. It is also particularly relevant that both murine CD22 and CD33 preferentially engage ligands containing Neu5Gc, which is found at high levels on pDCs (**Figure 4.10**), rather than Neu5Ac (Blixt et al., 2003; Brinkman-Van der Linden et al., 2000; Kelm et al., 1998; Collins et al., 2002; Brinkman-Van der Linden et al., 2003). It is therefore possible that CD22 and/or CD33 act to dampen type I IFN production in pDCs and that impaired function due to both the absence of Neu5Gc and increased 9-*O*-acetylation of Sia in *Cmah*$^{-/-}$ mice may be linked to the pDC phenotype observed in these animals.

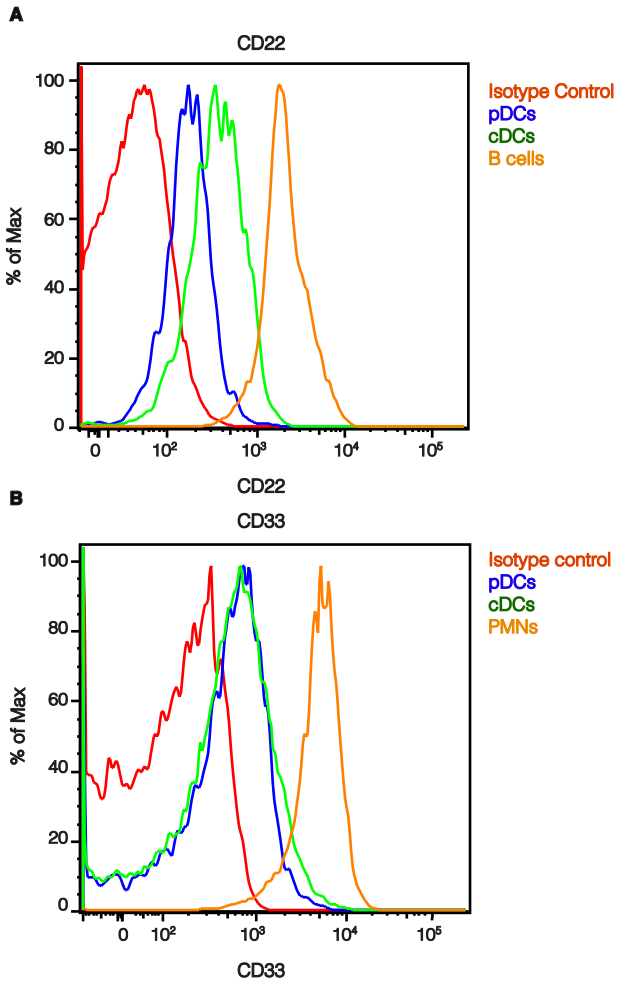

Figure 4.15. Expression of Siglecs on pDCs. Wild type pDCs and cDCs from spleens of 10-wk-old animals were stained for expression of CD22 and CD33 and analyzed by flow cytometry. CD22 expression on B cells and CD33 expression on polymorphonuclear leukocytes (PMNs) served as positive controls.

Discussion

The primary goal of these studies was to determine whether the low levels of 9-*O*-AcSia that characterize pDCs and their progenitors are necessary for the development of this lineage. Our initial experiments in *Siae*$^{-/-}$ mice could not provide an answer, as levels of 9-*O*-AcSia on pDCs and their progenitors did not change in animals that lacked this *O*-acetylesterase. In mice that lacked *Cmah*, the enzyme responsible for converting the Neu5Ac form of Sia to Neu5Gc, 9-*O*-AcSia levels increased in pDCs and pre-pDCs; the development of pDCs in the bone marrow, however, was not comprised. Based on these results, it appears that low surface levels of 9-*O*-AcSia are not required for pDC development.

Our investigations did reveal additional phenotypes in the pDC compartment in both *Siae*$^{-/-}$ and *Cmah*$^{-/-}$ mice that bore some similarity. While pDC development in the bone marrow remained intact, absolute numbers of pDCs were reduced in the periphery of both types of mutant animals. As described above, pDC to cDC conversion was not a likely explanation for the loss of pDCs in either knockout mouse. Instead, pDCs in *Cmah*$^{-/-}$ animals appeared hyperactivated, producing greater amounts of IFN-α in response to TLR7 stimulation than their wild type counterparts. It is plausible that activation-induced death contributes to the decrease in pDC numbers observed in *Cmah*-null mice.

We considered that this hyperactivation in *Cmah*-null pDCs might be due to impaired function of inhibitory receptors that restrain the type I IFN response. In line with this possibility, we demonstrated that pDCs express CD22 and CD33. Both of these Siglecs require that their Sia-containing ligands are not 9-*O*-acetylated and both preferentially engage Neu5Gc versus Neu5Ac in the mouse. Thus, their function might be prevented by both increased 9-*O*-AcSia and the absence of Neu5Gc on *Cmah*$^{-/-}$ pDCs. Further investigations to understand how these Siglecs might act to attenuate the type I IFN response in pDCs, possibly through their cytoplasmic ITIM motifs, is warranted. As described in Chapter 1, Siglec-H is a specific marker for murine pDCs (Blasius et al., 2004; Zhang et al., 2006) that has been demonstrated to dampen TLR-induced type I IFN secretion in pDCs (Blasius et al., 2004; Blasius et al., 2006a). Siglec-H possesses all of the conserved structural features that contribute to Sia recognition (Pillai et al., 2012). In spite of this, in vitro solid-phase assays to evaluate binding of Siglec-H-Fc recombinant protein to red blood cells and attempts to detect Siglec-H binding to sialylated polyacrylamide conjugates (that bind avidly to other Siglecs) have failed to demonstrate recognition of Sia by this Siglec (Zhang et al., 2006). Importantly, these studies tested binding of Siglec-H only to Neu5Ac-based glycoconjugates, and whether Siglec-H preferentially engages Neu5Gc-containing ligands has not been evaluated. We have shown here that pDCs

express high surface levels of Neu5Gc, and Siglec-H binding to this species of Sia (versus Neu5Ac, 9-*O*-Neu5Gc, and 9-*O*-Neu5Ac) should be assessed.

In addition, BrdU labeling studies to compare the rate of pDC turnover in *Cmah*$^{-/-}$ mice and wild type animals should be initiated. Previous work has demonstrated that while cDCs turn over rapidly, and have a half-life of 5-7 days, pDCs are long-lived, with slow BrdU incorporation rates, and a half-life approaching 14 days (O'Keeffe et al., 2002; Liu et al., 2007). If pDCs are in fact undergoing activation-induced attrition in *Cmah*$^{-/-}$ mice, there should be a corresponding increase in their BrdU incorporation rates. In contrast, measurements of cDC turnover in *Cmah*$^{-/-}$ and wild type mice should reveal minimal differences as cDC numbers are not reduced in *Cmah*-null mice.

Increased activation and accelerated turnover of pDCs may also be occurring in *Siae*$^{-/-}$ mice. Impaired Siglec function might not be the mechanism in this case, since the steady state levels of 9-*O*-AcSia on pDCs in these animals do not change. Whether or not transient increases in 9-*O*-acetylation do occur in vivo remains to be determined. Regardless, production of type I IFNs by *Siae*$^{-/-}$ pDCs should be tested and BrdU labeling studies of these cells should also be performed.

An important question is whether the phenotypes of pDCs in *Cmah* and *Siae*$^{-/-}$ mice are cell-intrinsic phenomena. In earlier studies, we have demonstrated that there is enhanced BCR signaling in both of these knockout

mice and that in *Siae* mutants, the B cell defect is lymophocyte-intrinsic, characterized by development of anti-chromatin antibodies, and an immune complex glomerulonephritis (Cariappa et al., 2009). As described in Chapter 1, numerous investigations focused on elevation of type I IFN levels as a pathogenesis factor in several autoimmune diseases have uncovered a role for pDCs in immune-complex mediated disorders like SLE (Ronnblom et al., 2001). In this context, aggregates of antinuclear antibodies and endogenous nucleic acids or nucleoproteins are delivered to the endosomal compartment of pDCs via FcγRII, where they may trigger pDCs through TLR7/9 (Ronnblom et al., 2001; Bave et al., 2003). It is therefore plausible that the changes observed in both the *Cmah* and *Siae* knockout mice reflect their activation by immune complexes, rather than an inherent deficiency of *Cmah* or *Siae* in pDCs, respectively. We can address this possibility by performing competitive transfers of BM pre-pDCs from each of these mutant mice with wild type counterparts into wild type recipients. A pDC-intrinsic defect would be implied if the number of mature pDCs derived from mutant pre-pDCs is less than the number generated from control pre-pDCs.

In addition to the pDC phenotype in *Siae*$^{-/-}$ mice, we noted several alterations in various myeloid cell types. As shown in Chapter 2, the total cDC compartment is characterized by high levels of 9-*O*-AcSia, although disparate levels are found on the surface of functionally distinct cDC subsets. Lower

intensity 9-*O*-AcSia staining is found on $CD8\alpha^+$ cDCs in comparison to the highest levels found on $CD4^-CD8\alpha^-$ and $CD4^+$ cDCs. In *Siae*-null mice, surface levels of 9-*O*-AcSia on $CD8\alpha^+$ cDCs increases to the levels found on the $CD4^-$ $CD8\alpha^-$ and $CD4^+$ cDCs, whose high levels are maintained. $CD4^-CD8\alpha^-$ and $CD4^+$ cDCs express CD11b (Shortman and Liu, 2002), reside in the marginal zone in the steady state, and migrate to the T-cell areas only upon activation where they are efficient drivers of Th_2 responses (Hochrein et al., 2001; Maldonado-Lopez et al., 1999; Moser and Murphy, 2000; Pulendran et al., 1999; Reis e Sousa et al., 1997). $CD8\alpha^+$ cDCs, on the other hand, lack CD11b expression (Shortman and Liu, 2002), are situated in T-cell areas at rest, and upon activation produce ample IL-12 to initiate Th_1 activity. Most importantly, they are the chief cross-presenters (Dudziak et al., 2007; Heath and Carbone, 2001; Lin et al., 2008). Interestingly, there is no evidence that the T cell coreceptors used for this categorization of cDCs are of functional significance (Shortman and Liu, 2002). Whether the different levels of 9-*O*-AcSia in cDC subsets are functionally relevant and if the increased CHE-FcD staining intensity in $Siae^{-/-}$ $CD8\alpha^+$ cDCs is accompanied by functional changes in these cells, remains to be determined. Recent investigations in our laboratory have demonstrated that $CD4^+$ T cell memory responses in *Siae*-null mice are enhanced in immunization studies and there is also an increase in $CD8\alpha^+$ memory phenotype T cells in these animals (H. Mattoo and E. Demissie, unpublished

observations). Whether these findings reflect enhanced antigen-presentation or cross-presentation by *Siae*$^{-/-}$ CD8α^{+} cDCs remains to be elucidated.

In addition to the changes in the cDC compartment, our studies revealed that levels of 9-*O*-AcSia increased on red pulp macrophages in *Siae* knockout mice. This alteration may impact the activity of Siglec-1 (sialoadhesin), whose expression is highly specific for macrophages (Pillai et al., 2012). Several roles for sialoadhesin in Sia-dependent pathogen interactions have been described. This Siglec behaves as a phagocytic receptor for bacterial and protozoal pathogens such as *Neisseria meningitides* (Delputte et al., 2011) and *Trypanosoma cruzi* (Monteiro et al., 2005), which coat themselves with Sias in an attempt to evade other forms of immune recognition; on the other hand, sialoadhesin on alveolar macrophages can be "hijacked" as an endocytic receptor for the respiratory syncytial virus (Vanderheijden et al., 2003), which derives its envelope surface Sias from the mammalian cells from which it originally buds. In all cases, sialoadhesin engages sialoglyconjugates with multiple clustered O-linked glycans, but only if they are not 9-*O*-acetylated, similar to CD22 (Sjoberg et al., 1994). It is possible then that 9-*O*-AcSia on the surface of macrophages engages sialoadhesin in cis interactions, acting to prevent its trans interactions with pathogens, and that in the absence of *Siae*, increased CHE-FcD staining reflects increased "masking" of this Siglec.

The increased surface levels of 9-*O*-AcSia on both CD8α^{+} cDCs and red pulp macrophages in *Siae* knockout animals is likely to reflect a cell-intrinsic role of the *O*-acetylesterase activity of *Siae* in these cell types. Aside from the effects on 9-*O*-AcSia, we also observed other phenotypes in certain myeloid cells in the absence of *Siae*. Interestingly, even though levels of 9-*O*-AcSia did not change on *Siae*$^{-/-}$ granulocytes, there was a notable increase in their numbers in both the bone marrow and in the periphery. It is possible that the increase in granulopoiesis in these mutant mice is an indirect consequence of pDC hyperactivation.

In trying to decipher the mechanism of enhanced granulopoiesis beyond this phenomenon, it is important to consider other physiological situations in which an increase in granulocyte production occurs. Previous studies have demonstrated that an increase in bone marrow granulopoiesis characterized by an expansion of early granulocyte precursors and rapid mobilization of mature granulocytes occurs during infections (Cheers and Stanley, 1988; Watari et al., 1989; Hirai et al., 2006; Ueda et al., 2009; Satake et al., 2012) in order to meet host demands. In addition, microarray studies have revealed that PBMCs from SLE patients have a granulopoeisis signature (Bennett et al., 2003), and a central role for neutrophils in lupus pathogenesis has been confirmed. SLE neutrophils undergo accelerated death upon exposure to SLE-derived anti-ribonucleoprotein antibodies, releasing neutrophil extracellular traps (NETs) comprised of cationic

proteins (e.g., LLR7 and HMGB1) and DNA. These NETs combine with serum autoantibodies to form immune complexes that activate pDCs in a TLR9-dependent manner to produce high levels of IFN-α (Lande et al., 2011; Garcia-Romo et al., 2011). A similar "NETosis" may occur in *Siae*$^{-/-}$ mice that have a lupus-like phenotype with immune complex disease, and an accompanying increase in granulopoeisis would not be unlikely.

Low levels of 9-*O*-AcSia have helped us identify pDC progenitors as well as more tightly define mature pDCs. However these low levels of Sia *O*-acetylation are not a prerequisite for pDC development per se as has been established by the study of *Cmah*$^{-/-}$ mice. In both *Siae*$^{-/-}$ and *Cmah*$^{-/-}$ mice, enhanced 9-*O*-AcSia is correlated with enhanced pDC activation and a decrease in the numbers of mature pDCs. It remains to be determined if these changes are cell- intrinsic and if they result from the inability of inhibitory Siglecs to bind to their ligands and to thus dampen pDC activation.

Chapter 5:

General Discussion

The studies presented in this thesis demonstrate the importance of 9-*O*-AcSia in the context of both hematopoiesis and pDC development. Classic bifurcation models of hematopoiesis affirm that HSCs develop initially into myelo-erythroid or lymphoid restricted progenitors that subsequently undergo restricted, stepwise differentiation into mature cell types. Some recent investigations have challenged this view, and these studies indicate that commitment to terminally differentiated cells occurs at HSC-proximal stages. Naik et al. used "cellular barcoding" to trace the in vivo fate of multipotent progenitors (MPPs) and HSCs and demonstrated that while HSCs generate all cell types, MPPs are heterogeneous in the cell types they produce, with developmental potential for only one or two distinct lineages (Naik et al., 2013). Our own studies delineating the pathway of pDC development support the view that early bone marrow progenitors have significantly restricted lineage outputs. Pro-pDCs, which fall within the MPP pool, lack differentiation potential for myeloid or lymphoid cells and differentiate into pre-pDCs that are committed to pDC development. An obvious next challenge is to identify the nature, expression, and timing of early-acting factors that govern this type of commitment for pDCs and other lineages.

The analysis of the output of transferred sibling cells derived from single MPPs demonstrated conserved fates for siblings in some, but not all cases (Naik et al., 2013). The former (conserved fates of sibling cells) suggests that early progenitor fate is imprinted, while the latter (the lack of conservation between

sibling cells) implies that fate may be determined stochastically or by the microenvironment after cell transfer. The precise contributions of each of these mechanisms to the diverse patterns of commitment found among early progenitors remains to be determined. Comparative gene expression analyses of distinct progenitor types and mature cell types will help resolve some of this ambiguity. In addition, recent manipulations of the bone marrow microenvironment have revealed that distinct milieus are important for discrete progenitor types. HSCs have been demonstrated to require a perivascular niche, while early lymphoid progenitors appear to rely on an endosteal niche (Oguro et al., 2013; Ding and Morrison, 2013). It remains to be determined whether the effects of such niche interactions contribute primarily to maintaining the cell viability and self-renewal potential of committed progenitors, or if they also drive early commitment events. The latter scenario would imply that discrete niches exist for the earliest progenitors of each lineage.

It is clear from our investigations that low levels of 9-*O*-AcSia mark commitment to the pDC lineage. Our experiments in *Cmah*$^{-/-}$ mice, however, in which pDC development in the bone marrow is not compromised despite the increased levels of 9-*O*-AcSia on pDCs and their progenitors in these animals suggest that low levels of 9-*O*-AcSia are not required for pDC development. Still, a function for the high versus low levels of 9-*O*-AcSia that divides the pool of early bone marrow progenitors in governing cell fate cannot be ruled out. Drake

et al. have demonstrated a role for polySia in hematopoietic development (Drake et al., 2008; Drake et al., 2009). Murine MPPs were found to use the sialyltransferase ST8Sia IV to express polySia on their cell surfaces (Drake et al., 2008). In *ST8Sia IV*$^{-/-}$ animals, there was a 30% reduction in total thymocytes and a concomitant deficiency in early T-lineage progenitors (ETPs) (Drake et al., 2009). Functional experiments demonstrated that *ST8Sia IV*$^{-/-}$ progenitors lacking polySia exhibited a specific defect in T-cell development because of an impaired ability to mobilize from the bone marrow and therefore access the thymus. The nature of the polySia-containing glycoconjugate(s) on progenitor cells and whether 9-*O*-acetylation modifies Sia residues on these glycans should be investigated.

Additional insight into the possible role of 9-*O*-AcSia will come from establishing the point in hematopoiesis when the 9-*O*-acetylation modification is first observed. Our experiments revealed that bone marrow HSCs can be separated into two groups based on high versus low levels of 9-*O*-AcSia. Is 9-*O*-AcSia found on the surface of progenitors generated in the extraembryonic yolk sac, the aorta/gonad/mesonephros (AGM) region, and the fetal liver that mark the earliest sites of hematopoiesis in the embryo? Answers to these and similar questions may guide further investigations to understand the potential functions of 9-*O*-acetylation of Sia in hematopoietic cell development.

Clarifying the specific enzymatic machinery involved in adding and

removing the 9-*O*-acetyl moiety from Sia-containing glycoconjugates to various cell types including pDCs is also crucial. Our experiments revealed that levels of 9-*O*-AcSia did not increase on pDCs and their progenitors in the absence of *Siae*, an *O*-acetylesterase that removes 9-*O*-acetyl moieties from Sia on the surface of B cells (Cariappa et al., 2009; Surolia et al., 2010). These results suggest the existence of additional *O*-acetylesterases, although it is formally possible that deacetylation of some glycoconjugates does not occur in vivo. It is important to identify other candidate *O*-acetylesterases and to interrogate knockout mice lacking each of these enzymes.

Similarly, determining the identify of candidate *O*-acetyltransferases responsible for adding the 9-*O*-acetyl moiety to Sia on pDCs and other cells and investigating knockout mice for each of these is also essential. One such possible candidate is the human CASD1 protein, whose overexpression in combination with α-N-acetyl-neuraminide α-2-8-sialyltransferase 1 (GD3 synthase) resulted in a 40% increase in biosynthesis of 7-*O*-acetylated ganglioside GD3 (Arming et al., 2011). In addition, high levels of CASD1 transcripts were detected in human tonsillar T and B cells, which express 9-*O*-acetylated and 7-*O*-acetylated GD3 (Wipfler et al., 2011). Distinct levels of 9-*O*-AcSia modulate many functions, including Siglec activity and cell-cell and host-pathogen interactions. Beyond establishing the specific enzymes that add and remove the 9-*O*-acetyl moiety from Sia in particular cell types, it will be crucial to understand the balance between

these and other enzymes (e.g., sialyltransferases) involved in Sia metabolism.

In addition to its role as a tool to better understand hematopoiesis, the distinct low levels of 9-*O*-AcSia demonstrated on pDCs and their progenitors also contributed to the discovery of pre-pDCs, progenitor cells that are committed to pDC development. Moreover, using low levels of 9-*O*-AcSia to phenotypically define pDCs enabled a rigorous method to unequivocally identify mature cells of this lineage. Gene expression studies and epigenetic analyses of pre-pDCs and pDCs may reveal key molecular determinants of pDC function and development. Functional assays employing pre-pDCs and pDCs may also improve our understanding of pDC type I IFN production, and clarify the role of pDCs, distinct from cDCs, in priming helper, cytotoxic, and regulatory T cells, both in physiologic and pathophysiologic contexts. Insight gathered from such investigations will elucidate pDC behavior in immunity, tolerance, and autoimmunity, and facilitate the development of novel pDC-targeted protein and small-molecule therapeutics.

Chapter 6:

Bibliography

Akashi, K., Traver, D., Miyamoto, T., and Weissman, I.L. (2000). A clonogenic common myeloid progenitor that gives rise to all myeloid lineages. Nature *404*, 193-197.

Allen, J.S., Pang, K., Skowera, A., Ellis, R., Rackham, C., Lozanoska-Ochser, B., Tree, T., Leslie, R.D., Tremble, J.M., Dayan, C.M.*, et al.* (2009). Plasmacytoid dendritic cells are proportionally expanded at diagnosis of type 1 diabetes and enhance islet autoantigen presentation to T-cells through immune complex capture. Diabetes *58*, 138-145.

Altheide, T.K., Hayakawa, T., Mikkelsen, T.S., Diaz, S., Varki, N., and Varki, A. (2006). System-wide genomic and biochemical comparisons of sialic acid biology among primates and rodents: Evidence for two modes of rapid evolution. J Biol Chem *281*, 25689-25702.

Angata, T., and Varki, A. (2002). Chemical diversity in the sialic acids and related alpha-keto acids: an evolutionary perspective. Chem Rev *102*, 439-469.

Arming, S., Wipfler, D., Mayr, J., Merling, A., Vilas, U., Schauer, R., Schwartz-Albiez, R., and Vlasak, R. (2011). The human Cas1 protein: a sialic acid-specific O-acetyltransferase? Glycobiology *21*, 553-564.

Asselin-Paturel, C., Boonstra, A., Dalod, M., Durand, I., Yessaad, N., Dezutter-Dambuyant, C., Vicari, A., O'Garra, A., Biron, C., Briere, F.*, et al.* (2001). Mouse type I IFN-producing cells are immature APCs with plasmacytoid morphology. Nat Immunol *2*, 1144-1150.

Asselin-Paturel, C., Brizard, G., Chemin, K., Boonstra, A., O'Garra, A., Vicari, A., and Trinchieri, G. (2005). Type I interferon dependence of plasmacytoid dendritic cell activation and migration. J Exp Med *201*, 1157-1167.

Asselin-Paturel, C., and Trinchieri, G. (2005). Production of type I interferons: plasmacytoid dendritic cells and beyond. J Exp Med *202*, 461-465.

Auffray, C., Fogg, D.K., Narni-Mancinelli, E., Senechal, B., Trouillet, C., Saederup, N., Leemput, J., Bigot, K., Campisi, L., Abitbol, M.*, et al.* (2009). CX3CR1+ CD115+ CD135+ common macrophage/DC precursors and the role of CX3CR1 in their response to inflammation. J Exp Med *206*, 595-606.

Banchereau, J., and Pascual, V. (2006). Type I interferon in systemic lupus erythematosus and other autoimmune diseases. Immunity *25*, 383-392.

Bao, Y., Han, Y., Chen, Z., Xu, S., and Cao, X. (2011). IFN-alpha-producing PDCA-1+ Siglec-H- B cells mediate innate immune defense by activating NK cells. Eur J Immunol *41*, 657-668.

Barchet, W., Cella, M., and Colonna, M. (2005). Plasmacytoid dendritic cells--virus experts of innate immunity. Semin Immunol *17*, 253-261.

Barchet, W., Cella, M., Odermatt, B., Asselin-Paturel, C., Colonna, M., and Kalinke, U. (2002). Virus-induced interferon alpha production by a dendritic cell subset in the absence of feedback signaling in vivo. J Exp Med *195*, 507-516.

Bardor, M., Nguyen, D.H., Diaz, S., and Varki, A. (2005). Mechanism of uptake and incorporation of the non-human sialic acid N-glycolylneuraminic acid into human cells. J Biol Chem *280*, 4228-4237.

Barrat, F.J., Meeker, T., Gregorio, J., Chan, J.H., Uematsu, S., Akira, S., Chang, B., Duramad, O., and Coffman, R.L. (2005). Nucleic acids of mammalian origin can act as endogenous ligands for Toll-like receptors and may promote systemic lupus erythematosus. J Exp Med *202*, 1131-1139.

Barton, G.M., Kagan, J.C., and Medzhitov, R. (2006). Intracellular localization of Toll-like receptor 9 prevents recognition of self DNA but facilitates access to viral DNA. Nat Immunol *7*, 49-56.

Bave, U., Magnusson, M., Eloranta, M.L., Perers, A., Alm, G.V., and Ronnblom, L. (2003). Fc gamma RIIa is expressed on natural IFN-alpha-producing cells (plasmacytoid dendritic cells) and is required for the IFN-alpha production induced by apoptotic cells combined with lupus IgG. J Immunol *171*, 3296-3302.

Bax, M., Garcia-Vallejo, J.J., Jang-Lee, J., North, S.J., Gilmartin, T.J., Hernandez, G., Crocker, P.R., Leffler, H., Head, S.R., Haslam, S.M*., et al.* (2007). Dendritic cell maturation results in pronounced changes in glycan expression affecting recognition by siglecs and galectins. J Immunol *179*, 8216-8224.

Bax, M., van Vliet, S.J., Litjens, M., Garcia-Vallejo, J.J., and van Kooyk, Y. (2009). Interaction of polysialic acid with CCL21 regulates the migratory capacity of human dendritic cells. PLoS One *4*, e6987.

Bell, J.J., and Bhandoola, A. (2008). The earliest thymic progenitors for T cells possess myeloid lineage potential. Nature *452*, 764-767.

Benjamini, Y.H., Y. (1995). Controlling the false discovery rate: a practical and powerful approach to multiple testing Journal of the Royal Statistical Society *57*, 289-300.

Bennett, L., Palucka, A.K., Arce, E., Cantrell, V., Borvak, J., Banchereau, J., and Pascual, V. (2003). Interferon and granulopoiesis signatures in systemic lupus erythematosus blood. J Exp Med *197*, 711-723.

Bergfeld, A.K., Pearce, O.M., Diaz, S.L., Pham, T., and Varki, A. (2012). Metabolism of vertebrate amino sugars with N-glycolyl groups: elucidating the intracellular fate of the non-human sialic acid N-glycolylneuraminic acid. J Biol Chem *287*, 28865-28881.

Bernstein, B.E., Mikkelsen, T.S., Xie, X., Kamal, M., Huebert, D.J., Cuff, J., Fry, B., Meissner, A., Wernig, M., Plath, K.*, et al.* (2006). A bivalent chromatin structure marks key developmental genes in embryonic stem cells. Cell *125*, 315-326.

Bjorck, P., Leong, H.X., and Engleman, E.G. (2011). Plasmacytoid dendritic cell dichotomy: identification of IFN-alpha producing cells as a phenotypically and functionally distinct subset. J Immunol *186*, 1477-1485.

Blanco, P., Palucka, A.K., Gill, M., Pascual, V., and Banchereau, J. (2001). Induction of dendritic cell differentiation by IFN-alpha in systemic lupus erythematosus. Science *294*, 1540-1543.

Blasius, A., Vermi, W., Krug, A., Facchetti, F., Cella, M., and Colonna, M. (2004). A cell-surface molecule selectively expressed on murine natural interferon-producing cells that blocks secretion of interferon-alpha. Blood *103*, 4201-4206.

Blasius, A.L., Cella, M., Maldonado, J., Takai, T., and Colonna, M. (2006)a. Siglec-H is an IPC-specific receptor that modulates type I IFN secretion through DAP12. Blood *107*, 2474-2476.

Blasius, A.L., and Colonna, M. (2006). Sampling and signaling in plasmacytoid dendritic cells: the potential roles of Siglec-H. Trends Immunol *27*, 255-260.

Blasius, A.L., Giurisato, E., Cella, M., Schreiber, R.D., Shaw, A.S., and Colonna, M. (2006)b. Bone marrow stromal cell antigen 2 is a specific marker of type I IFN-producing cells in the naive mouse, but a promiscuous cell surface antigen following IFN stimulation. J Immunol *177*, 3260-3265.

Blixt, O., Collins, B.E., van den Nieuwenhof, I.M., Crocker, P.R., and Paulson, J.C. (2003). Sialoside specificity of the siglec family assessed using novel multivalent probes: identification of potent inhibitors of myelin-associated glycoprotein. J Biol Chem *278*, 31007-31019.

Boog, C.J., Neefjes, J.J., Boes, J., Ploegh, H.L., and Melief, C.J. (1989). Specific immune responses restored by alteration in carbohydrate chains of surface molecules on antigen-presenting cells. Eur J Immunol *19*, 537-542.

Brawand, P., Fitzpatrick, D.R., Greenfield, B.W., Brasel, K., Maliszewski, C.R., and De Smedt, T. (2002). Murine plasmacytoid pre-dendritic cells generated from Flt3 ligand-supplemented bone marrow cultures are immature APCs. J Immunol *169*, 6711-6719.

Brinkman-Van der Linden, E.C., Angata, T., Reynolds, S.A., Powell, L.D., Hedrick, S.M., and Varki, A. (2003). CD33/Siglec-3 binding specificity, expression pattern, and consequences of gene deletion in mice. Mol Cell Biol *23*, 4199-4206.

Brinkman-Van der Linden, E.C., Sjoberg, E.R., Juneja, L.R., Crocker, P.R., Varki, N., and Varki, A. (2000). Loss of N-glycolylneuraminic acid in human evolution. Implications for sialic acid recognition by siglecs. J Biol Chem *275*, 8633-8640.

Cabral, M.G., Piteira, A.R., Silva, Z., Ligeiro, D., Brossmer, R., and Videira, P.A. (2010). Human dendritic cells contain cell surface sialyltransferase activity. Immunol Lett *131*, 89-96.

Cao, W., Bover, L., Cho, M., Wen, X., Hanabuchi, S., Bao, M., Rosen, D.B., Wang, Y.H., Shaw, J.L., Du, Q.*, et al.* (2009). Regulation of TLR7/9 responses in plasmacytoid dendritic cells by BST2 and ILT7 receptor interaction. J Exp Med *206*, 1603-1614.

Cao, W., and Liu, Y.J. (2007). Innate immune functions of plasmacytoid dendritic cells. Curr Opin Immunol *19*, 24-30.

Cao, W., Rosen, D.B., Ito, T., Bover, L., Bao, M., Watanabe, G., Yao, Z., Zhang, L., Lanier, L.L., and Liu, Y.J. (2006). Plasmacytoid dendritic cell-specific receptor ILT7-Fc epsilonRI gamma inhibits Toll-like receptor-induced interferon production. J Exp Med *203*, 1399-1405.

Cao, W., Zhang, L., Rosen, D.B., Bover, L., Watanabe, G., Bao, M., Lanier, L.L., and Liu, Y.J. (2007). BDCA2/Fc epsilon RI gamma complex signals through a novel BCR-like pathway in human plasmacytoid dendritic cells. PLoS Biol *5*, e248.

Cariappa, A., Takematsu, H., Liu, H., Diaz, S., Haider, K., Boboila, C., Kalloo, G., Connole, M., Shi, H.N., Varki, N.*, et al.* (2009). B cell antigen receptor signal strength and peripheral B cell development are regulated by a 9-O-acetyl sialic acid esterase. J Exp Med *206*, 125-138.

Cheers, C., and Stanley, E.R. (1988). Macrophage production during murine listeriosis: colony-stimulating factor 1 (CSF-1) and CSF-1-binding cells in genetically resistant and susceptible mice. Infect Immun *56*, 2972-2978.

Chellappa, V., Taylor, K.N., Pedrick, K., Donado, C., Netravali, I.A., Haider, K., Cariappa, A., Dalomba, N.F., and Pillai, S. (2013). M89V Sialic acid Acetyl Esterase (SIAE) and all other non-synonymous common variants of this gene are catalytically normal. PLoS One *8*, e53453.

Chi, A.W., Chavez, A., Xu, L., Weber, B.N., Shestova, O., Schaffer, A., Wertheim, G., Pear, W.S., Izon, D., and Bhandoola, A. (2011). Identification of Flt3(+)CD150(-) myeloid progenitors in adult mouse bone marrow that harbor T lymphoid developmental potential. Blood *118*, 2723-2732.

Chklovskaia, E., Nowbakht, P., Nissen, C., Gratwohl, A., Bargetzi, M., and Wodnar-Filipowicz, A. (2004). Reconstitution of dendritic and natural killer-cell subsets after allogeneic stem cell transplantation: effects of endogenous flt3 ligand. Blood *103*, 3860-3868.

Chou, H.H., Takematsu, H., Diaz, S., Iber, J., Nickerson, E., Wright, K.L., Muchmore, E.A., Nelson, D.L., Warren, S.T., and Varki, A. (1998). A mutation in human CMP-sialic acid hydroxylase occurred after the Homo-Pan divergence. Proc Natl Acad Sci U S A *95*, 11751-11756.

Cisse, B., Caton, M.L., Lehner, M., Maeda, T., Scheu, S., Locksley, R., Holmberg, D., Zweier, C., den Hollander, N.S., Kant, S.G.*, et al.* (2008). Transcription factor E2-2 is an essential and specific regulator of plasmacytoid dendritic cell development. Cell *135*, 37-48.

Coffman, R.L., and Weissman, I.L. (1981). B220: a B cell-specific member of th T200 glycoprotein family. Nature *289*, 681-683.

Collins, B.E., Blixt, O., Bovin, N.V., Danzer, C.P., Chui, D., Marth, J.D., Nitschke, L., and Paulson, J.C. (2002). Constitutively unmasked CD22 on B cells of ST6Gal I knockout mice: novel sialoside probe for murine CD22. Glycobiology *12*, 563-571.

Corcoran, L., Ferrero, I., Vremec, D., Lucas, K., Waithman, J., O'Keeffe, M., Wu, L., Wilson, A., and Shortman, K. (2003). The lymphoid past of mouse plasmacytoid cells and thymic dendritic cells. J Immunol *170*, 4926-4932.

Crespo, H.J., Cabral, M.G., Teixeira, A.V., Lau, J.T., Trindade, H., and Videira, P.A. (2009). Effect of sialic acid loss on dendritic cell maturation. Immunology *128*, e621-631.

Crick, F. (1970). Central dogma of molecular biology. Nature *227*, 561-563.

Crocker, P.R., Paulson, J.C., and Varki, A. (2007). Siglecs and their roles in the immune system. Nat Rev Immunol *7*, 255-266.

Crozat, K., Guiton, R., Guilliams, M., Henri, S., Baranek, T., Schwartz-Cornil, I., Malissen, B., and Dalod, M. (2010). Comparative genomics as a tool to reveal functional equivalences between human and mouse dendritic cell subsets. Immunol Rev *234*, 177-198.

D'Amico, A., and Wu, L. (2003). The early progenitors of mouse dendritic cells and plasmacytoid predendritic cells are within the bone marrow hemopoietic precursors expressing Flt3. J Exp Med *198*, 293-303.

Dai, X.M., Ryan, G.R., Hapel, A.J., Dominguez, M.G., Russell, R.G., Kapp, S., Sylvestre, V., and Stanley, E.R. (2002). Targeted disruption of the mouse colony-stimulating factor 1 receptor gene results in osteopetrosis, mononuclear phagocyte deficiency, increased primitive progenitor cell frequencies, and reproductive defects. Blood *99*, 111-120.

Daley, J.M., Thomay, A.A., Connolly, M.D., Reichner, J.S., and Albina, J.E. (2008). Use of Ly6G-specific monoclonal antibody to deplete neutrophils in mice. J Leukoc Biol *83*, 64-70.

Dalod, M., Salazar-Mather, T.P., Malmgaard, L., Lewis, C., Asselin-Paturel, C., Briere, F., Trinchieri, G., and Biron, C.A. (2002). Interferon alpha/beta and interleukin 12 responses to viral infections: pathways regulating dendritic cell cytokine expression in vivo. J Exp Med *195*, 517-528.

Deane, J.A., Pisitkun, P., Barrett, R.S., Feigenbaum, L., Town, T., Ward, J.M., Flavell, R.A., and Bolland, S. (2007). Control of toll-like receptor 7 expression is essential to restrict autoimmunity and dendritic cell proliferation. Immunity *27*, 801-810.

Delputte, P.L., Van Gorp, H., Favoreel, H.W., Hoebeke, I., Delrue, I., Dewerchin, H., Verdonck, F., Verhasselt, B., Cox, E., and Nauwynck, H.J. (2011). Porcine sialoadhesin (CD169/Siglec-1) is an endocytic receptor that allows targeted delivery of toxins and antigens to macrophages. PLoS One *6*, e16827.

Devine, P.L., Clark, B.A., Birrell, G.W., Layton, G.T., Ward, B.G., Alewood, P.F., and McKenzie, I.F. (1991). The breast tumor-associated epitope defined by monoclonal antibody 3E1.2 is an O-linked mucin carbohydrate containing N-glycolylneuraminic acid. Cancer Res *51*, 5826-5836.

Diana, J., Simoni, Y., Furio, L., Beaudoin, L., Agerberth, B., Barrat, F., and Lehuen, A. (2013). Crosstalk between neutrophils, B-1a cells and plasmacytoid dendritic cells initiates autoimmune diabetes. Nat Med *19*, 65-73.

Diao, J., Winter, E., Cantin, C., Chen, W., Xu, L., Kelvin, D., Phillips, J., and Cattral, M.S. (2006). In situ replication of immediate dendritic cell (DC) precursors contributes to conventional DC homeostasis in lymphoid tissue. J Immunol *176*, 7196-7206.

Diaz, S.L., Padler-Karavani, V., Ghaderi, D., Hurtado-Ziola, N., Yu, H., Chen, X., Brinkman-Van der Linden, E.C., Varki, A., and Varki, N.M. (2009). Sensitive and specific detection of the non-human sialic Acid N-glycolylneuraminic acid in human tissues and biotherapeutic products. PLoS One *4*, e4241.

Ding, L., and Morrison, S.J. (2013). Haematopoietic stem cells and early lymphoid progenitors occupy distinct bone marrow niches. Nature *495*, 231-235.

Drake, P.M., Nathan, J.K., Stock, C.M., Chang, P.V., Muench, M.O., Nakata, D., Reader, J.R., Gip, P., Golden, K.P., Weinhold, B.*, et al.* (2008). Polysialic acid, a glycan with highly restricted expression, is found on human and murine leukocytes and modulates immune responses. J Immunol *181*, 6850-6858.

Drake, P.M., Stock, C.M., Nathan, J.K., Gip, P., Golden, K.P., Weinhold, B., Gerardy-Schahn, R., and Bertozzi, C.R. (2009). Polysialic acid governs T-cell development by regulating progenitor access to the thymus. Proc Natl Acad Sci U S A *106*, 11995-12000.

Dudziak, D., Kamphorst, A.O., Heidkamp, G.F., Buchholz, V.R., Trumpfheller, C., Yamazaki, S., Cheong, C., Liu, K., Lee, H.W., Park, C.G.*, et al.* (2007). Differential antigen processing by dendritic cell subsets in vivo. Science *315*, 107-111.

Fancke, B., Suter, M., Hochrein, H., and O'Keeffe, M. (2008). M-CSF: a novel plasmacytoid and conventional dendritic cell poietin. Blood *111*, 150-159.

Farkas, L., Beiske, K., Lund-Johansen, F., Brandtzaeg, P., and Jahnsen, F.L. (2001). Plasmacytoid dendritic cells (natural interferon- alpha/beta-producing cells) accumulate in cutaneous lupus erythematosus lesions. Am J Pathol *159*, 237-243.

Fogg, D.K., Sibon, C., Miled, C., Jung, S., Aucouturier, P., Littman, D.R., Cumano, A., and Geissmann, F. (2006). A clonogenic bone marrow progenitor specific for macrophages and dendritic cells. Science *311*, 83-87.

Garcia-Romo, G.S., Caielli, S., Vega, B., Connolly, J., Allantaz, F., Xu, Z., Punaro, M., Baisch, J., Guiducci, C., Coffman, R.L.*, et al.* (2011). Netting neutrophils are major inducers of type I IFN production in pediatric systemic lupus erythematosus. Sci Transl Med *3*, 73ra20.

Ghosh, H.S., Cisse, B., Bunin, A., Lewis, K.L., and Reizis, B. (2010). Continuous expression of the transcription factor e2-2 maintains the cell fate of mature plasmacytoid dendritic cells. Immunity *33*, 905-916.

Gilliet, M., Boonstra, A., Paturel, C., Antonenko, S., Xu, X.L., Trinchieri, G., O'Garra, A., and Liu, Y.J. (2002). The development of murine plasmacytoid dendritic cell precursors is differentially regulated by FLT3-ligand and granulocyte/macrophage colony-stimulating factor. J Exp Med *195*, 953-958.

Gilliet, M., Cao, W., and Liu, Y.J. (2008). Plasmacytoid dendritic cells: sensing nucleic acids in viral infection and autoimmune diseases. Nat Rev Immunol *8*, 594-606.

Grouard, G., Rissoan, M.C., Filgueira, L., Durand, I., Banchereau, J., and Liu, Y.J. (1997). The enigmatic plasmacytoid T cells develop into dendritic cells with interleukin (IL)-3 and CD40-ligand. J Exp Med *185*, 1101-1111.

Guiducci, C., Gong, M., Xu, Z., Gill, M., Chaussabel, D., Meeker, T., Chan, J.H., Wright, T., Punaro, M., Bolland, S.*, et al.* (2010). TLR recognition of self nucleic acids hampers glucocorticoid activity in lupus. Nature *465*, 937-941.

Guiducci, C., Ott, G., Chan, J.H., Damon, E., Calacsan, C., Matray, T., Lee, K.D., Coffman, R.L., and Barrat, F.J. (2006). Properties regulating the nature of the plasmacytoid dendritic cell response to Toll-like receptor 9 activation. J Exp Med *203*, 1999-2008.

Guimaraes, M.J., Bazan, J.F., Castagnola, J., Diaz, S., Copeland, N.G., Gilbert, D.J., Jenkins, N.A., Varki, A., and Zlotnik, A. (1996). Molecular cloning and characterization of lysosomal sialic acid O-acetylesterase. J Biol Chem *271*, 13697-13705.

Hadeiba, H., Lahl, K., Edalati, A., Oderup, C., Habtezion, A., Pachynski, R., Nguyen, L., Ghodsi, A., Adler, S., and Butcher, E.C. (2012). Plasmacytoid dendritic cells transport peripheral antigens to the thymus to promote central tolerance. Immunity *36*, 438-450.

Hardy, R.R., Carmack, C.E., Shinton, S.A., Kemp, J.D., and Hayakawa, K. (1991). Resolution and characterization of pro-B and pre-pro-B cell stages in normal mouse bone marrow. J Exp Med *173*, 1213-1225.

Harman, B.C., Miller, J.P., Nikbakht, N., Gerstein, R., and Allman, D. (2006). Mouse plasmacytoid dendritic cells derive exclusively from estrogen-resistant myeloid progenitors. Blood *108*, 878-885.

Heath, W.R., and Carbone, F.R. (2001). Cross-presentation in viral immunity and self-tolerance. Nat Rev Immunol *1*, 126-134.

Hedlund, M., Tangvoranuntakul, P., Takematsu, H., Long, J.M., Housley, G.D., Kozutsumi, Y., Suzuki, A., Wynshaw-Boris, A., Ryan, A.F., Gallo, R.L.*, et al.* (2007). N-glycolylneuraminic acid deficiency in mice: implications for human biology and evolution. Mol Cell Biol *27*, 4340-4346.

Heng, T.S., and Painter, M.W. (2008). The Immunological Genome Project: networks of gene expression in immune cells. Nat Immunol *9*, 1091-1094.

Herrler, G., Rott, R., Klenk, H.D., Muller, H.P., Shukla, A.K., and Schauer, R. (1985). The receptor-destroying enzyme of influenza C virus is neuraminate-O-acetylesterase. Embo J *4*, 1503-1506.

Higashi, H., Hirabayashi, Y., Fukui, Y., Naiki, M., Matsumoto, M., Ueda, S., and Kato, S. (1985). Characterization of N-glycolylneuraminic acid-containing gangliosides as tumor-associated Hanganutziu-Deicher antigen in human colon cancer. Cancer Res *45*, 3796-3802.

Hirabayashi, Y., Higashi, H., Kato, S., Taniguchi, M., and Matsumoto, M. (1987). Occurrence of tumor-associated ganglioside antigens with Hanganutziu-Deicher antigenic activity on human melanomas. Jpn J Cancer Res *78*, 614-620.

Hirai, H., Zhang, P., Dayaram, T., Hetherington, C.J., Mizuno, S., Imanishi, J., Akashi, K., and Tenen, D.G. (2006). C/EBPbeta is required for 'emergency' granulopoiesis. Nat Immunol *7*, 732-739.

Hochrein, H., Shortman, K., Vremec, D., Scott, B., Hertzog, P., and O'Keeffe, M. (2001). Differential production of IL-12, IFN-alpha, and IFN-gamma by mouse dendritic cell subsets. J Immunol *166*, 5448-5455.

Honda, K., Ohba, Y., Yanai, H., Negishi, H., Mizutani, T., Takaoka, A., Taya, C., and Taniguchi, T. (2005). Spatiotemporal regulation of MyD88-IRF-7 signalling for robust type-I interferon induction. Nature *434*, 1035-1040.

Huang, X., Hultgren, B., Dybdal, N., and Stewart, T.A. (1994). Islet expression of interferon-alpha precedes diabetes in both the BB rat and streptozotocin-treated mice. Immunity *1*, 469-478.

Huang, X., Yuang, J., Goddard, A., Foulis, A., James, R.F., Lernmark, A., Pujol-Borrell, R., Rabinovitch, A., Somoza, N., and Stewart, T.A. (1995). Interferon expression in the pancreases of patients with type I diabetes. Diabetes *44*, 658-664.

Idoyaga, J., Suda, N., Suda, K., Park, C.G., and Steinman, R.M. (2009). Antibody to Langerin/CD207 localizes large numbers of CD8alpha+ dendritic cells to the marginal zone of mouse spleen. Proc Natl Acad Sci U S A *106*, 1524-1529.

Irie, A., Koyama, S., Kozutsumi, Y., Kawasaki, T., and Suzuki, A. (1998). The molecular basis for the absence of N-glycolylneuraminic acid in humans. J Biol Chem *273*, 15866-15871.

Irizarry, R.A., Bolstad, B.M., Collin, F., Cope, L.M., Hobbs, B., and Speed, T.P. (2003). Summaries of Affymetrix GeneChip probe level data. Nucleic Acids Res *31*, e15.

Iwasaki, A. (2007). Mucosal dendritic cells. Annu Rev Immunol *25*, 381-418.

Izaguirre, A., Barnes, B.J., Amrute, S., Yeow, W.S., Megjugorac, N., Dai, J., Feng, D., Chung, E., Pitha, P.M., and Fitzgerald-Bocarsly, P. (2003). Comparative analysis of IRF and IFN-alpha expression in human plasmacytoid and monocyte-derived dendritic cells. J Leukoc Biol *74*, 1125-1138.

Jakubzick, C., Bogunovic, M., Bonito, A.J., Kuan, E.L., Merad, M., and Randolph, G.J. (2008). Lymph-migrating, tissue-derived dendritic cells are minor constituents within steady-state lymph nodes. J Exp Med *205*, 2839-2850.

Jego, G., Palucka, A.K., Blanck, J.P., Chalouni, C., Pascual, V., and Banchereau, J. (2003). Plasmacytoid dendritic cells induce plasma cell differentiation through type I interferon and interleukin 6. Immunity *19*, 225-234.

Jenner, J., Kerst, G., Handgretinger, R., and Muller, I. (2006). Increased alpha2,6-sialylation of surface proteins on tolerogenic, immature dendritic cells and regulatory T cells. Exp Hematol *34*, 1212-1218.

Jouvenet, N., Neil, S.J., Zhadina, M., Zang, T., Kratovac, Z., Lee, Y., McNatt, M., Hatziioannou, T., and Bieniasz, P.D. (2009). Broad-spectrum inhibition of retroviral and filoviral particle release by tetherin. J Virol *83*, 1837-1844.

Kariko, K., Buckstein, M., Ni, H., and Weissman, D. (2005). Suppression of RNA recognition by Toll-like receptors: the impact of nucleoside modification and the evolutionary origin of RNA. Immunity *23*, 165-175.

Karsunky, H., Merad, M., Cozzio, A., Weissman, I.L., and Manz, M.G. (2003). Flt3 ligand regulates dendritic cell development from Flt3+ lymphoid and myeloid-committed progenitors to Flt3+ dendritic cells in vivo. J Exp Med *198*, 305-313.

Kawachi, S., Saida, T., Uhara, H., Uemura, K., Taketomi, T., and Kano, K. (1988). Heterophile Hanganutziu-Deicher antigen in ganglioside fractions of human melanoma tissues. Int Arch Allergy Appl Immunol *85*, 381-383.

Kelm, S., Brossmer, R., Isecke, R., Gross, H.J., Strenge, K., and Schauer, R. (1998). Functional groups of sialic acids involved in binding to siglecs (sialoadhesins) deduced from interactions with synthetic analogues. Eur J Biochem *255*, 663-672.

Kelm, S., and Schauer, R. (1997). Sialic acids in molecular and cellular interactions. Int Rev Cytol *175*, 137-240.

Kerkmann, M., Rothenfusser, S., Hornung, V., Towarowski, A., Wagner, M., Sarris, A., Giese, T., Endres, S., and Hartmann, G. (2003). Activation with CpG-A and CpG-B oligonucleotides reveals two distinct regulatory pathways of type I IFN synthesis in human plasmacytoid dendritic cells. J Immunol *170*, 4465-4474.

Klein, A., Krishna, M., Varki, N.M., and Varki, A. (1994). 9-O-acetylated sialic acids have widespread but selective expression: analysis using a chimeric dual-function probe derived from influenza C hemagglutinin-esterase. Proc Natl Acad Sci U S A *91*, 7782-7786.

Kondo, M., Weissman, I.L., and Akashi, K. (1997). Identification of clonogenic common lymphoid progenitors in mouse bone marrow. Cell *91*, 661-672.

Kornfeld, R., and Kornfeld, S. (1985). Assembly of asparagine-linked oligosaccharides. Annu Rev Biochem *54*, 631-664.

Koski, G.K., Kariko, K., Xu, S., Weissman, D., Cohen, P.A., and Czerniecki, B.J. (2004). Cutting edge: innate immune system discriminates between RNA containing bacterial versus eukaryotic structural features that prime for high-level IL-12 secretion by dendritic cells. J Immunol *172*, 3989-3993.

Krieg, A.M. (2002). CpG motifs in bacterial DNA and their immune effects. Annu Rev Immunol *20*, 709-760.

Krieg, A.M., and Vollmer, J. (2007). Toll-like receptors 7, 8, and 9: linking innate immunity to autoimmunity. Immunol Rev *220*, 251-269.

Krishna, M., and Varki, A. (1997). 9-O-Acetylation of sialomucins: a novel marker of murine CD4 T cells that is regulated during maturation and activation. J Exp Med *185*, 1997-2013.

Lande, R., Ganguly, D., Facchinetti, V., Frasca, L., Conrad, C., Gregorio, J., Meller, S., Chamilos, G., Sebasigari, R., Riccieri, V.*, et al.* (2011). Neutrophils activate plasmacytoid dendritic cells by releasing self-DNA-peptide complexes in systemic lupus erythematosus. Sci Transl Med *3*, 73ra19.

Lande, R., Gregorio, J., Facchinetti, V., Chatterjee, B., Wang, Y.H., Homey, B., Cao, W., Su, B., Nestle, F.O., Zal, T.*, et al.* (2007). Plasmacytoid dendritic cells sense self-DNA coupled with antimicrobial peptide. Nature *449*, 564-569.

Laouar, Y., Welte, T., Fu, X.Y., and Flavell, R.A. (2003). STAT3 is required for Flt3L-dependent dendritic cell differentiation. Immunity *19*, 903-912.

Lau, C.M., Broughton, C., Tabor, A.S., Akira, S., Flavell, R.A., Mamula, M.J., Christensen, S.R., Shlomchik, M.J., Viglianti, G.A., Rifkin, I.R.*, et al.* (2005). RNA-associated autoantigens activate B cells by combined B cell antigen receptor/Toll-like receptor 7 engagement. J Exp Med *202*, 1171-1177.

Li, C., and Wong, W.H. (2001). Model-based analysis of oligonucleotide arrays: expression index computation and outlier detection. Proc Natl Acad Sci U S A *98*, 31-36.

Li, J., Park, J., Foss, D., and Goldschneider, I. (2009). Thymus-homing peripheral dendritic cells constitute two of the three major subsets of dendritic cells in the steady-state thymus. J Exp Med *206*, 607-622.

Li, Q., Xu, B., Michie, S.A., Rubins, K.H., Schreriber, R.D., and McDevitt, H.O. (2008). Interferon-alpha initiates type 1 diabetes in nonobese diabetic mice. Proc Natl Acad Sci U S A *105*, 12439-12444.

Lin, M.L., Zhan, Y., Villadangos, J.A., and Lew, A.M. (2008). The cell biology of cross-presentation and the role of dendritic cell subsets. Immunol Cell Biol *86*, 353-362.

Lindstedt, M., Lundberg, K., and Borrebaeck, C.A. (2005). Gene family clustering identifies functionally associated subsets of human in vivo blood and tonsillar dendritic cells. J Immunol *175*, 4839-4846.

Liou, L.Y., Blasius, A.L., Welch, M.J., Colonna, M., Oldstone, M.B., and Zuniga, E.I. (2008). In vivo conversion of BM plasmacytoid DC into CD11b+ conventional DC during virus infection. Eur J Immunol *38*, 3388-3394.

Liu, K., Victora, G.D., Schwickert, T.A., Guermonprez, P., Meredith, M.M., Yao, K., Chu, F.F., Randolph, G.J., Rudensky, A.Y., and Nussenzweig, M. (2009). In vivo analysis of dendritic cell development and homeostasis. Science *324*, 392-397.

Liu, K., Waskow, C., Liu, X., Yao, K., Hoh, J., and Nussenzweig, M. (2007). Origin of dendritic cells in peripheral lymphoid organs of mice. Nat Immunol *8*, 578-583.

Liu, Y.J. (2005). IPC: professional type 1 interferon-producing cells and plasmacytoid dendritic cell precursors. Annu Rev Immunol *23*, 275-306.

Lovgren, T., Eloranta, M.L., Bave, U., Alm, G.V., and Ronnblom, L. (2004). Induction of interferon-alpha production in plasmacytoid dendritic cells by immune complexes containing nucleic acid released by necrotic or late apoptotic cells and lupus IgG. Arthritis Rheum *50*, 1861-1872.

Luc, S., Luis, T.C., Boukarabila, H., Macaulay, I.C., Buza-Vidas, N., Bouriez-Jones, T., Lutteropp, M., Woll, P.S., Loughran, S.J., Mead, A.J.*, et al.* (2012). The earliest thymic T cell progenitors sustain B cell and myeloid lineage potential. Nat Immunol *13*, 412-419.

MacDonald, K.P., Rowe, V., Bofinger, H.M., Thomas, R., Sasmono, T., Hume, D.A., and Hill, G.R. (2005). The colony-stimulating factor 1 receptor is expressed on dendritic cells during differentiation and regulates their expansion. J Immunol *175*, 1399-1405.

Maldonado-Lopez, R., De Smedt, T., Michel, P., Godfroid, J., Pajak, B., Heirman, C., Thielemans, K., Leo, O., Urbain, J., and Moser, M. (1999). CD8alpha+ and CD8alpha- subclasses of dendritic cells direct the development of distinct T helper cells in vivo. J Exp Med *189*, 587-592.

Malykh, Y.N., Schauer, R., and Shaw, L. (2001). N-Glycolylneuraminic acid in human tumours. Biochimie *83*, 623-634.

Maraskovsky, E., Brasel, K., Teepe, M., Roux, E.R., Lyman, S.D., Shortman, K., and McKenna, H.J. (1996). Dramatic increase in the numbers of functionally mature dendritic cells in Flt3 ligand-treated mice: multiple dendritic cell subpopulations identified. J Exp Med *184*, 1953-1962.

Marshak-Rothstein, A. (2006). Toll-like receptors in systemic autoimmune disease. Nat Rev Immunol *6*, 823-835.

Martin, L.T., Verhagen, A., and Varki, A. (2003). Recombinant influenza C hemagglutinin-esterase as a probe for sialic acid 9-O-acetylation. Methods Enzymol *363*, 489-498.

McKenna, H.J., Stocking, K.L., Miller, R.E., Brasel, K., De Smedt, T., Maraskovsky, E., Maliszewski, C.R., Lynch, D.H., Smith, J., Pulendran, B.*, et al.* (2000). Mice lacking flt3 ligand have deficient hematopoiesis affecting hematopoietic progenitor cells, dendritic cells, and natural killer cells. Blood *95*, 3489-3497.

Means, T.K., Latz, E., Hayashi, F., Murali, M.R., Golenbock, D.T., and Luster, A.D. (2005). Human lupus autoantibody-DNA complexes activate DCs through cooperation of CD32 and TLR9. J Clin Invest *115*, 407-417.

Mebius, R.E., Miyamoto, T., Christensen, J., Domen, J., Cupedo, T., Weissman, I.L., and Akashi, K. (2001). The fetal liver counterpart of adult common lymphoid progenitors gives rise to all lymphoid lineages, CD45+CD4+CD3- cells, as well as macrophages. J Immunol *166*, 6593-6601.

Meyers, J.H., Justement, J.S., Hallahan, C.W., Blair, E.T., Sun, Y.A., O'Shea, M.A., Roby, G., Kottilil, S., Moir, S., Kovacs, C.M.*, et al.* (2007). Impact of HIV on cell survival and antiviral activity of plasmacytoid dendritic cells. PLoS One *2*, e458.

Mikkelsen, T.S., Ku, M., Jaffe, D.B., Issac, B., Lieberman, E., Giannoukos, G., Alvarez, P., Brockman, W., Kim, T.K., Koche, R.P.*, et al.* (2007). Genome-wide maps of chromatin state in pluripotent and lineage-committed cells. Nature *448*, 553-560.

Miller, G., Pillarisetty, V.G., Shah, A.B., Lahrs, S., and DeMatteo, R.P. (2003). Murine Flt3 ligand expands distinct dendritic cells with both tolerogenic and immunogenic properties. J Immunol *170*, 3554-3564.

Miyagi, E., Andrew, A.J., Kao, S., and Strebel, K. (2009). Vpu enhances HIV-1 virus release in the absence of Bst-2 cell surface down-modulation and intracellular depletion. Proc Natl Acad Sci U S A *106*, 2868-2873.

Miyoshi, I., Higashi, H., Hirabayashi, Y., Kato, S., and Naiki, M. (1986). Detection of 4-O-acetyl-N-glycolylneuraminyl lactosylceramide as one of tumor-associated antigens in human colon cancer tissues by specific antibody. Mol Immunol *23*, 631-638.

Monteiro, V.G., Lobato, C.S., Silva, A.R., Medina, D.V., de Oliveira, M.A., Seabra, S.H., de Souza, W., and DaMatta, R.A. (2005). Increased association of Trypanosoma cruzi with sialoadhesin positive mice macrophages. Parasitol Res *97*, 380-385.

Moser, M., and Murphy, K.M. (2000). Dendritic cell regulation of TH1-TH2 development. Nat Immunol *1*, 199-205.

Muchmore, E.A., and Varki, A. (1987). Selective inactivation of influenza C esterase: a probe for detecting 9-O-acetylated sialic acids. Science *236*, 1293-1295.

Naik, S.H., Metcalf, D., van Nieuwenhuijze, A., Wicks, I., Wu, L., O'Keeffe, M., and Shortman, K. (2006). Intrasplenic steady-state dendritic cell precursors that are distinct from monocytes. Nat Immunol *7*, 663-671.

Naik, S.H., Perie, L., Swart, E., Gerlach, C., van Rooij, N., de Boer, R.J., and Schumacher, T.N. (2013). Diverse and heritable lineage imprinting of early haematopoietic progenitors. Nature *496*, 229-232.

Naik, S.H., Sathe, P., Park, H.Y., Metcalf, D., Proietto, A.I., Dakic, A., Carotta, S., O'Keeffe, M., Bahlo, M., Papenfuss, A.*, et al.* (2007). Development of plasmacytoid and conventional dendritic cell subtypes from single precursor cells derived in vitro and in vivo. Nat Immunol *8*, 1217-1226.

Naito, Y., Takematsu, H., Koyama, S., Miyake, S., Yamamoto, H., Fujinawa, R., Sugai, M., Okuno, Y., Tsujimoto, G., Yamaji, T.*, et al.* (2007). Germinal center marker GL7 probes activation-dependent repression of N-glycolylneuraminic acid, a sialic acid species involved in the negative modulation of B-cell activation. Mol Cell Biol *27*, 3008-3022.

Napirei, M., Karsunky, H., Zevnik, B., Stephan, H., Mannherz, H.G., and Moroy, T. (2000). Features of systemic lupus erythematosus in Dnase1-deficient mice. Nat Genet *25*, 177-181.

Neil, S.J., Zang, T., and Bieniasz, P.D. (2008). Tetherin inhibits retrovirus release and is antagonized by HIV-1 Vpu. Nature *451*, 425-430.

Nestle, F.O., Conrad, C., Tun-Kyi, A., Homey, B., Gombert, M., Boyman, O., Burg, G., Liu, Y.J., and Gilliet, M. (2005). Plasmacytoid predendritic cells initiate psoriasis through interferon-alpha production. J Exp Med *202*, 135-143.

Nitschke, L., Carsetti, R., Ocker, B., Kohler, G., and Lamers, M.C. (1997). CD22 is a negative regulator of B-cell receptor signalling. Curr Biol *7*, 133-143.

O'Keeffe, M., Fancke, B., Suter, M., Ramm, G., Clark, J., Wu, L., and Hochrein, H. (2012). Nonplasmacytoid, high IFN-alpha-producing, bone marrow dendritic cells. J Immunol *188*, 3774-3783.

O'Keeffe, M., Hochrein, H., Vremec, D., Caminschi, I., Miller, J.L., Anders, E.M., Wu, L., Lahoud, M.H., Henri, S., Scott, B.*, et al.* (2002). Mouse plasmacytoid cells: long-lived cells, heterogeneous in surface phenotype and function, that differentiate into CD8(+) dendritic cells only after microbial stimulus. J Exp Med *196*, 1307-1319.

Oguro, H., Ding, L., and Morrison, S.J. (2013). SLAM family markers resolve functionally distinct subpopulations of hematopoietic stem cells and multipotent progenitors. Cell Stem Cell *13*, 102-116.

Olweus, J., BitMansour, A., Warnke, R., Thompson, P.A., Carballido, J., Picker, L.J., and Lund-Johansen, F. (1997). Dendritic cell ontogeny: a human dendritic cell lineage of myeloid origin. Proc Natl Acad Sci U S A *94*, 12551-12556.

Onai, N., Kurabayashi, K., Hosoi-Amaike, M., Toyama-Sorimachi, N., Matsushima, K., Inaba, K., and Ohteki, T. (2013). A clonogenic progenitor with prominent plasmacytoid dendritic cell developmental potential. Immunity *38*, 943-957.

Onai, N., Manz, M.G., and Schmid, M.A. (2010). Isolation of common dendritic cell progenitors (CDP) from mouse bone marrow. Methods Mol Biol *595*, 195-203.

Onai, N., Obata-Onai, A., Schmid, M.A., Ohteki, T., Jarrossay, D., and Manz, M.G. (2007). Identification of clonogenic common Flt3+M-CSFR+ plasmacytoid and conventional dendritic cell progenitors in mouse bone marrow. Nat Immunol *8*, 1207-1216.

Otipoby, K.L., Andersson, K.B., Draves, K.E., Klaus, S.J., Farr, A.G., Kerner, J.D., Perlmutter, R.M., Law, C.L., and Clark, E.A. (1996). CD22 regulates thymus-independent responses and the lifespan of B cells. Nature *384*, 634-637.

Pelayo, R., Hirose, J., Huang, J., Garrett, K.P., Delogu, A., Busslinger, M., and Kincade, P.W. (2005). Derivation of 2 categories of plasmacytoid dendritic cells in murine bone marrow. Blood *105*, 4407-4415.

Pillai, S., Cariappa, A., and Pirnie, S.P. (2009). Esterases and autoimmunity: the sialic acid acetylesterase pathway and the regulation of peripheral B cell tolerance. Trends Immunol *30*, 488-493.

Pillai, S., Netravali, I.A., Cariappa, A., and Mattoo, H. (2012). Siglecs and immune regulation. Annu Rev Immunol *30*, 357-392.

Pisetsky, D.S., and Fairhurst, A.M. (2007). The origin of extracellular DNA during the clearance of dead and dying cells. Autoimmunity *40*, 281-284.

Pulendran, B., Smith, J.L., Caspary, G., Brasel, K., Pettit, D., Maraskovsky, E., and Maliszewski, C.R. (1999). Distinct dendritic cell subsets differentially regulate the class of immune response in vivo. Proc Natl Acad Sci U S A *96*, 1036-1041.

Reis e Sousa, C., Hieny, S., Scharton-Kersten, T., Jankovic, D., Charest, H., Germain, R.N., and Sher, A. (1997). In vivo microbial stimulation induces rapid CD40 ligand-independent production of interleukin 12 by dendritic cells and their redistribution to T cell areas. J Exp Med *186*, 1819-1829.

Reizis, B., Bunin, A., Ghosh, H.S., Lewis, K.L., and Sisirak, V. (2011). Plasmacytoid dendritic cells: recent progress and open questions. Annu Rev Immunol *29*, 163-183.

Rey-Gallardo, A., Delgado-Martin, C., Gerardy-Schahn, R., Rodriguez-Fernandez, J.L., and Vega, M.A. (2011). Polysialic acid is required for neuropilin-2a/b-mediated control of CCL21-driven chemotaxis of mature dendritic cells and for their migration in vivo. Glycobiology *21*, 655-662.

Rey-Gallardo, A., Escribano, C., Delgado-Martin, C., Rodriguez-Fernandez, J.L., Gerardy-Schahn, R., Rutishauser, U., Corbi, A.L., and Vega, M.A. (2010). Polysialylated neuropilin-2 enhances human dendritic cell migration through the basic C-terminal region of CCL21. Glycobiology *20*, 1139-1146.

Reya, T., Morrison, S.J., Clarke, M.F., and Weissman, I.L. (2001). Stem cells, cancer, and cancer stem cells. Nature *414*, 105-111.

Rogers, G.N., Herrler, G., Paulson, J.C., and Klenk, H.D. (1986). Influenza C virus uses 9-O-acetyl-N-acetylneuraminic acid as a high affinity receptor determinant for attachment to cells. J Biol Chem *261*, 5947-5951.

Ronnblom, L., and Alm, G.V. (2001). A pivotal role for the natural interferon alpha-producing cells (plasmacytoid dendritic cells) in the pathogenesis of lupus. J Exp Med *194*, F59-63.

Ronnblom, L., Eloranta, M.L., and Alm, G.V. (2003). Role of natural interferon-alpha producing cells (plasmacytoid dendritic cells) in autoimmunity. Autoimmunity *36*, 463-472.

Rubtsov, A.V., Rubtsova, K., Fischer, A., Meehan, R.T., Gillis, J.Z., Kappler, J.W., and Marrack, P. (2011). Toll-like receptor 7 (TLR7)-driven accumulation of a novel CD11c(+) B-cell population is important for the development of autoimmunity. Blood *118*, 1305-1315.

Sandgren, S., Wittrup, A., Cheng, F., Jonsson, M., Eklund, E., Busch, S., and Belting, M. (2004). The human antimicrobial peptide LL-37 transfers extracellular DNA plasmid to the nuclear compartment of mammalian cells via lipid rafts and proteoglycan-dependent endocytosis. J Biol Chem *279*, 17951-17956.

Sano, H., and Morimoto, C. (1982). Dna isolated from DNA/anti-DNA antibody immune complexes in systemic lupus erythematosus is rich in guanine-cytosine content. J Immunol *128*, 1341-1345.

Satake, S., Hirai, H., Hayashi, Y., Shime, N., Tamura, A., Yao, H., Yoshioka, S., Miura, Y., Inaba, T., Fujita, N.*, et al.* (2012). C/EBPbeta is involved in the amplification of early granulocyte precursors during candidemia-induced "emergency" granulopoiesis. J Immunol *189*, 4546-4555.

Sathe, P., Vremec, D., Wu, L., Corcoran, L., and Shortman, K. (2013). Convergent differentiation: myeloid and lymphoid pathways to murine plasmacytoid dendritic cells. Blood *121*, 11-19.

Sato, S., Miller, A.S., Inaoki, M., Bock, C.B., Jansen, P.J., Tang, M.L., and Tedder, T.F. (1996). CD22 is both a positive and negative regulator of B lymphocyte antigen receptor signal transduction: altered signaling in CD22-deficient mice. Immunity *5*, 551-562.

Satpathy, A.T., Kc, W., Albring, J.C., Edelson, B.T., Kretzer, N.M., Bhattacharya, D., Murphy, T.L., and Murphy, K.M. (2012). Zbtb46 expression distinguishes classical dendritic cells and their committed progenitors from other immune lineages. J Exp Med *209*, 1135-1152.

Schlenzka, W., Shaw, L., Kelm, S., Schmidt, C.L., Bill, E., Trautwein, A.X., Lottspeich, F., and Schauer, R. (1996). CMP-N-acetylneuraminic acid hydroxylase: the first cytosolic Rieske iron-sulphur protein to be described in Eukarya. FEBS Lett *385*, 197-200.

Schlitzer, A., Heiseke, A.F., Einwachter, H., Reindl, W., Schiemann, M., Manta, C.P., See, P., Niess, J.H., Suter, T., Ginhoux, F.*, et al.* (2012). Tissue-specific differentiation of a circulating CCR9- pDC-like common dendritic cell precursor. Blood *119*, 6063-6071.

Schlitzer, A., Loschko, J., Mair, K., Vogelmann, R., Henkel, L., Einwachter, H., Schiemann, M., Niess, J.H., Reindl, W., and Krug, A. (2011). Identification of CCR9- murine plasmacytoid DC precursors with plasticity to differentiate into conventional DCs. Blood *117*, 6562-6570.

Schmid, M.A., Kingston, D., Boddupalli, S., and Manz, M.G. (2010). Instructive cytokine signals in dendritic cell lineage commitment. Immunol Rev *234*, 32-44.

Schraml, B.U., van Blijswijk, J., Zelenay, S., Whitney, P.G., Filby, A., Acton, S.E., Rogers, N.C., Moncaut, N., Carvajal, J.J., and Reis e Sousa, C. (2013). Genetic tracing via DNGR-1 expression history defines dendritic cells as a hematopoietic lineage. Cell *154*, 843-858.

Segura, E., Wong, J., and Villadangos, J.A. (2009). Cutting edge: B220+CCR9- dendritic cells are not plasmacytoid dendritic cells but are precursors of conventional dendritic cells. J Immunol *183*, 1514-1517.

Sharon, N., and Lis, H. (1982). Glycoproteins: research booming on long-ignored ubiquitous compounds. Mol Cell Biochem *42*, 167-187.

Shigematsu, H., Reizis, B., Iwasaki, H., Mizuno, S., Hu, D., Traver, D., Leder, P., Sakaguchi, N., and Akashi, K. (2004). Plasmacytoid dendritic cells activate lymphoid-specific genetic programs irrespective of their cellular origin. Immunity *21*, 43-53.

Shortman, K., and Liu, Y.J. (2002). Mouse and human dendritic cell subtypes. Nat Rev Immunol *2*, 151-161.

Sjoberg, E.R., Powell, L.D., Klein, A., and Varki, A. (1994). Natural ligands of the B cell adhesion molecule CD22 beta can be masked by 9-O-acetylation of sialic acids. J Cell Biol *126*, 549-562.

Soumelis, V., and Liu, Y.J. (2006). From plasmacytoid to dendritic cell: morphological and functional switches during plasmacytoid pre-dendritic cell differentiation. Eur J Immunol *36*, 2286-2292.

Stacey, K.J., Young, G.R., Clark, F., Sester, D.P., Roberts, T.L., Naik, S., Sweet, M.J., and Hume, D.A. (2003). The molecular basis for the lack of immunostimulatory activity of vertebrate DNA. J Immunol *170*, 3614-3620.

Stamatos, N.M., Carubelli, I., van de Vlekkert, D., Bonten, E.J., Papini, N., Feng, C., Venerando, B., d'Azzo, A., Cross, A.S., Wang, L.X*., et al.* (2010). LPS-induced cytokine production in human dendritic cells is regulated by sialidase activity. J Leukoc Biol *88*, 1227-1239.

Stamatos, N.M., Liang, F., Nan, X., Landry, K., Cross, A.S., Wang, L.X., and Pshezhetsky, A.V. (2005). Differential expression of endogenous sialidases of human monocytes during cellular differentiation into macrophages. Febs J *272*, 2545-2556.

Stoddart, A., Zhang, Y., and Paige, C.J. (1996). Molecular cloning of the cDNA encoding a murine sialic acid-specific 9-O-acetylesterase and RNA expression in cells of hematopoietic and non-hematopoietic origin. Nucleic Acids Res *24*, 4003-4008.

Surolia, I., Pirnie, S.P., Chellappa, V., Taylor, K.N., Cariappa, A., Moya, J., Liu, H., Bell, D.W., Driscoll, D.R., Diederichs, S.*, et al.* (2010). Functionally defective germline variants of sialic acid acetylesterase in autoimmunity. Nature *466*, 243-247.

Swiecki, M., and Colonna, M. (2010). Unraveling the functions of plasmacytoid dendritic cells during viral infections, autoimmunity, and tolerance. Immunol Rev *234*, 142-162.

Takagi, H., Fukaya, T., Eizumi, K., Sato, Y., Sato, K., Shibazaki, A., Otsuka, H., Hijikata, A., Watanabe, T., Ohara, O.*, et al.* (2011). Plasmacytoid dendritic cells are crucial for the initiation of inflammation and T cell immunity in vivo. Immunity *35*, 958-971.

Takematsu, H., Diaz, S., Stoddart, A., Zhang, Y., and Varki, A. (1999). Lysosomal and cytosolic sialic acid 9-O-acetylesterase activities can Be encoded by one gene via differential usage of a signal peptide-encoding exon at the N terminus. J Biol Chem *274*, 25623-25631.

Takeuchi, S., and Katz, S.I. (2006). Use of interleukin 7 receptor-alpha knockout donor cells demonstrates the lymphoid independence of dendritic cells. Blood *107*, 184-186.

Tangvoranuntakul, P., Gagneux, P., Diaz, S., Bardor, M., Varki, N., Varki, A., and Muchmore, E. (2003). Human uptake and incorporation of an immunogenic nonhuman dietary sialic acid. Proc Natl Acad Sci U S A *100*, 12045-12050.

Taylor, P.R., Martinez-Pomares, L., Stacey, M., Lin, H.H., Brown, G.D., and Gordon, S. (2005). Macrophage receptors and immune recognition. Annu Rev Immunol *23*, 901-944.

ten Boekel, E., Melchers, F., and Rolink, A. (1995). The status of Ig loci rearrangements in single cells from different stages of B cell development. Int Immunol *7*, 1013-1019.

Tezuka, H., Abe, Y., Asano, J., Sato, T., Liu, J., Iwata, M., and Ohteki, T. (2011). Prominent role for plasmacytoid dendritic cells in mucosal T cell-independent IgA induction. Immunity *34*, 247-257.

Tian, J., Avalos, A.M., Mao, S.Y., Chen, B., Senthil, K., Wu, H., Parroche, P., Drabic, S., Golenbock, D., Sirois, C.*, et al.* (2007). Toll-like receptor 9-dependent activation by DNA-containing immune complexes is mediated by HMGB1 and RAGE. Nat Immunol *8*, 487-496.

Troy, F.A., 2nd (1992). Polysialylation: from bacteria to brains. Glycobiology *2*, 5-23.
Tussiwand, R., Onai, N., Mazzucchelli, L., and Manz, M.G. (2005). Inhibition of natural type I IFN-producing and dendritic cell development by a small molecule receptor tyrosine kinase inhibitor with Flt3 affinity. J Immunol *175*, 3674-3680.

Ueda, Y., Cain, D.W., Kuraoka, M., Kondo, M., and Kelsoe, G. (2009). IL-1R type I-dependent hemopoietic stem cell proliferation is necessary for inflammatory granulopoiesis and reactive neutrophilia. J Immunol *182*, 6477-6484.

Van Damme, N., Goff, D., Katsura, C., Jorgenson, R.L., Mitchell, R., Johnson, M.C., Stephens, E.B., and Guatelli, J. (2008). The interferon-induced protein BST-2 restricts HIV-1 release and is downregulated from the cell surface by the viral Vpu protein. Cell Host Microbe *3*, 245-252.

Vanderheijden, N., Delputte, P.L., Favoreel, H.W., Vandekerckhove, J., Van Damme, J., van Woensel, P.A., and Nauwynck, H.J. (2003). Involvement of sialoadhesin in entry of porcine reproductive and respiratory syndrome virus into porcine alveolar macrophages. J Virol *77*, 8207-8215.

Varki, A. (2001). Loss of N-glycolylneuraminic acid in humans: Mechanisms, consequences, and implications for hominid evolution. Am J Phys Anthropol *Suppl 33*, 54-69.

Varki, A., and Angata, T. (2006). Siglecs--the major subfamily of I-type lectins. Glycobiology *16*, 1R-27R.

Varki, A., and Crocker, P.R. (2009). I-type Lectins. In Essentials of Glycobiology, A.

Varki, R.D. Cummings, J.D. Esko, H.H. Freeze, P. Stanley, C.R. Bertozzi, G.W. Hart, and M.E. Etzler, eds. (Cold Spring Harbor (NY)).

Varki, A., and Gagneux, P. (2012). Multifarious roles of sialic acids in immunity. Ann N Y Acad Sci *1253*, 16-36.

Varki, A., and Schauer, R. (2009). Sialic Acids. In Essentials of Glycobiology, A. Varki, R.D. Cummings, J.D. Esko, H.H. Freeze, P. Stanley, C.R. Bertozzi, G.W. Hart, and M.E. Etzler, eds. (Cold Spring Harbor (NY)).

Videira, P.A., Garcia, A.P., and Sa-Correia, I. (2005). Functional and topological analysis of the Burkholderia cenocepacia priming glucosyltransferase BceB, involved in the biosynthesis of the cepacian exopolysaccharide. J Bacteriol *187*, 5013-5018.

Vinay, D.S., Lee, S.J., Kim, C.H., Oh, H.S., and Kwon, B.S. (2012). Exposure of a distinct PDCA-1+ (CD317) B cell population to agonistic anti-4-1BB (CD137) inhibits T and B cell responses both in vitro and in vivo. PLoS One *7*, e50272.

Vlasak, R., Krystal, M., Nacht, M., and Palese, P. (1987). The influenza C virus glycoprotein (HE) exhibits receptor-binding (hemagglutinin) and receptor-destroying (esterase) activities. Virology *160*, 419-425.

Vogt, T.K., Link, A., Perrin, J., Finke, D., and Luther, S.A. (2009). Novel function for interleukin-7 in dendritic cell development. Blood *113*, 3961-3968.

Vollmer, J., Tluk, S., Schmitz, C., Hamm, S., Jurk, M., Forsbach, A., Akira, S., Kelly, K.M., Reeves, W.H., Bauer, S.*, et al.* (2005). Immune stimulation mediated by autoantigen binding sites within small nuclear RNAs involves Toll-like receptors 7 and 8. J Exp Med *202*, 1575-1585.

Vollstedt, S., O'Keeffe, M., Odermatt, B., Beat, R., Glanzmann, B., Riesen, M., Shortman, K., and Suter, M. (2004). Treatment of neonatal mice with Flt3 ligand leads to changes in dendritic cell subpopulations associated with enhanced IL-12 and IFN-alpha production. Eur J Immunol *34*, 1849-1860.

Vremec, D. (2010). The isolation of mouse dendritic cells from lymphoid tissues and the identification of dendritic cell subtypes by multiparameter flow cytometry. Methods Mol Biol *595*, 205-229.

Wada, H., Masuda, K., Satoh, R., Kakugawa, K., Ikawa, T., Katsura, Y., and Kawamoto, H. (2008). Adult T-cell progenitors retain myeloid potential. Nature *452*, 768-772.

Waskow, C., Liu, K., Darrasse-Jeze, G., Guermonprez, P., Ginhoux, F., Merad, M., Shengelia, T., Yao, K., and Nussenzweig, M. (2008). The receptor tyrosine kinase Flt3 is required for dendritic cell development in peripheral lymphoid tissues. Nat Immunol *9*, 676-683.

Watari, K., Asano, S., Shirafuji, N., Kodo, H., Ozawa, K., Takaku, F., and Kamachi, S. (1989). Serum granulocyte colony-stimulating factor levels in healthy volunteers and patients with various disorders as estimated by enzyme immunoassay. Blood *73*, 117-122.

Welner, R.S., Esplin, B.L., Garrett, K.P., Pelayo, R., Luche, H., Fehling, H.J., and Kincade, P.W. (2009). Asynchronous RAG-1 expression during B lymphopoiesis. J Immunol *183*, 7768-7777.

Wilson, A., and Trumpp, A. (2006). Bone-marrow haematopoietic-stem-cell niches. Nat Rev Immunol *6*, 93-106.

Wipfler, D., Srinivasan, G.V., Sadick, H., Kniep, B., Arming, S., Willhauck-Fleckenstein, M., Vlasak, R., Schauer, R., and Schwartz-Albiez, R. (2011). Differentially regulated expression of 9-O-acetyl GD3 (CD60b) and 7-O-acetyl-GD3 (CD60c) during differentiation and maturation of human T and B lymphocytes. Glycobiology *21*, 1161-1172.

Wrammert, J., Kallberg, E., Agace, W.W., and Leanderson, T. (2002). Ly6C expression differentiates plasma cells from other B cell subsets in mice. Eur J Immunol *32*, 97-103.

Yamamoto, R., Morita, Y., Ooehara, J., Hamanaka, S., Onodera, M., Rudolph, K.L., Ema, H., and Nakauchi, H. (2013). Clonal analysis unveils self-renewing lineage-restricted progenitors generated directly from hematopoietic stem cells. Cell *154*, 1112-1126.

Yang, G.X., Lian, Z.X., Kikuchi, K., Moritoki, Y., Ansari, A.A., Liu, Y.J., Ikehara, S., and Gershwin, M.E. (2005). Plasmacytoid dendritic cells of different origins have distinct characteristics and function: studies of lymphoid progenitors versus myeloid progenitors. Journal of immunology *175*, 7281-7287.

Yasuda, K., Yu, P., Kirschning, C.J., Schlatter, B., Schmitz, F., Heit, A., Bauer, S., Hochrein, H., and Wagner, H. (2005). Endosomal translocation of vertebrate DNA activates dendritic cells via TLR9-dependent and -independent pathways. J Immunol *174*, 6129-6136.

Yasutomo, K., Horiuchi, T., Kagami, S., Tsukamoto, H., Hashimura, C., Urushihara, M., and Kuroda, Y. (2001). Mutation of DNASE1 in people with systemic lupus erythematosus. Nat Genet *28*, 313-314.

Zasloff, M. (2002). Antimicrobial peptides of multicellular organisms. Nature *415*, 389-395.

Zeng, Q., Langereis, M.A., van Vliet, A.L., Huizinga, E.G., and de Groot, R.J. (2008). Structure of coronavirus hemagglutinin-esterase offers insight into corona and influenza virus evolution. Proc Natl Acad Sci U S A *105*, 9065-9069.

Zhang, J., Raper, A., Sugita, N., Hingorani, R., Salio, M., Palmowski, M.J., Cerundolo, V., and Crocker, P.R. (2006). Characterization of Siglec-H as a novel endocytic receptor expressed on murine plasmacytoid dendritic cell precursors. Blood *107*, 3600-3608.

Zimmer, G., Reuter, G., and Schauer, R. (1992). Use of influenza C virus for detection of 9-O-acetylated sialic acids on immobilized glycoconjugates by esterase activity. Eur J Biochem *204*, 209-215.

Zuniga, E.I., McGavern, D.B., Pruneda-Paz, J.L., Teng, C., and Oldstone, M.B. (2004). Bone marrow plasmacytoid dendritic cells can differentiate into myeloid dendritic cells upon virus infection. Nat Immunol *5*, 1227-1234.